MECHANISMS OF MITOCHONDRIAL FUSION AND FISSION

Thesis by

Erik Griffin

In Partial Fulfillment of the Requirements

for the Degree of

Doctor of Philosophy

California Institute of Technology

Pasadena, California

2006

(Defended May 3, 2006)

© 2006

Erik Griffin

All Rights Reserved

Acknowledgements

I would first like to thank my graduate advisor, David Chan. David provided me with the scientific input, laboratory environment, and encouragement that made training with him a pleasure.

I would also like to thank past and current members of the Chan lab. Scott Detmer, Toby Rosen, Zhiyin Song, Yan Zhang, Hsiuchen Chen, Takumi Koshiba, Lloyd Little, Meru Sadhu, and Agi Hamburger have made the Chan lab great place to work.

I feel as if I really lucked out in coming to Caltech because of the friends and classmates and friends I had here. McKell Carter, Karli Watson, Laura Croal, Chris Otey, Eric Mosser, Harry Green, Jun Huh, Johannes Graumann, Nazli Ghaboosi...you guys rock.

Mom, Dad, Todd and Esther: Thank you for always supporting me.

Finally, I would like to thank Tara Suntoke for everything. From our trips for afternoon tea, our trips up the coast or to the mountains, I'd have to say we owned this place. I will never forget our time together on the left coast.

Abstract

We have studied the mechanisms of mitochondrial fusion and fission in *S. cerevisiae*. Using a proteomics-based approach, we have identified the WD domain protein Caf4p as a Fis1p binding partner that, along with its paralog Mdv1p, functions as a molecular adaptor between Fis1p and Dnm1p. This work defines a role for Mdv1p and Caf4p in the recruitment of Dnm1p to mitochondrial fission complexes. In a separate study, we focus on the role of Fzo1p during mitochondrial fusion. Fzo1p and its mammalian homologs, Mfn1 and Mfn2, are conserved transmembrane GTPases that are required for mitochondrial fusion. A structure/function analysis has established an essential role for three Fzo1p heptad repeat regions during mitochondrial fusion. Furthermore, we show that Fzo1p functions as an oligomer and forms critical interactions between the HRN/GTPase and HR1/HR2 regions. Finally, we have identified Om14p as a novel regulator of mitochondrial morphology. Om14p interacts with Fzo1p and Ugo1p and may be the first inhibitor of mitochondrial fusion.

Table of Contents

Acknowledgements iii

Abstract iv

Table of Contents v

List of Tables and Figures viii

Chapter 1: Introduction 1

Molecular mechanisms of mitochondrial membrane fusion

Abstract 1

Introduction 2

Virus/host membrane fusion 3

SNARE-mediated intracellular fusion 4

General considerations for mitochondrial membrane fusion 5

The Players: FZO family 7

MGM1/OPA1 12

UGO1 16

Ergosterol 17

How are outer and inner membrane fusion coordinated? 18

Perspectives 19

Mechanisms of mitochondrial fission 21

Membrane fission 21

The evolution of mitochondrial division 23

Mechanisms of mitochondrial fission in *S. cerevisiae* 26

References 30

Chapter 2: The WD40 protein Caf4p is a component of the mitochondrial fission machinery and recruits Dnm1p to mitochondria 48

Abstract 49

Introduction 49

Results 50

Discussion 56

Materials and Methods 57

References 59

Supplemental Tables 61

Chapter 3: Domain interactions within Fzo1p oligomers are required for mitochondrial fusion 69

Abstract 70

Introduction 70

Experimental Procedures 72

Results 76

Discussion 82

References 85

Figures and Tables 88

Chapter 4: Identification of Om14p as a regulator of mitochondrial morphology 100

Abstract 101

Introduction 101

Materials and Methods 102

Results 105

Discussion 108

References 111

Figures and Tables 116

Appendix 123

Future Directions 143

List of Figures and Tables

Chapter 1:

Figure 1: The mitochondrial fusion complex in yeast 47

Chapter 2:

Figure 1: Construction of M_9TH-*FIS1* and Caf4p/Mdv1p alignment 50

Figure 2: Caf4p and Mdv1p coimmunoprecipitation experiments 51

Table I: Caf4p and Mdv1p interact with Dnm1p and Fis1p in a yeast two-hybrid assay 52

Figure 3: *CAF4* regulates mitochondrial morphology 52

Figure 4: *CAF4* mediates residual fission in *mdv1Δ* cells 53

Figure 5: Caf4p overexpression blocks mitochondrial fission 54

Figure 6: Suppression of glycerol growth defects of *fzo1Δ* cells 54

Figure 7: Mitochondrial localization of Caf4p and Mdv1p requires Fis1p 55

Figure 8: Fis1p mediates Dnm1p-GFP localization through either Mdv1p or Caf4p 56

Table II: Quantitification of Dnm1p-GFP puncta localization 57

Table S1: Proteins identified in MudPIT experiments with M_9TH-Fis1p 61

Table S2: Yeast strains 67

Table S3: Primer sequences 68

Chapter 3

Table 1: Summary of intragenic complementation data 91

Table 2: Mitochondrial fusion assay 92

Figure 1: Identification of critical regions of Fzo1p 93

Figure 2: Allelic complementation between null alleles of *FZO1* 94

Figure 3: Self-association of Fzo1p 95

Figure 4: Fzo1p null mutants form homotypic oligomers 96

Figure 5: Two interacting fragments of Fzo1p 97

Figure 6: The GTPase and heptad repeat regions are required for the interaction between Fzo1p-HRN/GTPase and Fzo1p-HR1/HR2 98

Figure 7: Co-expression of the Fzo1p-HRN/GTPase and Fzo1p-HR1/HR2 fragments of Fzo1p complements *fzo1Δ* 99

Chapter 4

Table 1: Yeast Strains 111

Figure 1: Om14p interacts with Ugo1p and Fzo1p 118

Figure 2: Om14p is upregulated in glycerol and galactose cultures 119

Figure 3: Mitochondrial morphology defect in *om14Δ* cells 120

Figure 4: *om14Δ* is an *fzo1-1* suppressor 121

Figure 5: *om14Δ* suppresses *fzo1-1* by increasing mitochondrial fusion 122

Appendix

Table 1: Common contaminants in TAP-MudPIT experiments 126

Table 2: Results from Mdv1p TAP-MudPIT 128

Table 3: Results from Caf4p TAP-MudPIT 129

Table 4: Results from Dnm1p TAP-MudPIT 132

Table 5: Results from Mdm30p TAP-MudPIT 132

Table 6: Results from Fzo1p TAP-MudPIT (Dextrose cultures) 134

Table 7: Results from Fzo1p TAP-MudPIT (Dextrose cultures

and mitochondrial isolation) 135

Table 8: Results from Fzo1p TAP-MudPIT (Glycerol cultures) 136

Table 9: Results from Ugo1p TAP-MudPIT (Glycerol cultures) 138

Chapter 1: Introduction to Mitochondrial Fusion and Fission

Molecular mechanism of mitochondrial membrane fusion

Erik E. Griffin, Scott A. Detmer, and David C. Chan

Published in Biochimica et Biophysica Acta (BBA)-Molecular Cell Research
March 9 2006

Abstract

Mitochondrial fusion requires coordinated fusion of the outer and inner membranes. This process leads to exchange of contents, controls the shape of mitochondria, and is important for mitochondrial function. Two types of mitochondrial GTPases are essential for mitochondrial fusion. On the outer membrane, the *fuzzy onions*/mitofusin proteins form complexes in *trans* that mediate homotypic physical interactions between adjacent mitochondria and are likely directly involved in outer membrane fusion. Associated with the inner membrane, the OPA1 dynamin-family GTPase maintains membrane structure and is a good candidate for mediating inner membrane fusion. In yeast, Ugo1p binds to both of these GTPases to form a fusion complex, although a related protein has yet to be found in mammals. An understanding of the molecular mechanism of fusion may have implications for Charcot-Marie-Tooth subtype 2A and autosomal dominant optic atrophy, neurodegenerative diseases caused by mutations in *Mfn2* and *OPA1*.

Introduction

It has been known for decades that mitochondria have plasticity of form and undergo fusion and fission (Lehninger, 1965), but only recently has there been progress in elucidating the molecular basis of these processes. A breakthrough was the identification of the *fuzzy onions* gene product (Fzo) in the fusion of mitochondria during *Drosophila* sperm differentiation (Hales and Fuller, 1997). Fzo is the founding member of a family of mitochondrial outer membrane GTPases essential for mitochondrial fusion from yeast to mammals (Chen et al., 2003; Hales and Fuller, 1997; Hermann et al., 1998). Subsequent genetic studies have identified additional components of the fusion and fission machinery.

The balance between fusion and fission plays a central role in controlling mitochondrial morphology. In the absence of fusion, mitochondria fragment into small spheres due to ongoing fission (Chen et al., 2005; Chen et al., 2003; Hermann et al., 1998; Rapaport et al., 1998). Beyond its role in morphology, mitochondrial fusion is required for mitochondrial function. Mammalian cells lacking mitochondrial fusion grow slowly due to low respiratory capacity (Chen et al., 2005). Mice deficient in mitochondrial fusion die in midgestation (Chen et al., 2003). Moreover, mutations in components of the fusion pathway have been implicated in human neurodegenerative diseases: *Mfn2* in the peripheral neuropathy Charcot-Marie-Tooth Disease subtype 2A and *OPA1* in autosomal dominant optic atrophy (Alexander et al., 2000; Delettre et al., 2000; Kijima et al., 2005; Lawson et al., 2005; Zuchner et al., 2004).

In this review, we discuss our current understanding of how mitochondrial membranes fuse. To begin, we outline how lipid bilayers fuse in the two best-studied

experimental systems– virus-mediated fusion and vesicle fusion– in order to highlight general principles of membrane trafficking that may be applicable to mitochondrial fusion.

Virus/host membrane fusion

In order for an enveloped virus to gain access to the cellular compartment, it must direct fusion between the viral membrane and the host cell membrane. This reaction is mediated by virally encoded transmembrane glycoproteins embedded in the viral envelope. Specificity of fusion is provided by the binding of the viral glycoprotein to specific cell surface receptors on the host cell. Class I viral fusion proteins contain a short hydrophobic helix termed the fusion peptide that is crucial to the fusion reaction. On native virions (the prefusogenic state), the fusion peptide is buried in a hydrophobic pocket in the glycoprotein interior (Eckert and Kim, 2001; Skehel and Wiley, 1998). Importantly, this native structure is metastable. That is, it is stably folded but can be triggered to undergo a conformational change to a more thermodynamically stable structure. Contact with host receptors (in the case of HIV-1 gp41) or a pH change following transport to the endosome (in the case of influenza HA2) triggers a dramatic structural transition that results in extension and insertion of the fusion peptide into the host membrane. In this extended conformation, the transmembrane fusion protein now bridges the viral and host membrane, although a gap remains between the membranes (Eckert and Kim, 2001). This conformation is a transient intermediate, and the fusion protein subsequently undergoes a second structural transition to snap the fusion peptide and transmembrane regions together. This final structure is highly stable and results from

the pairing of two regions containing hydrophobic heptad repeats, sequence motifs that form coiled-coil-like structures (Eckert and Kim, 2001). In this fusogenic conformation, the viral and host membranes are forced into close apposition. Therefore, the charge repulsion between the lipid bilayers is overcome by coupling membrane apposition with the formation of a highly stable helical bundle. This sequence of events appears to occur for a broad range of Class I viral fusion proteins (Eckert and Kim, 2001; Skehel and Wiley, 1998).

SNARE-mediated intracellular fusion

Most intracellular membrane fusion events utilize a very similar mechanism. Rab GTPases, Rab effector molecules, and SNAREs are the core components of the membrane fusion machinery (Bonifacino and Glick, 2004; Ungar and Hughson, 2003). Their segregation patterns are largely responsible for marking membranes that are capable of fusing with each other. The interaction of Rab GTPases and Rab effectors in *trans* provides the initial tethering between membranes and helps ensure that only the correct pairs of membranes can proceed to fusion. At this stage, the membranes are reversibly associated but still separated by a considerable gap.

After this tethering stage, membrane fusion itself is likely to be mediated by SNARE proteins residing in the two membranes. SNAREs are membrane-associated proteins containing a loosely conserved ~60 residue SNARE motif that contains hydrophobic heptad repeats. SNAREs can be engineered to fuse liposomes (Weber et al., 1998) and cells (Hu et al., 2003) and are necessary in most intracellular membrane fusion systems, although there are exceptions (Ungar and Hughson, 2003). Prior to fusion,

distinct Q- and R-SNAREs are segregated between the two membranes and "primed" for fusion. Following Rab-mediated tethering, the Q-SNAREs interact specifically with their cognate R-SNARE partners in *trans*. The specificity of SNARE pairing further ensures the fidelity of the fusion reaction (McNew et al., 2000; Parlati et al., 2000). The *trans* SNARE complex adopts an extremely stable structure, in which four SNARE motifs form a four–helix bundle to draw the two membranes together (Sutton et al., 1998). Similar to the viral fusion proteins, the energetic benefit of forming the *trans* SNARE structure is coupled to overcoming the charge repulsion between the membranes.

General considerations of mitochondrial membrane fusion

There are several important characteristics of mitochondria that make their fusion mechanism particularly intriguing. First, unlike almost all other intracellular fusion events, neither SNAREs nor the AAA-ATPase NSF have been implicated in the mitochondrial fusion reaction (Nunnari et al., 1997). Indeed, the three known mitochondrial fusion molecules appear solely dedicated to mitochondrial fusion, suggesting the machinery evolved independently and is uniquely tailored for this organelle. Interestingly, a different machinery may exist in plants, because there are no identifiable homologs of the animal genes involved in fusion (Sheahan et al., 2005). Second, mitochondria have an outer and inner membrane, with a membrane potential across the latter. Therefore, the fusion of four sets of lipid bilayers must be coordinated. Third, unlike viral fusion and most SNARE-mediated fusion, mitochondrial fusion is homotypic. This implies a symmetry in the distribution of molecules between the adjacent membranes and is undoubtedly reflected in their fusion mechanism. Finally,

although the regulation of mitochondrial fusion is not understood, it is likely to be influenced by cellular energetic demands, apoptotic stimuli and developmental cues. Taken together, these characteristics suggest that mitochondria fuse through a novel mechanism that reflects their unique endosymbiont origin and double membrane architecture.

In spite of these unique features, mitochondrial fusion likely has some general features in common with virus-mediated and SNARE-mediated membrane fusion. First, the specificity of membrane fusion is likely determined by the formation of specific protein complexes formed in *trans* between the fusing membranes. As detailed below, mitofusin complexes on the outer membrane may provide the specificity for homotypic inter-mitochondrial interactions. Second, conformational changes in *trans* protein complexes will likely provide the energy necessary to appose two negatively charged lipid bilayers. Again, mitofusins may be critical for this process.

A number of experimental systems have been developed to study mitochondrial fusion. In some studies, tubulation of mitochondria is interpreted as evidence for fusion. However, the assessment of mitochondrial fusion by morphology alone is risky, because factors other than fusion, such as loss of fission, can influence the tubulation of mitochondria. Therefore, direct *in vivo* assays for fusion are the foundation for most of our knowledge of the genetic and energetic requirements for mitochondrial fusion. In yeast, fusion between differentially labeled mitochondria is scored following mating of *a* and α cells (Nunnari et al., 1997). In mammalian tissue culture, cells with distinctly labeled mitochondria are co-plated and fused by treatment with polyethylene glycol (PEG). The resulting cell hybrids are scored for the intermixing of mitochondrial

markers (Chen et al., 2003; Legros et al., 2002; Mattenberger et al., 2003). Alternatively, the diffusion of a photoactivated mitochondrial GFP can be used to quantitate mitochondrial fusion (Karbowski et al., 2004). Recently, the development of an *in vitro* mitochondrial fusion assay has opened the door to integration of genetic and biochemical approaches (Meeusen et al., 2004).

The players

Genetic strategies have identified three core components of the fusion pathway in yeast (Figure 1). Two of these genes, Fzo1p and Mgm1p, encode large mitochondrial GTPases. The third, Ugo1p, resides in the mitochondrial outer membrane and interacts with both Fzo1p and Mgm1p. There are two mammalian homologs of *FZO1*, termed mitofusins (*Mfn1* and *Mfn2*) and one homolog of *MGM1*, *OPA1*. A mammalian homolog of *UGO1* has not been identified. In yeast, two additional components, Mdm30p and Pcp1p/Rbd1p, regulate the activity of Fzo1p and Mgm1p, respectively.

FZO family

FZO family members are required for mitochondrial fusion

Fzo family members are the best candidates for molecules that directly mediate mitochondrial fusion. *Fzo/Mfn* mutations in yeast, flies, and mammals completely abolish mitochondrial fusion, indicating they play essential, conserved roles in fusion (Chen et al., 2005; Hales and Fuller, 1997; Hermann et al., 1998). In *fzo1Δ* yeast, even mitochondria that are adjacent to one another are unable to fuse, suggesting Fzo1p acts at a late step in the fusion pathway (Hermann et al., 1998). Similarly, *Mfn*-null embryonic

fibroblast cell lines (lacking both *Mfn1* and *Mfn2*) have severely fragmented mitochondrial morphology and display no fusion in the PEG mitochondrial fusion assay (Chen et al., 2005).

Studies of embryonic fibroblast cell lines derived from *Mfn1* mutant and *Mfn2* mutant mice indicate that Mfn1 and Mfn2 are partially redundant molecules (Chen et al., 2003). In contrast to *Mfn*-null cells, *Mfn1*-null cells and *Mfn2*-null cells retain low levels of mitochondrial fusion (Chen et al., 2005; Chen et al., 2003). Both of these mutant cell lines also have fragmented mitochondrial morphologies. *Mfn1*-null cells have mitochondria that are extremely short and rod-shaped, while *Mfn2*-null cells have mitochondria that range from small fragments to large spheres and short tubules. Significantly, a highly tubular mitochondrial population can be restored in either *Mfn1*-null, *Mfn2*-null, or *Mfn*-null cells by the over-expression of either Mfn1 or Mfn2. This morphological rescue is accompanied by restoration of full fusion activity. These data indicate that a single mitofusin is sufficient for mitochondrial fusion and that the defects observed in the single mutant cell lines result from the reduced level of total mitofusin expression rather than the specific requirement for either molecule.

The architecture of Fzo family members

Fzo family members encode large transmembrane GTPases that are distributed uniformly across the mitochondrial outer membrane. The transmembrane region spans the outer membrane twice, placing the N- and C-terminal portions in the cytosol where they are in position to mediate important steps during fusion (Figure 1) (Fritz et al., 2001; Hermann et al., 1998; Rapaport et al., 1998).

Fzo family members share an N-terminal GTPase domain that includes the canonical G1–G4 motifs. Mutations designed to block GTP nucleotide binding or hydrolysis completely block fusion (Chen et al., 2003; Hales and Fuller, 1997; Hermann et al., 1998). However, despite its required role in fusion, there are few data that indicate how GTPase activity contributes to the fusion reaction. The GTPase domain may function in a regulatory/signaling capacity similar to that of Rab GTPases during SNARE-mediated fusion. In this model, the nucleotide state of Fzo/Mfn would regulate the recruitment or activity of other factors during fusion. Alternatively, Fzo/Mfn could function in a manner similar to dynamin GTPases, and couple GTP hydrolysis to a mechanochemical activity such as membrane deformation or close membrane apposition. Indeed, it has been suggested that Fzo/Mfn is a dynamin family member on the basis of its large size, membrane association, and ability to oligomerize (Praefcke and McMahon, 2004).

Fzo family members contain two heptad repeat regions, HR1 and HR2, situated on either side of the transmembrane region. The yeast homolog encodes a third heptad repeat region N-terminal of the GTPase domain that is not found in the mammalian mitofusins. As discussed previously, hydrophobic heptad repeats are predicted to form coiled-coil-like structures and play critical functions in the fusion mechanism of both SNAREs and viral fusion proteins. Given their location proximal to the transmembrane region, it is tempting to speculate that HR1 and/or HR2 might form helical fusogenic structures analogous to those formed by SNAREs or viral glycoproteins.

Like dynamins, Fzo/Mfn molecules are capable of complex intermolecular interactions. Coimmunoprecipitation studies have demonstrated that the mitofusins can

interact to form three distinct molecular complexes: Mfn1 homotypic complexes, Mfn2 homotypic complexes, and Mfn1/Mfn2 heterotypic complexes (Chen et al., 2003; Eura et al., 2003). Co-expression of a mitochondrially localized C-terminal construct of Mfn2 can sequester an otherwise cytoplasmic N-terminal Mfn2 construct (Rojo et al., 2002). This recruitment is dependent on the presence of both HR1 and HR2, and suggests they may interact with each other (Rojo et al., 2002). Additionally, the C-terminus of Mfn2, lacking the transmembrane region, can be immunoprecipitated with the N-terminus of Mfn2 in a reaction that depends on the GTPase domain and HR1 (Honda et al., 2005). The stoichiometry of these complexes is unknown and direct interactions have not been demonstrated.

Fzo/Mfn forms a trans complex

During both viral and SNARE-mediated fusion, the formation of specific *trans* complexes is critical for ensuring specificity and for mediating membrane apposition. For these reasons, it is important to understand what *trans* complexes form between adjacent mitochondria during mitochondrial fusion. Because mitochondrial fusion is homotypic, specificity could be achieved by an interaction between the same protein on adjacent mitochondria. Several lines of evidence implicate Fzo/Mfn in the formation of a *trans* complex. Mfn-null mitochondria fail to fuse with wild-type mitochondria, indicating that mitofusins are required on adjacent mitochondria (Koshiba et al., 2004). In addition, *Mfn1*-null mitochondria can fuse to *Mfn2*-null mitochondria, suggesting that a *trans* Mfn1/Mfn2 complex is also fusion-competent (Chen et al., 2005). Finally,

mitochondrial fusion *in vitro* requires functional *FZO1* on both mitochondria, supporting its role in mediating a *trans* complex (Meeusen et al., 2004).

The C-terminal HR2 domain of Mfn1 appears to be important for formation of a *trans* complex. HR2 forms a dimeric, anti-parallel coiled coil that is 95 Å long (Koshiba et al., 2004). In contrast to the fusogenic states of viral fusion proteins and SNAREs, the anti-parallel HR2 dimer positions the transmembrane domains on opposite ends of the helical bundle. Therefore, formation of this structure between Mfn1 molecules on adjacent mitochondria would tether the membranes together, but not close enough to directly mediate fusion. Expression of a truncated Mfn1 lacking the GTPase domain results in severe mitochondrial clumping (Koshiba et al., 2004). EM images of these clumped mitochondria reveal tight and uniform spacing compatible with the length of the dimeric HR2 coiled coil. Formation of these structures depends on the HR2 structure and may represent a tethered intermediate in the fusion pathway (Koshiba et al., 2004). Because these tethered intermediates are unable to progress to membrane fusion, the GTPase domain likely acts downstream of mitochondrial tethering. A *trans* Mfn1 complex has also been identified *in vitro* by immunoprecipitation (Ishihara et al., 2004).

MDM30 controls Fzo1p levels

MDM30 was identified in a visual screen for non-essential yeast genes required to maintain normal mitochondrial morphology (Dimmer et al., 2002). Mdm30p is a member of the F-box family of proteins, which target substrates to the SCF (Skp1p/Cdc53p/F-box) ubiquitin ligase complex. Ubiquitinated substrates are then degraded by the 26S proteasome (Deshaies, 1999). *mdm30Δ* cells have elevated Fzo1p

levels that result in fragmentation and aggregation of the mitochondrial reticulum (Fritz et al., 2003). In the zygotic fusion assay, *mdm30Δ* cells have no fusion activity, but *mdm30D dnm1Δ* double mutants (*DNM1* is required for mitochondrial fission) retain some activity, indicating *MDM30* is important but not strictly required for mitochondrial fusion (Fritz et al., 2003).

In the simplest model, Mdm30p could regulate the turnover rate and the steady-state levels of Fzo1p by directly targeting Fzo1p for degradation. Alternatively, it has been suggested that Mdm30p may degrade non-productive Fzo1p fusion intermediates, whose accumulation in *mdm30Δ* yeast could inhibit fusion (Fritz et al., 2003). An important step in testing these models will be to determine the direct targets of Mdm30p, and specifically if Fzo1p is one of them. It has not been possible to demonstrate the presence of ubiquitin conjugated Fzo1p molecules, and it remains possible that the elevated Fzo1p expression levels in *mdm30Δ* yeast is an indirect effect (Fritz et al., 2003). In addition to Mdm30p-dependent turnover of Fzo1p, it has also been noted that Fzo1p degradation following mating factor treatment is Mdm30p-independent (Neutzner and Youle, 2005). Therefore, at least two distinct modes of Fzo1p turnover exist.

MGM1/OPA1

The role of MGM1/OPA1 in mitochondrial fusion

Mgm1p/OPA1 is a member of the dynamin-related protein (DRP) subfamily. DRPs and classical dynamins all encode GTPase, middle, and GTPase effector (GED) domains. Unlike dynamins, DRPs lack a pleckstrin homology and a proline-rich domain (Praefcke and McMahon, 2004). Several dynamin family members have well-

characterized roles in membrane fission in diverse cellular contexts including endocytosis, vesicular trafficking, and mitochondrial division. During endocytosis, dynamin assembles into a collar around the neck of the invaginating vesicle. GTP hydrolysis is thought to stimulate constriction or elongation of the collar, leading to membrane scission. It has not been determined if Mgm1p shares the membrane-constricting activity of the other dynamin family members, and it is unclear how such an activity would contribute to mitochondrial fusion.

The requirement of Mgm1p for mitochondrial fusion in yeast has been clearly established. *mgm1Δ* cells display no mitochondrial fusion, even when the mitochondria are in close contact, indicating that Mgm1p, like Fzo1p, is required at a late step in the fusion pathway (Sesaki et al., 2003b; Wong et al., 2003). There has been significant confusion over the function of OPA1 because, paradoxically, both overexpression and knock-down of OPA1 results in fragmentation of the mitochondrial network (Chen et al., 2005; Cipolat et al., 2004; Griparic et al., 2004; Olichon et al., 2002). In one experimental system, OPA1 expression leads to increased tubulation (Cipolat et al., 2004). While the over-expression phenotype remains to be resolved, it is clear that mitochondrial fragmentation in OPA1 knock-down cells results from a complete block in both outer and inner membrane fusion activity (Chen et al., 2005; Cipolat et al., 2004).

In addition to the defects in fusion, cells lacking OPA1 have highly disorganized cristae (Griparic et al., 2004; Olichon et al., 2002). Similarly, *mgm1Δ* yeast have dramatically swollen and poorly involuted cristae (Sesaki et al., 2003b). These observations raise the issue of whether the fusion defects in Mgm1p/OPA1-deficient cells might be secondary to disorganization of the mitochondrial inner membrane. However,

the cristae defects in *mgm1Δ* cells are largely suppressed in *dnm1D mgm1Δ* cells, but these cells nevertheless are completely defective for mitochondrial fusion (Sesaki et al., 2003b; Wong et al., 2003). Taken together, these observations implicate Mgm1p/OPA1 directly in the fusion reaction.

Maturation of Mgm1p

Correct processing of Mgm1p is critical to its function in mitochondrial dynamics. In yeast, proteolytic processing results in a long and a short isoform, l-Mgm1p and s-Mgm1p. Unprocessed Mgm1p contains an N-terminal mitochondrial targeting sequence (MTS) followed by an extended hydrophobic region. After translation in the cytosol, Mgm1p is targeted to the mitochondrial inner membrane by the MTS (Herlan et al., 2003). The MTS is inserted through the inner membrane and into the matrix, where it is cleaved by the mitochondrial processing peptidase (MPP), resulting in l-Mgm1p (Herlan et al., 2003). l-Mgm1p is believed to be anchored in the inner membrane through the N-terminal hydrophobic domain, leaving the rest of the protein facing the intermembrane space.

Mgm1p can be also be processed by the rhomboid-like protease Rbd1p/Pcp1p to yield s-Mgm1p (Herlan et al., 2004; Herlan et al., 2003; McQuibban et al., 2003; Sesaki et al., 2003a). Rhomboids are a functionally conserved family of intramembrane proteases best characterized for their processing of epidermal growth factor receptor ligands in *Drosophila* (Urban et al., 2001). s-Mgm1p remains membrane associated in the IMS, although whether s-Mgm1p is associated with the IMS face of the IM or OM is unclear (Herlan et al., 2003). It has been proposed that sorting of Mgm1p in the inner

membrane is responsible for the production of l-Mgm1p versus s-Mgm1p (Herlan et al., 2004). During cleavage of the MTS, the N-terminus of Mgm1p lies within the translocon of the inner membrane (TIM). If Mgm1p exits laterally out of the TIM complex, l-Mgm1p is produced. If Mgm1p exit is delayed, further insertion of the hydrophobic domain allows processing by Rbd1p/Pcp1p to produce s-Mgm1p. This model is consistent with the observation that l-Mgm1p and s-Mgm1p do not have a precursor-product relationship (Shepard and Yaffe, 1999).

rbd1/pcp1Δ cells produce only l-Mgm1p (Herlan et al., 2003; McQuibban et al., 2003; Sesaki et al., 2003a). These cells display severely fragmented mitochondrial morphology, indicating l-Mgm1p is not sufficient to support normal levels of mitochondrial fusion. Assessing the activity of s-Mgm1p is more difficult because it lacks an MTS. However, s-Mgm1p targeted to mitochondria by fusion of a heterologous N-terminal MTS fails to complement the fusion defect in *mgm1Δ* cells (Herlan et al., 2003). The ratio of the two isoforms is critical for fusion, because mutations that cause differences in the ratio of the two isoforms cause defects in mitochondrial morphology (Herlan et al., 2004; Herlan et al., 2003; McQuibban et al., 2003; Sesaki et al., 2003a). Allelic complementation between temperature-sensitive *mgm1* mutants indicate Mgm1p is multimeric, and it would be interesting to know if the two isoforms interact with each other, or if they form distinct complexes (Wong et al., 2003).

OPA1 in mammalian cells is also localized to the mitochondrial inter-membrane space and is peripherally associated with the inner membrane (Arnoult et al., 2005; Griparic et al., 2004). The mammalian homolog of Rbd1p/Pcp1p, PARL, is indeed localized to mitochondria. However, its putative role in OPA1 processing remains to be

confirmed. An additional complication is that extensive alternative splicing results in eight mRNA isoforms (Delettre et al., 2000; Satoh et al., 2003).

UGO1

FZO1 and *MGM1* are just two of the ~340 genes required for respiration in *S. cerevisiae*. They are unique, however, because their respiration defect can be suppressed by mutations in the mitochondrial fission pathway (Cerveny et al., 2001; Fekkes et al., 2000; Mozdy et al., 2000; Tieu and Nunnari, 2000). This property of mitochondrial fusion mutants enabled the identification of *UGO1* as a third component of the fusion pathway (Sesaki and Jensen, 2001). Ugo1p is a 58 kDa protein embedded in the mitochondrial outer membrane, with the N-terminal region facing the cytosol and the C-terminal region facing the inter-membrane space (Sesaki and Jensen, 2001). Ugo1p contains two energy transfer motifs found in mitochondrial carrier proteins. However, no Ugo1p homologs have been identified outside of fungi, suggesting that its role in mitochondrial fusion is not conserved.

Ugo1p, Fzo1p and Mgm1p assemble into a fusion complex. The N-terminal cytoplasmic domain of Ugo1p binds Fzo1p near its transmembrane region, and the C-terminal half of Ugo1p binds Mgm1p in the inter-membrane space. Indeed, Ugo1p is required for the formation of a Fzo1p/Mgm1p complex (Sesaki and Jensen, 2004; Wong et al., 2003). Interestingly, the GTPase activities of Fzo1p and Mgm1p are not required for binding to Ugo1p, suggesting that Ugo1p binding does not require the GTPase cycles of either protein (Sesaki and Jensen, 2004). Based on these data, Ugo1p may provide a scaffold for the assembly of a fusion complex that spans the outer and inner membranes,

and could provide a link that coordinates their fusion. The requirement for this interaction would explain why Mgm1p is required for outer membrane fusion despite its inter-membrane space localization (Sesaki et al., 2003b).

Ergosterol

Ergosterol is a membrane-associated sterol with a recently established role in vacuolar and peroxisomal fusion. Interestingly, several lipids including ergosterol, PI(3)P, PI(4,5)P_2, and diacylglycerol (DAG) organize specific vacuolar membrane subdomains where fusion proteins are concentrated (Fratti et al., 2004). Disruption of ergosterol biosynthesis leads to vacuolar fusion defects both *in vitro* and *in vivo* (Kato and Wickner, 2001). Similarly, ergosterol, PI(3)P, and PI(4,5)P_2 inhibitors block peroxisomal fusion *in vitro* by preventing fusion proteins from dynamically partitioning in membrane subdomains (Boukh-Viner et al., 2005).

A striking conclusion from two recent genome wide screens for morphology defects in yeast is the identification of severe mitochondrial morphology defects in mutants of the ergosterol biosynthesis pathway (Altmann and Westermann, 2005; Dimmer et al., 2002). These mutants all possess fragmented or aggregated mitochondria, suggesting a fusion defect. Although a direct role in fusion has not been established with either the zygotic or *in vitro* mitochondrial fusion assay, an intriguing possibility is that ergosterol is necessary to organize fusion molecules into subdomains in the outer membrane. Both Fzo1p and Ugo1p are uniformly distributed across the outer membrane, so either other unknown components or fusion-active subpopulations of these proteins may be concentrated into ergosterol-rich domains.

How are outer and inner membrane fusion coordinated?

The double membrane architecture of mitochondria means that fusion necessarily entails merging four membranes into two membranes. Time-lapse imaging studies *in vivo* indicate that outer and inner mitochondrial membrane fusion are tightly coordinated. Manipulation of mitochondrial fusion *in vitro*, however, has distinguished outer membrane and inner membrane fusion as two mechanistically distinct processes (Meeusen et al., 2004). Under limiting GTP concentrations, mitochondria *in vitro* will fuse their outer membranes, but not inner membranes. Supplementation with a GTP-regenerating system allows for subsequent inner membrane fusion (Meeusen et al., 2004).

Similarly, outer membrane fusion can be distinguished from inner membrane fusion in mammalian cells. Dissipation of mitochondrial membrane potential has been reported to block mitochondrial fusion (Ishihara et al., 2003; Legros et al., 2004; Mattenberger et al., 2003). Surprisingly, this effect is specific for inner membrane fusion. Treatment of human 143B cells with an H+ ionophore (CCCP) or a K+ ionophore (valinomycin) blocked inner membrane but not outer membrane fusion (Malka et al., 2005). In contrast, CCCP treatment *in vitro* nearly completely blocks outer membrane fusion in yeast (Meeusen et al., 2004). It will be interesting to determine whether the membrane fusion defects observed with depolarized mitochondria are due to a direct mechanistic role of membrane potential during the fusion process, or secondary to inner membrane ultrastructural defects observed following depolarization.

The requirement for high levels of GTP for inner membrane fusion *in vitro* implicates a GTPase in inner membrane fusion. A likely candidate is the inter-membrane

space GTPase Mgm1p. As discussed above, because Mgm1p is necessary for outer membrane fusion *in vivo*, it has not been possible to address its role specifically in inner membrane fusion (Sesaki et al., 2003b). Because the *in vitro* mitochondrial fusion assay allows distinction between outer membrane and inner membrane fusion, it should be useful in addressing this issue through the use of temperature-sensitive alleles of *MGM1*.

Perspectives

Based on the studies discussed, the outlines of a model for mitochondrial fusion can be proposed to motivate future studies. It seems likely that Fzo1p/Mfns and Mgm1p/OPA1 are core components of the fusion machinery. Fzo1p/Mfn on the outer membrane appears to mediate homotypic interactions between mitochondria. They play a direct role in at least tethering mitochondria to each other, and may have subsequent roles in membrane merger. Based on its location, Mgm1p/OPA1 is the best candidate for mediating inner membrane fusion. It is unclear how its putative dynamin-like properties would contribute to fusion. One possibility is that OPA1 is be important in tubulation of the inner membrane during the fusion process. In yeast, Ugo1p may help to coordinate outer membrane fusion by Fzo1p with inner membrane fusion by Mgm1p, but nothing is known about its possible counterpart in mammalian cells.

A clear priority for the near future is the identification of new components of the fusion pathway. Genetic screens in yeast have been very successful in identifying much of the core machinery, and these can now be complemented with biochemical approaches. In the near future, it may be possible to identify the core mitochondrial fusion machinery and to determine how it apposes mitochondrial membranes for fusion.

To achieve this goal, a combination of structural information and *in vitro* reconstitution using purified components will be necessary.

Molecular Mechanism of Mitochondrial Fission

Balanced rates of mitochondrial fusion and fission are necessary to maintain the dynamic mitochondrial reticulum (Nunnari et al., 1997; Sesaki and Jensen, 1999). In the absence of mitochondrial fission, ongoing fusion causes the formation of mitochondrial nets with few tubular ends (Bleazard et al., 1999; Sesaki and Jensen, 1999; Smirnova et al., 1998) In flies, defects in mitochondrial fission disrupt axonal transport of mitochondria, causing profound neuronal dysfunction (Verstreken et al., 2005). Mitochondrial fission is associated with apoptosis in mammals (Frank et al., 2001), worms (Jagasia et al., 2005), and potentially in yeast (Fannjiang et al., 2004; Ivanovska and Hardwick, 2005). Here, we review the evolution and mechanism of mitochondrial division.

Membrane fission

Membrane fission occurs is a wide variety of cellular contexts including cytokinesis, vesicle budding, endocytosis, and organelle division. In principle, membrane fission involves the establishment and marking of the fission site so membrane fission proteins can be recruited. Next, the fission proteins either constrict or elongate the membrane until it severs. Two membrane fission events that are particularly relevant to mitochondrial division are bacterial cytokinesis and eukaryotic endocytosis.

FtsZ

In bacteria, membrane scission during cytokinesis is mediated by the tubulin-like self-assembling GTPase FtsZ (Margolin, 2005; Osteryoung and Nunnari, 2003). In *E. coli*, cytokinesis is initiated by the assembly of FtsZ into a membrane-tethered ring structure at the middle of the cell. The FtsZ ring recruits of other division factors to the cytoplasmic face of the inner membrane. Progressive contraction of the FtsZ ring coincides with membrane invagination and cell division (Margolin, 2005). Currently, it remains unresolved whether FtsZ ring contraction is a cause or a consequence of membrane invagination (Margolin, 2005).

Dynamins

In eukaryotes, membrane scission during endocytosis is mediated by dynamin GTPases (Praefcke and McMahon, 2004). Three characteristic features of dynamins are their membrane association, GTP dependent assembly, and assembly stimulated GTP hydrolysis (Warnock et al., 1996). During endocytosis, GTP-bound dynamin 1 associates with the plasma membrane through its pleckstrin homology domain. On the membrane, dynamin 1 assembles into a collar-like, or spiral, structure around the neck of the nascent endocytic vesicle (Hinshaw and Schmid, 1995; Takei et al., 1995). Formation of this structure brings the C-terminal GTPase effector domain, or GED, into proximity with the GTPase domain (Zhang and Hinshaw, 2001). The GED domain functions as a GAP to directly stimulate GTP hydrolysis (Sever et al., 1999).

There are two models for how dynamin contributes to membrane scission. In the mechanochemical model, GTP hydrolysis induces sufficient constriction or elongation of

the collar to directly cause membrane fission (Stowell et al., 1999; Sweitzer and Hinshaw, 1998; Zhang and Hinshaw, 2001). An alternative model is that GTP-bound dynamin recruits other factors to the endocytic collar which then drive fission. This model is based on the dynamin GED mutant, R725A, which fails to stimulate GTP hydrolysis upon oligomerization, yet increases the rate of endocytosis in a cell-based assay (Sever et al., 2000; Sever et al., 1999). In contrast to what the mechanochemical model would predict, dynamin R725A suggests decreased GTP hydrolysis increases dynamin's membrane severing activity. This interpretation is highly controversial because hydrolysis-deficient dynamin mutants do not support endocytosis and because an extensive body of work has demonstrated GTP hydrolysis is coupled to constriction of dynamin spirals *in vitro* (Marks et al., 2001; Praefcke and McMahon, 2004). While it is clear dynamin is intimately involved in membrane scission, a precise mechanism for dynamin activity awaits structural information on GTP-bound and GDP-bound dynamin.

The evolution of mitochondrial division

Many aspects of mitochondrial and chloroplast biology reflect their evolution from endosymbiotic bacteria. For example, while most mitochondrial and chloroplast proteins are encoded in the nucleus, both organelles retain genomes of bacterial origin (Gray, 1999). Additionally, chloroplast division and protist mitochondrial division evolved from a combination of bacterial cytokinesis proteins and eukaryotic endocytosis proteins (Osteryoung and Nunnari, 2003). Homologs of the bacterial division protein FtsZ and the eukaryotic endocytosis protein dynamin assemble on the organellar inner membrane and outer membrane, respectively. This architecture suggests endosymbiotic

bacteria initially co-opted the endocytosis machinery for outer membrane division (van der Bliek, 2000). In higher eukaryotes, FtsZ has been lost, and mitochondrial division is mediated solely by dynamin-related proteins (Margolin, 2005; Osteryoung and Nunnari, 2003).

Chloroplast Division

Like mitochondria, chloroplast biogenesis involves the regulated division of chloroplasts. Both FtsZ (Kiessling et al., 2000; Osteryoung et al., 1998; Vitha et al., 2001) and dynamins (Gao et al., 2003; Miyagishima et al., 2003) are involved in chloroplast division, suggesting chloroplasts use a hybrid of bacterial and eukaryotic machinery for division. For example, in *Arabidopsis*, two FtsZ homologues co-localize in ring structures in the chloroplast stroma (McAndrew et al., 2001) and a dynamin family member, ARC5, assembles into a ring on the cytosolic side of the outer membrane (Gao et al., 2003). Similarly, in the red alga *C. merolae*, a FtsZ homologue, CmFtsZ2, initiates chloroplast division by assembling into a ring in the stroma. A dynamin family member, CmDnm2, subsequently assembles into a ring on the outer membrane that contracts during division (Miyagishima et al., 2003). Taken together, these data indicate chloroplasts likely use the FtsZ machinery for inner membrane scission and dynamin-related proteins for outer membrane fission.

Mitochondrial Division

Mitochondrial division in primitive eukaryotes is similar to chloroplast division. For example, FtsZ homologues localize and are important for the division of

mitochondria in the red algae *Mallomonas splendens* and *Cyanidioschyon merolae*, as well as the amoeba *Dictyostelium discoideum* (Beech et al., 2000; Gilson et al., 2003; Nishida et al., 2003). In the red alga *C. merolae*, mitochondrial division shares several similarities with chloroplasts. A mitochondria-specific FtsZ (CmFtsZ1) forms a ring in the matrix side of the inner membrane (Nishida et al., 2003). Next, an electron-dense structure termed the mitochondrial dividing, or MD, ring forms on the cytoplasmic side of the OM. The MD ring is clearly evident in electron micrographs, although its composition has not been determined (Nishida et al., 2003). Finally, a dynamin-related protein (CmDnm1) assembles on the cytoplasmic face of the OM, allowing completion of the mitochondrial fission (Nishida et al., 2003).

In contrast to chloroplast division or mitochondrial division in red algae, mitochondrial division in higher eukaryotes such as *S. cerevisiae*, *C. elegans*, *A. thaliana*, and mammals is mediated solely by dynamins (Arimura and Tsutsumi, 2002; Bleazard et al., 1999; Labrousse et al., 1999; Sesaki and Jensen, 1999; Smirnova et al., 1998). Indeed, no FtsZ homologs are evident in the genomes of yeast, worms, or mammals (Margolin, 2005). This simplified mitochondrial division machinery suggests that either 1) the outer membrane dynamin ring has evolved the capacity to also sever the inner membrane or 2) the role of FtsZ in inner membrane fission may have been replaced by other proteins that await discovery.

In support of the latter possibility, there is evidence for dynamin-independent mitochondrial constriction at an early step in the fission reaction. Dnm1p localizes specifically to sites of mitochondrial constriction (Bleazard et al., 1999; Ingerman et al., 2005). Time-lapse imaging of mitochondrial fission events indicate that the first step in

fission is constriction of the mitochondrial tubule. Dnm1p is recruited to mitochondrial constrictions and forms large puncta that mark sites of subsequent membrane fission (Legesse-Miller et al., 2003). In addition, mitochondria in DRP-1 deficient worms have a "beads on a string" appearance that suggest these mutants are defective for a late stage in mitochondrial fission, yet are still able to form constrictions (Labrousse et al., 1999). Finally, the mitochondrial fission proteins also mediate peroxisomal fission (Hoepfner et al., 2001; Koch et al., 2003; Koch et al., 2005; Li and Gould, 2003). In DRP1-deficient cells, peroxisomes form prominent constrictions but fail to divide, suggesting DRP1 must be recruited to these constrictions to complete the fission reaction (Koch et al., 2004). Taken together, these data suggest the first step in fission may be a dynamin-independent mitochondrial constriction. These constrictions sites could then serve as sites for DRP/Dnm1p recruitment and eventually fission. A priority for the future is to identify the components that generate dynamin-independent mitochondrial constrictions.

Mechanisms of Mitochondrial Fission in *S. cerevisiae*

Dynamin-related proteins (Dnm1p/DRP1/DLP1) were originally identified on the basis of the mitochondrial morphology defect in *dnm1Δ* yeast (Hermann et al., 1997) and were subsequently shown to be required for fission in yeast (Bleazard et al., 1999; Sesaki and Jensen, 1999), worms (Labrousse et al., 1999), and mammals (Smirnova et al., 1998). Like other dynamins, DRP1 can assemble into spirals *in vitro* (Yoon et al., 2001) and oligomerization stimulates GTP hydrolysis (Fukushima et al., 2001; Ingerman et al., 2005). Interestingly, Dnm1p assembles into spirals *in vitro* that are two times the diameter of dynamin 1 spirals and similar to the diameter of mitochondrial fission sites

(~100 nm in diameter), suggesting Dnm1p forms spirals tailored to mitochondria (Ingerman et al., 2005). Given the direct involvement of dynamins in membrane fission during endocytosis, Dnm1p is thought to directly sever the mitochondrial membranes during fission.

An early step in the mitochondrial fission pathway is the assembly of Dnm1p on the mitochondrial outer membrane. In wild-type cells, Dnm1p localizes to dozens of mitochondrial puncta and a few cytosolic puncta (Bleazard et al., 1999). Dnm1p localizes to mitochondrial constriction and the formation of Dnm1p puncta precedes all mitochondrial fission events, suggesting Dnm1p puncta are intimately involved in executing the mitochondrial fission reaction. Other factors likely contribute to Dnm1p activity because only a minority of Dnm1p puncta progress to complete division (Legesse-Miller et al., 2003). Additionally, unlike classical dynamins, which directly associate with membranes their through pleckstrin homology domains, dynamin-related proteins lacking pleckstrin homology domains assemble on mitochondria through interactions with other mitochondrial proteins. Thus, understanding how Dnm1p is assembled into active fission complexes is critical to understanding the mitochondrial fission reaction.

Fis1p and Mdv1p

Fis1p is a 17.7 kDa protein distributed uniformly on the mitochondrial outer membrane via a C-terminal transmembrane domain and is required for mitochondrial fission (Fekkes et al., 2000; Mozdy et al., 2000). The cytosolic N-terminal portion of Fis1p is comprised of a six-helix bundle consisting of two tetratrico-peptide repeat (TPR)

motifs (Dohm et al., 2004; Suzuki et al., 2003; Suzuki et al., 2005). In *fis1Δ* cells, Dnm1p localization is severely altered. Instead of forming dozens of mitochondrial puncta, Dnm1p is found almost exclusively in the cytosol (Cerveny et al., 2001; Fekkes et al., 2000; Mozdy et al., 2000; Tieu and Nunnari, 2000). The few mitochondrial puncta that do form are larger than wild-type puncta, and are likely non-functional Dnm1p aggregates (Mozdy et al., 2000). Thus, Fis1p is thought to mediate the recruitment of cytosolic Dnm1p puncta to mitochondria (Mozdy et al., 2000; Tieu and Nunnari, 2000). In an alternative model, Dnm1p localizes to the mitochondrial outer membrane in a Fis1p independent manner, and Fis1p is required to mediate even distribution of mitochondrial Dnm1p puncta (Cerveny and Jensen, 2003).

Mdv1p is required for wild-type levels of mitochondrial fission. Mdv1p interacts with Dnm1p through its C-terminal WD40 domain and with Fis1p through its N-terminal extension, suggesting it may act as an adaptor between Fis1p and Dnm1p (Tieu et al., 2002). Overexpressed Mdv1p-GFP fusion proteins localize to Dnm1p puncta on mitochondria, suggesting Mdv1p is present at sites of mitochondrial fission (Cerveny and Jensen, 2003; Tieu et al., 2002). Surprisingly, in *mdv1Δ* cells, Dnm1p localization is completely normal, indicating Mdv1p is dispensable for Dnm1p recruitment. Thus, Fis1p does not require Mdv1p to recruit Dnm1p to mitochondria (Cerveny and Jensen, 2003; Tieu et al., 2002).

The Dnm1p localization patterns in *fis1Δ* and *mdv1Δ* cells led to a two-step model for Dnm1p recruitment (Shaw and Nunnari, 2002). In this model, Fis1p acts early to recruit Dnm1p to mitochondria in an Mdv1p-independent manner. Because the Dnm1p-Fis1p complexes formed in *mdv1Δ* cells are not able to support fission, the complex must

subsequently be rearranged to include Mdv1p to allow fission (Shaw and Nunnari, 2002; Tieu et al., 2002). This model raises an important question: How does Fis1p recruit Dnm1p to mitochondria? The simplest model is that Fis1p would directly interact with Dnm1p. However, there is no evidence to support a direct interaction between Fis1p and Dnm1p.

Identification and characterization of Caf4p

In this work, we describe the identification of the Mdv1p paralog, Caf4p, as a Fis1p interacting protein and characterize its role in the formation of fission complexes. Caf4p is not required for mitochondrial fission, yet it supports low levels of fission in the absence of Mdv1p. Most importantly, Caf4p and Mdv1p share similar biochemical properties and have redundant roles as molecular adaptors between Fis1p and Dnm1p. These data indicate Fis1p recruits Dnm1p to sites of mitochondrial fission through either of two molecular adaptors, Caf4p or Mdv1p, and we propose a significant revision of the current model for mitochondrial fission.

Domain interactions within Fzo1p oligomers are required for mitochondrial fusion

In this work, we describe a structure-function and domain interaction analysis of the mitochondrial fusogen Fzo1p, which has identified three heptad repeats of Fzo1p that are required for mitochondrial fusion. We provide allelic complementation and coimmunoprecipitation data that indicate Fzo1p functions as an oligomer during mitochondrial fusion. Finally, we have identified two non-overlapping fragments, Fzo1p (HRN/GTPase) and Fzo1p (HR1/HR2), that interact with each other and can support

mitochondrial fusion when co-expressed, suggesting their interaction between these regions is critical for mitochondrial fusion.

Identification of Om14p as a regulator of mitochondrial morphology

In this chapter, we describe the identification and initial characterization of Om14p as a novel regulator of mitochondrial dynamics. Om14p interacts with Fzo1p and Ugo1p and appears to function as a negative regulator of mitochondrial fusion.

Appendix

In this appendix, we present candidate binding partners of fusion and fission molecules through tandem affinity purification MudPIT (Graumann et al., 2004; Link et al., 1999). In the fusion pathway, candidate interactors were identified for Fzo1p, Ugo1p, and Mdm30p. In the fission pathway, candidate binding partners were identified for Fis1p (Chapter 2), Mdv1p, Caf4p and Dnm1p.

REFERENCES

Alexander, C., M. Votruba, U.E. Pesch, D.L. Thiselton, S. Mayer, A. Moore, M. Rodriguez, U. Kellner, B. Leo-Kottler, G. Auburger, S.S. Bhattacharya, and B. Wissinger. 2000. OPA1, encoding a dynamin-related GTPase, is mutated in autosomal dominant optic atrophy linked to chromosome 3q28. *Nat Genet.* 26:211-5.

Altmann, K., and B. Westermann. 2005. Role of essential genes in mitochondrial morphogenesis in *Saccharomyces cerevisiae*. *Mol Biol Cell*. 16:5410–7.

Arimura, S., and N. Tsutsumi. 2002. A dynamin-like protein (ADL2b), rather than FtsZ, is involved in *Arabidopsis* mitochondrial division. *Proc Natl Acad Sci U S A*. 99:5727-31.

Arnoult, D., A. Grodet, Y.J. Lee, J. Estaquier, and C. Blackstone. 2005. Release of OPA1 during apoptosis participates in the rapid and complete release of cytochrome c and subsequent mitochondrial fragmentation. *J Biol Chem*. 280:35742–50.

Beech, P.L., T. Nheu, T. Schultz, S. Herbert, T. Lithgow, P.R. Gilson, and G.I. McFadden. 2000. Mitochondrial FtsZ in a chromophyte alga. *Science*. 287:1276–9.

Bleazard, W., J.M. McCaffery, E.J. King, S. Bale, A. Mozdy, Q. Tieu, J. Nunnari, and J.M. Shaw. 1999. The dynamin-related GTPase Dnm1 regulates mitochondrial fission in yeast. *Nat Cell Biol*. 1:298–304.

Bonifacino, J.S., and B.S. Glick. 2004. The mechanisms of vesicle budding and fusion. *Cell*. 116:153–66.

Boukh-Viner, T., T. Guo, A. Alexandrian, A. Cerracchio, C. Gregg, S. Haile, R. Kyskan, S. Milijevic, D. Oren, J. Solomon, V. Wong, J.M. Nicaud, R.A. Rachubinski, A.M. English, and V.I. Titorenko. 2005. Dynamic ergosterol- and ceramide-rich domains in the peroxisomal membrane serve as an organizing platform for peroxisome fusion. *J Cell Biol*. 168:761–73.

Cerveny, K.L., and R.E. Jensen. 2003. The WD-repeats of Net2p interact with Dnm1p and Fis1p to regulate division of mitochondria. *Mol Biol Cell*. 14:4126–39.

Cerveny, K.L., J.M. McCaffery, and R.E. Jensen. 2001. Division of mitochondria requires a novel DMN1-interacting protein, Net2p. *Mol Biol Cell*. 12:309–21.

Chen, H., A. Chomyn, and D.C. Chan. 2005. Disruption of fusion results in mitochondrial heterogeneity and dysfunction. *J Biol Chem*. 280:26185–92.

Chen, H., S.A. Detmer, A.J. Ewald, E.E. Griffin, S.E. Fraser, and D.C. Chan. 2003. Mitofusins Mfn1 and Mfn2 coordinately regulate mitochondrial fusion and are essential for embryonic development. *J Cell Biol*. 160:189–200.

Cipolat, S., O. Martins de Brito, B. Dal Zilio, and L. Scorrano. 2004. OPA1 requires mitofusin 1 to promote mitochondrial fusion. *Proc Natl Acad Sci U S A*. 101:15927–32.

Delettre, C., G. Lenaers, J.M. Griffoin, N. Gigarel, C. Lorenzo, P. Belenguer, L. Pelloquin, J. Grosgeorge, C. Turc-Carel, E. Perret, C. Astarie-Dequeker, L. Lasquellec, B. Arnaud, B. Ducommun, J. Kaplan, and C.P. Hamel. 2000. Nuclear gene OPA1, encoding a mitochondrial dynamin-related protein, is mutated in dominant optic atrophy. *Nat Genet*. 26:207–10.

Deshaies, R.J. 1999. SCF and Cullin/Ring H2-based ubiquitin ligases. *Annu Rev Cell Dev Biol*. 15:435–67.

Dimmer, K.S., S. Fritz, F. Fuchs, M. Messerschmitt, N. Weinbach, W. Neupert, and B. Westermann. 2002. Genetic basis of mitochondrial function and morphology in *Saccharomyces cerevisiae*. *Mol Biol Cell*. 13:847–53.

Dohm, J.A., S.J. Lee, J.M. Hardwick, R.B. Hill, and A.G. Gittis. 2004. Cytosolic domain of the human mitochondrial fission protein fis1 adopts a TPR fold. *Proteins*. 54:153–6.

Eckert, D.M., and P.S. Kim. 2001. Mechanisms of viral membrane fusion and its inhibition. *Annu Rev Biochem*. 70:777–810.

Eura, Y., N. Ishihara, S. Yokota, and K. Mihara. 2003. Two mitofusin proteins, mammalian homologues of FZO, with distinct functions are both required for mitochondrial fusion. *J Biochem (Tokyo)*. 134:333–44.

Fannjiang, Y., W.C. Cheng, S.J. Lee, B. Qi, J. Pevsner, J.M. McCaffery, R.B. Hill, G. Basanez, and J.M. Hardwick. 2004. Mitochondrial fission proteins regulate programmed cell death in yeast. *Genes Dev*. 18:2785–97.

Fekkes, P., K.A. Shepard, and M.P. Yaffe. 2000. Gag3p, an outer membrane protein required for fission of mitochondrial tubules. *J Cell Biol*. 151:333–40.

Frank, S., B. Gaume, E.S. Bergmann-Leitner, W.W. Leitner, E.G. Robert, F. Catez, C.L. Smith, and R.J. Youle. 2001. The role of dynamin-related protein 1, a mediator of mitochondrial fission, in apoptosis. *Dev Cell*. 1:515–25.

Fratti, R.A., Y. Jun, A.J. Merz, N. Margolis, and W. Wickner. 2004. Interdependent assembly of specific regulatory lipids and membrane fusion proteins into the vertex ring domain of docked vacuoles. *J Cell Biol*. 167:1087–98.

Fritz, S., D. Rapaport, E. Klanner, W. Neupert, and B. Westermann. 2001. Connection of the mitochondrial outer and inner membranes by Fzo1 is critical for organellar fusion. *J Cell Biol*. 152:683–92.

Fritz, S., N. Weinbach, and B. Westermann. 2003. Mdm30 is an F-box protein required for maintenance of fusion-competent mitochondria in yeast. *Mol Biol Cell*. 14:2303–13.

Fukushima, N.H., E. Brisch, B.R. Keegan, W. Bleazard, and J.M. Shaw. 2001. The GTPase effector domain sequence of the Dnm1p GTPase regulates self-assembly and controls a rate-limiting step in mitochondrial fission. *Mol Biol Cell.* 12:2756–66.

Gao, H., D. Kadirjan-Kalbach, J.E. Froehlich, and K.W. Osteryoung. 2003. ARC5, a cytosolic dynamin-like protein from plants, is part of the chloroplast division machinery. *Proc Natl Acad Sci U S A.* 100:4328–33.

Gilson, P.R., X.C. Yu, D. Hereld, C. Barth, A. Savage, B.R. Kiefel, S. Lay, P.R. Fisher, W. Margolin, and P.L. Beech. 2003. Two Dictyostelium orthologs of the prokaryotic cell division protein FtsZ localize to mitochondria and are required for the maintenance of normal mitochondrial morphology. *Eukaryot Cell.* 2:1315–26.

Graumann, J., L.A. Dunipace, J.H. Seol, W.H. McDonald, J.R. Yates, 3rd, B.J. Wold, and R.J. Deshaies. 2004. Applicability of tandem affinity purification MudPIT to pathway proteomics in yeast. *Mol Cell Proteomics*. 3:226–37.

Gray, M.W. 1999. Evolution of organellar genomes. *Curr Opin Genet Dev*. 9:678–87.

Griparic, L., N.N. van der Wel, I.J. Orozco, P.J. Peters, and A.M. van der Bliek. 2004. Loss of the intermembrane space protein Mgm1/OPA1 induces swelling and localized constrictions along the lengths of mitochondria. *J Biol Chem.* 279:18792–8.

Hales, K.G., and M.T. Fuller. 1997. Developmentally regulated mitochondrial fusion mediated by a conserved, novel, predicted GTPase. *Cell.* 90:121–9.

Herlan, M., C. Bornhovd, K. Hell, W. Neupert, and A.S. Reichert. 2004. Alternative topogenesis of Mgm1 and mitochondrial morphology depend on ATP and a functional import motor. *J Cell Biol*. 165:167–73.

Herlan, M., F. Vogel, C. Bornhovd, W. Neupert, and A.S. Reichert. 2003. Processing of Mgm1 by the rhomboid-type protease Pcp1 is required for maintenance of mitochondrial morphology and of mitochondrial DNA. *J Biol Chem*. 278:27781–8.

Hermann, G.J., E.J. King, and J.M. Shaw. 1997. The yeast gene, MDM20, is necessary for mitochondrial inheritance and organization of the actin cytoskeleton. *J Cell Biol*. 137:141–53.

Hermann, G.J., J.W. Thatcher, J.P. Mills, K.G. Hales, M.T. Fuller, J. Nunnari, and J.M. Shaw. 1998. Mitochondrial fusion in yeast requires the transmembrane GTPase Fzo1p. *J Cell Biol*. 143:359–73.

Hinshaw, J.E., and S.L. Schmid. 1995. Dynamin self-assembles into rings suggesting a mechanism for coated vesicle budding. *Nature*. 374:190–2.

Hoepfner, D., M. van den Berg, P. Philippsen, H.F. Tabak, and E.H. Hettema. 2001. A role for Vps1p, actin, and the Myo2p motor in peroxisome abundance and inheritance in *Saccharomyces cerevisiae*. *J Cell Biol*. 155:979–90.

Honda, S., T. Aihara, M. Hontani, K. Okubo, and S. Hirose. 2005. Mutational analysis of action of mitochondrial fusion factor mitofusin-2. *J Cell Sci*. 118:3153–61.

Hu, C., M. Ahmed, T.J. Melia, T.H. Sollner, T. Mayer, and J.E. Rothman. 2003. Fusion of cells by flipped SNAREs. *Science*. 300:1745–9.

Ingerman, E., E.M. Perkins, M. Marino, J.A. Mears, J.M. McCaffery, J.E. Hinshaw, and J. Nunnari. 2005. Dnm1 forms spirals that are structurally tailored to fit mitochondria. *J Cell Biol*. 170:1021–7.

Ishihara, N., Y. Eura, and K. Mihara. 2004. Mitofusin 1 and 2 play distinct roles in mitochondrial fusion reactions via GTPase activity. *J Cell Sci*. 117:6535–46.

Ishihara, N., A. Jofuku, Y. Eura, and K. Mihara. 2003. Regulation of mitochondrial morphology by membrane potential, and DRP1-dependent division and FZO1-dependent fusion reaction in mammalian cells. *Biochem Biophys Res Commun*. 301:891–8.

Ivanovska, I., and J.M. Hardwick. 2005. Viruses activate a genetically conserved cell death pathway in a unicellular organism. *J Cell Biol*. 170:391–9.

Jagasia, R., P. Grote, B. Westermann, and B. Conradt. 2005. DRP-1-mediated mitochondrial fragmentation during EGL-1-induced cell death in *C. elegans*. *Nature*. 433:754–60.

Karbowski, M., D. Arnoult, H. Chen, D.C. Chan, C.L. Smith, and R.J. Youle. 2004. Quantitation of mitochondrial dynamics by photolabeling of individual organelles shows that mitochondrial fusion is blocked during the Bax activation phase of apoptosis. *J Cell Biol*. 164:493–9.

Kato, M., and W. Wickner. 2001. Ergosterol is required for the Sec18/ATP-dependent priming step of homotypic vacuole fusion. *Embo J*. 20:4035–40.

Kiessling, J., S. Kruse, S.A. Rensing, K. Harter, E.L. Decker, and R. Reski. 2000. Visualization of a cytoskeleton-like FtsZ network in chloroplasts. *J Cell Biol*. 151:945–50.

Kijima, K., C. Numakura, H. Izumino, K. Umetsu, A. Nezu, T. Shiiki, M. Ogawa, Y. Ishizaki, T. Kitamura, Y. Shozawa, and K. Hayasaka. 2005. Mitochondrial GTPase mitofusin 2 mutation in Charcot-Marie-Tooth neuropathy type 2A. *Hum Genet*. 116:23–7.

Koch, A., G. Schneider, G.H. Luers, and M. Schrader. 2004. Peroxisome elongation and constriction but not fission can occur independently of dynamin-like protein 1. *J Cell Sci*. 117:3995–4006.

Koch, A., M. Thiemann, M. Grabenbauer, Y. Yoon, M.A. McNiven, and M. Schrader. 2003. Dynamin-like protein 1 is involved in peroxisomal fission. *J Biol Chem*. 278:8597–605.

Koch, A., Y. Yoon, N.A. Bonekamp, M.A. McNiven, and M. Schrader. 2005. A role for Fis1 in both mitochondrial and peroxisomal fission in mammalian cells. *Mol Biol Cell*. 16:5077–86.

Koshiba, T., S.A. Detmer, J.T. Kaiser, H. Chen, J.M. McCaffery, and D.C. Chan. 2004. Structural basis of mitochondrial tethering by mitofusin complexes. *Science*. 305:858–62.

Labrousse, A.M., M.D. Zappaterra, D.A. Rube, and A.M. van der Bliek. 1999. *C. elegans* dynamin-related protein DRP-1 controls severing of the mitochondrial outer membrane. *Mol Cell*. 4:815–26.

Lawson, V.H., B.V. Graham, and K.M. Flanigan. 2005. Clinical and electrophysiologic features of CMT2A with mutations in the mitofusin 2 gene. *Neurology*. 65:197–204.

Legesse-Miller, A., R.H. Massol, and T. Kirchhausen. 2003. Constriction and Dnm1p recruitment are distinct processes in mitochondrial fission. *Mol Biol Cell*. 14:1953–63.

Legros, F., A. Lombes, P. Frachon, and M. Rojo. 2002. Mitochondrial fusion in human cells is efficient, requires the inner membrane potential, and is mediated by mitofusins. *Mol Biol Cell*. 13:4343–54.

Legros, F., F. Malka, P. Frachon, A. Lombes, and M. Rojo. 2004. Organization and dynamics of human mitochondrial DNA. *J Cell Sci*. 117:2653–62.

Lehninger, A.L. 1965. *The Mitochondrion*. W. A. Benjamin, Inc., New York. 263 pp.

Li, X., and S.J. Gould. 2003. The dynamin-like GTPase DLP1 is essential for peroxisome division and is recruited to peroxisomes in part by PEX11. *J Biol Chem*. 278:17012–20.

Link, A.J., J. Eng, D.M. Schieltz, E. Carmack, G.J. Mize, D.R. Morris, B.M. Garvik, and J.R. Yates, 3rd. 1999. Direct analysis of protein complexes using mass spectrometry. *Nat Biotechnol*. 17:676–82.

Malka, F., O. Guillery, C. Cifuentes-Diaz, E. Guillou, P. Belenguer, A. Lombes, and M. Rojo. 2005. Separate fusion of outer and inner mitochondrial membranes. *EMBO Rep*. 6:853–9.

Margolin, W. 2005. FtsZ and the division of prokaryotic cells and organelles. *Nat Rev Mol Cell Biol*. 6:862–71.

Marks, B., M.H. Stowell, Y. Vallis, I.G. Mills, A. Gibson, C.R. Hopkins, and H.T. McMahon. 2001. GTPase activity of dynamin and resulting conformation change are essential for endocytosis. *Nature*. 410:231–5.

Mattenberger, Y., D.I. James, and J.C. Martinou. 2003. Fusion of mitochondria in mammalian cells is dependent on the mitochondrial inner membrane potential and independent of microtubules or actin. *FEBS Lett*. 538:53–9.

McAndrew, R.S., J.E. Froehlich, S. Vitha, K.D. Stokes, and K.W. Osteryoung. 2001. Colocalization of plastid division proteins in the chloroplast stromal compartment establishes a new functional relationship between FtsZ1 and FtsZ2 in higher plants. *Plant Physiol*. 127:1656–66.

McNew, J.A., F. Parlati, R. Fukuda, R.J. Johnston, K. Paz, F. Paumet, T.H. Sollner, and J.E. Rothman. 2000. Compartmental specificity of cellular membrane fusion encoded in SNARE proteins. *Nature*. 407:153–9.

McQuibban, G.A., S. Saurya, and M. Freeman. 2003. Mitochondrial membrane remodelling regulated by a conserved rhomboid protease. *Nature*. 423:537-41.

Meeusen, S., J.M. McCaffery, and J. Nunnari. 2004. Mitochondrial fusion intermediates revealed in vitro. *Science*. 305:1747–52.

Miyagishima, S.Y., K. Nishida, T. Mori, M. Matsuzaki, T. Higashiyama, H. Kuroiwa, and T. Kuroiwa. 2003. A plant-specific dynamin-related protein forms a ring at the chloroplast division site. *Plant Cell*. 15:655–65.

Mozdy, A.D., J.M. McCaffery, and J.M. Shaw. 2000. Dnm1p GTPase-mediated mitochondrial fission is a multi-step process requiring the novel integral membrane component Fis1p. *J Cell Biol*. 151:367–80.

Neutzner, A., and R.J. Youle. 2005. Instability of the mitofusin Fzo1 regulates mitochondrial morphology during the mating response of the yeast *Saccharomyces cerevisiae*. *J Biol Chem*. 280:18598–603.

Nishida, K., M. Takahara, S.Y. Miyagishima, H. Kuroiwa, M. Matsuzaki, and T. Kuroiwa. 2003. Dynamic recruitment of dynamin for final mitochondrial severance in a primitive red alga. *Proc Natl Acad Sci U S A*. 100:2146–51.

Nunnari, J., W.F. Marshall, A. Straight, A. Murray, J.W. Sedat, and P. Walter. 1997. Mitochondrial transmission during mating in *Saccharomyces cerevisiae* is determined by mitochondrial fusion and fission and the intramitochondrial segregation of mitochondrial DNA. *Mol Biol Cell*. 8:1233–42.

Olichon, A., L.J. Emorine, E. Descoins, L. Pelloquin, L. Brichese, N. Gas, E. Guillou, C. Delettre, A. Valette, C.P. Hamel, B. Ducommun, G. Lenaers, and P. Belenguer. 2002. The human dynamin-related protein OPA1 is anchored to the mitochondrial inner membrane facing the inter-membrane space. *FEBS Lett*. 523:171-6.

Osteryoung, K.W., and J. Nunnari. 2003. The division of endosymbiotic organelles. *Science*. 302:1698–704.

Osteryoung, K.W., K.D. Stokes, S.M. Rutherford, A.L. Percival, and W.Y. Lee. 1998. Chloroplast division in higher plants requires members of two functionally divergent gene families with homology to bacterial ftsZ. *Plant Cell*. 10:1991–2004.

Parlati, F., J.A. McNew, R. Fukuda, R. Miller, T.H. Sollner, and J.E. Rothman. 2000. Topological restriction of SNARE-dependent membrane fusion. *Nature*. 407:194–8.

Praefcke, G.J., and H.T. McMahon. 2004. The dynamin superfamily: universal membrane tubulation and fission molecules? *Nat Rev Mol Cell Biol*. 5:133–47.

Rapaport, D., M. Brunner, W. Neupert, and B. Westermann. 1998. Fzo1p is a mitochondrial outer membrane protein essential for the biogenesis of functional mitochondria in *Saccharomyces cerevisiae*. *J Biol Chem*. 273:20150–5.

Rojo, M., F. Legros, D. Chateau, and A. Lombes. 2002. Membrane topology and mitochondrial targeting of mitofusins, ubiquitous mammalian homologs of the transmembrane GTPase Fzo. *J Cell Sci*. 115:1663–74.

Satoh, M., T. Hamamoto, N. Seo, Y. Kagawa, and H. Endo. 2003. Differential sublocalization of the dynamin-related protein OPA1 isoforms in mitochondria. *Biochem Biophys Res Commun*. 300:482–93.

Sesaki, H., and R.E. Jensen. 1999. Division versus fusion: Dnm1p and Fzo1p antagonistically regulate mitochondrial shape. *J Cell Biol*. 147:699–706.

Sesaki, H., and R.E. Jensen. 2001. UGO1 encodes an outer membrane protein required for mitochondrial fusion. *J Cell Biol*. 152:1123–34.

Sesaki, H., and R.E. Jensen. 2004. Ugo1p links the Fzo1p and Mgm1p GTPases for mitochondrial fusion. *J Biol Chem*. 279:28298–303.

Sesaki, H., S.M. Southard, A.E. Hobbs, and R.E. Jensen. 2003a. Cells lacking Pcp1p/Ugo2p, a rhomboid-like protease required for Mgm1p processing, lose mtDNA and mitochondrial structure in a Dnm1p-dependent manner, but remain competent for mitochondrial fusion. *Biochem Biophys Res Commun*. 308:276–83.

Sesaki, H., S.M. Southard, M.P. Yaffe, and R.E. Jensen. 2003b. Mgm1p, a dynamin-related GTPase, is essential for fusion of the mitochondrial outer membrane. *Mol Biol Cell*. 14:2342–56.

Sever, S., H. Damke, and S.L. Schmid. 2000. Dynamin:GTP controls the formation of constricted coated pits, the rate limiting step in clathrin-mediated endocytosis. *J Cell Biol.* 150:1137–48.

Sever, S., A.B. Muhlberg, and S.L. Schmid. 1999. Impairment of dynamin's GAP domain stimulates receptor-mediated endocytosis. *Nature*. 398:481–6.

Shaw, J.M., and J. Nunnari. 2002. Mitochondrial dynamics and division in budding yeast. *Trends Cell Biol.* 12:178–84.

Sheahan, M.B., D.W. McCurdy, and R.J. Rose. 2005. Mitochondria as a connected population: ensuring continuity of the mitochondrial genome during plant cell dedifferentiation through massive mitochondrial fusion. *Plant J.* 44:744–55.

Shepard, K.A., and M.P. Yaffe. 1999. The yeast dynamin-like protein, Mgm1p, functions on the mitochondrial outer membrane to mediate mitochondrial inheritance. *J Cell Biol.* 144:711–20.

Skehel, J.J., and D.C. Wiley. 1998. Coiled coils in both intracellular vesicle and viral membrane fusion. *Cell*. 95:871–4.

Smirnova, E., D.L. Shurland, S.N. Ryazantsev, and A.M. van der Bliek. 1998. A human dynamin-related protein controls the distribution of mitochondria. *J Cell Biol.* 143:351–8.

Stowell, M.H., B. Marks, P. Wigge, and H.T. McMahon. 1999. Nucleotide-dependent conformational changes in dynamin: evidence for a mechanochemical molecular spring. *Nat Cell Biol.* 1:27–32.

Sutton, R.B., D. Fasshauer, R. Jahn, and A.T. Brunger. 1998. Crystal structure of a SNARE complex involved in synaptic exocytosis at 2.4 A resolution. *Nature*. 395:347–53.

Suzuki, M., S.Y. Jeong, M. Karbowski, R.J. Youle, and N. Tjandra. 2003. The solution structure of human mitochondria fission protein Fis1 reveals a novel TPR-like helix bundle. *J Mol Biol*. 334:445–58.

Suzuki, M., A. Neutzner, N. Tjandra, and R.J. Youle. 2005. Novel structure of the N terminus in yeast Fis1 correlates with a specialized function in mitochondrial fission. *J Biol Chem*. 280:21444–52.

Sweitzer, S.M., and J.E. Hinshaw. 1998. Dynamin undergoes a GTP-dependent conformational change causing vesiculation. *Cell*. 93:1021–9.

Takei, K., P.S. McPherson, S.L. Schmid, and P. De Camilli. 1995. Tubular membrane invaginations coated by dynamin rings are induced by GTP-gamma S in nerve terminals. *Nature*. 374:186–90.

Tieu, Q., and J. Nunnari. 2000. Mdv1p is a WD repeat protein that interacts with the dynamin-related GTPase, Dnm1p, to trigger mitochondrial division. *J Cell Biol*. 151:353–66.

Tieu, Q., V. Okreglak, K. Naylor, and J. Nunnari. 2002. The WD repeat protein, Mdv1p, functions as a molecular adaptor by interacting with Dnm1p and Fis1p during mitochondrial fission. *J Cell Biol*. 158:445–52.

Ungar, D., and F.M. Hughson. 2003. SNARE protein structure and function. *Annu Rev Cell Dev Biol*. 19:493–517.

Urban, S., J.R. Lee, and M. Freeman. 2001. *Drosophila* rhomboid-1 defines a family of putative intramembrane serine proteases. *Cell*. 107:173–82.

van der Bliek, A.M. 2000. A mitochondrial division apparatus takes shape. *J Cell Biol*. 151:F1–4.

Verstreken, P., C.V. Ly, K.J. Venken, T.W. Koh, Y. Zhou, and H.J. Bellen. 2005. Synaptic mitochondria are critical for mobilization of reserve pool vesicles at *Drosophila* neuromuscular junctions. *Neuron*. 47:365–78.

Vitha, S., R.S. McAndrew, and K.W. Osteryoung. 2001. FtsZ ring formation at the chloroplast division site in plants. *J Cell Biol*. 153:111–20.

Warnock, D.E., J.E. Hinshaw, and S.L. Schmid. 1996. Dynamin self-assembly stimulates its GTPase activity. *J Biol Chem*. 271:22310–4.

Weber, T., B.V. Zemelman, J.A. McNew, B. Westermann, M. Gmachl, F. Parlati, T.H. Sollner, and J.E. Rothman. 1998. SNAREpins: minimal machinery for membrane fusion. *Cell*. 92:759–72.

Wong, E.D., J.A. Wagner, S.V. Scott, V. Okreglak, T.J. Holewinske, A. Cassidy-Stone, and J. Nunnari. 2003. The intramitochondrial dynamin-related GTPase, Mgm1p, is a component of a protein complex that mediates mitochondrial fusion. *J Cell Biol*. 160:303–11.

Yoon, Y., K.R. Pitts, and M.A. McNiven. 2001. Mammalian dynamin-like protein DLP1 tubulates membranes. *Mol Biol Cell*. 12:2894–905.

Zhang, P., and J.E. Hinshaw. 2001. Three-dimensional reconstruction of dynamin in the constricted state. *Nat Cell Biol*. 3:922–6.

Zuchner, S., I.V. Mersiyanova, M. Muglia, N. Bissar-Tadmouri, J. Rochelle, E.L. Dadali, M. Zappia, E. Nelis, A. Patitucci, J. Senderek, Y. Parman, O. Evgrafov, P.D. Jonghe, Y. Takahashi, S. Tsuji, M.A. Pericak-Vance, A. Quattrone, E. Battaloglu, A.V. Polyakov, V. Timmerman, J.M. Schroder, and J.M. Vance. 2004. Mutations in the mitochondrial GTPase mitofusin 2 cause Charcot-Marie-Tooth neuropathy type 2A. *Nat Genet*. 36:449–51.

FIGURE LEGENDS

Figure 1. The mitochondrial fusion complex in yeast. Fzo1p spans the outer membrane twice, placing the GTPase domain (green ellipse) and three heptad repeats (blue rods) in position to mediate important steps during fusion. The long and short isoforms of the dynamin-related GTPase Mgm1p are located in the intermembrane space and differ in the presence of an N-terminal transmembrane region. Ugo1p interacts with both Fzo1p and Mgm1p, and may help coordinate their activities. The mitofusins and OPA1 are the mammalian orthologs of *FZO1* and *MGM1*. Mitofusins contain HR1 and HR2 but lack the most N-terminal hydrophobic heptad repeat. No mammalian ortholog of *UGO1* has been identified.

Figure 1.

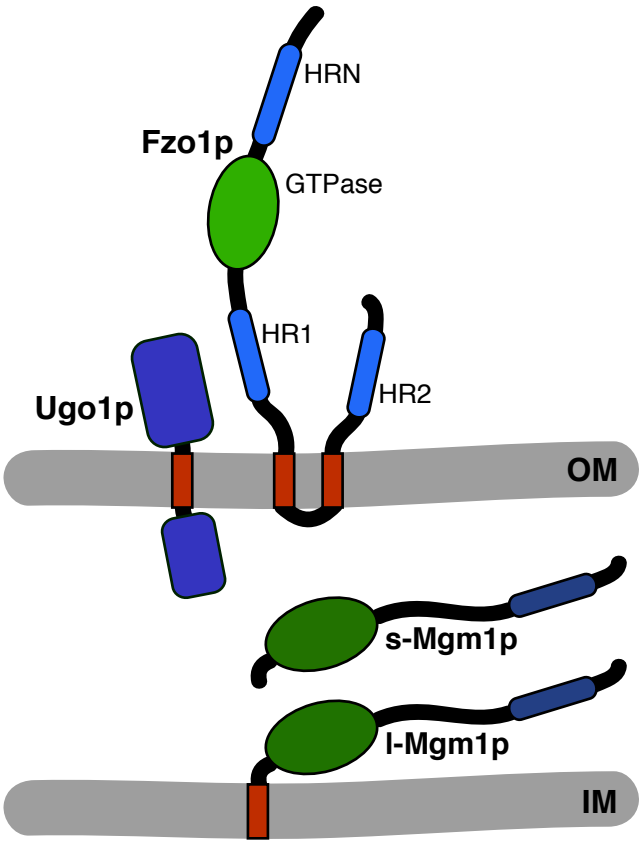

Chapter 2

The WD40 protein Caf4p is a component of the mitochondrial fission machinery and recruits Dnm1p to mitochondria

Erik E. Griffin, Johannes Graumann, David C. Chan

This chapter has been published in the *Journal of Cell Biology* (2005) 170: 237–248. Johannes Graumann is a graduate student in Ray Deshaies' lab at Caltech where he performed the MudPIT analysis described in this paper.

The WD40 protein Caf4p is a component of the mitochondrial fission machinery and recruits Dnm1p to mitochondria

Erik E. Griffin, Johannes Graumann, and David C. Chan

Division of Biology, California Institute of Technology, Pasadena, CA 91125

The mitochondrial division machinery regulates mitochondrial dynamics and consists of Fis1p, Mdv1p, and Dnm1p. Mitochondrial division relies on the recruitment of the dynamin-related protein Dnm1p to mitochondria. Dnm1p recruitment depends on the mitochondrial outer membrane protein Fis1p. Mdv1p interacts with Fis1p and Dnm1p, but is thought to act at a late step during fission because Mdv1p is dispensable for Dnm1p localization. We identify the WD40 repeat protein Caf4p as a Fis1p-associated protein that localizes to mitochondria in a Fis1p-dependent manner. Caf4p interacts with each component of the fission apparatus: with Fis1p and Mdv1p through its NH_2-terminal half and with Dnm1p through its COOH-terminal WD40 domain. We demonstrate that *mdv1Δ* yeast contain residual mitochondrial fission due to the redundant activity of Caf4p. Moreover, recruitment of Dnm1p to mitochondria is disrupted in *mdv1Δ caf4Δ* yeast, demonstrating that Mdv1p and Caf4p are molecular adaptors that recruit Dnm1p to mitochondrial fission sites. Our studies support a revised model for assembly of the mitochondrial fission apparatus.

Introduction

Mitochondria are dynamic organelles that undergo fusion and fission. These processes intermix the mitochondria within cells and control their morphology. In addition to controlling mitochondrial shape, recent studies have also implicated components of the fission machinery in regulation of programmed cell death (Frank et al., 2001; Fannjiang et al., 2004; Jagasia et al., 2005). Genetic approaches in *Saccharomyces cerevisiae* have identified *DNM1*, *FIS1*, and *MDV1* as components of the mitochondrial fission pathway (Shaw and Nunnari, 2002). Dnm1p and its mammalian homologue Drp1 are members of the extensively studied dynamin family of large, oligomeric GTPases. Although the precise mechanism remains controversial, dynamins may couple GTP hydrolysis to a conformational constriction that causes membrane scission (Praefcke and McMahon, 2004). In yeast cells, Dnm1p dynamically localizes to dozens of puncta that are primarily associated with mitochondria (Otsuga et al., 1998; Bleazard et al., 1999; Sesaki and Jensen, 1999; Legesse-Miller et al., 2003). A subset of these puncta are sites of future fission.

The assembly of functional Dnm1p complexes on mitochondria is a critical issue in understanding the mechanism of mitochondrial fission. The mitochondrial outer membrane protein Fis1p is required for the formation of normal Dnm1p puncta on mitochondria. In *fis1Δ* cells, Dnm1p puncta are primarily cytosolic or form abnormally large aggregates on mitochondria (Fekkes et al., 2000; Mozdy et al., 2000; Tieu and Nunnari, 2000). Mdv1p interacts with Fis1p through its NH_2-terminal half and with Dnm1p through its COOH-terminal WD40 domain. However, Mdv1p appears dispensable for Dnm1p assembly on mitochondria because *mdv1Δ* cells show little or no change in Dnm1p localization, even though mitochondrial fission is disrupted (Fekkes et al., 2000; Tieu and Nunnari, 2000; Tieu et al., 2002; Cerveny and Jensen, 2003). These observations have led to two important features of a recently proposed model for mitochondrial fission (Shaw and Nunnari, 2002; Tieu et al., 2002; Osteryoung and Nunnari, 2003). First, Fis1p acts to assemble and distribute Dnm1p on mitochondria in an Mdv1p-independent step. Second, Mdv1p acts downstream of Dnm1p localization to stimulate membrane scission. An alternative model proposes that Dnm1p marks the site of mitochondrial fission and recruits Fis1p and Mdv1p into an active fission complex (Cerveny and Jensen, 2003). Again, in this model Mdv1p functions downstream of Dnm1p localization.

Correspondence to David C. Chan: dchan@caltech.edu

Abbreviations used in this paper: CC, coiled coil; MudPIT, multidimensional protein identification technology; NTE, NH_2-terminal extension; TEV, tobacco etch virus; UTR, untranslated region.

The online version of this article includes supplemental material.

© The Rockefeller University Press $8.00
The Journal of Cell Biology, Vol. 170, No. 2, July 18, 2005 237–248
http://www.jcb.org/cgi/doi/10.1083/jcb.200503148

Supplemental Material can be found at:
http://www.jcb.org/cgi/content/full/jcb.200503148/DC1

THE JOURNAL OF CELL BIOLOGY

Downloaded from www.jcb.org on April 13, 2006

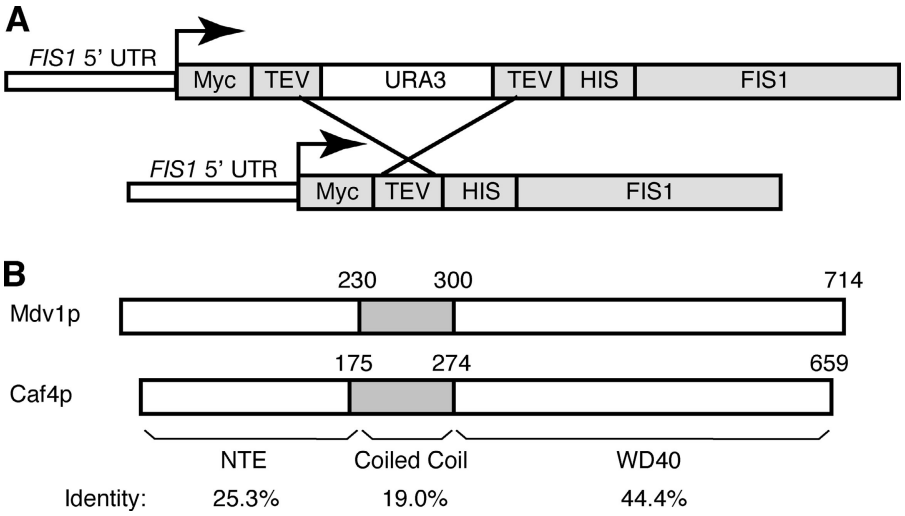

Figure 1. **Construction of M_9TH-*FIS1* and Caf4p/Mdv1p alignment.** (A) A 9xMyc-TEV-*URA3*-TEV-His_8 cassette was PCR amplified with *FIS1*-targeting primers and integrated in-frame into the NH_2 terminus of *FIS1*. Pop-out of the *URA3* cassette by recombination between flanking TEV sites yielded M_9TH-*FIS1* under the control of the endogenous *FIS1* promoter. UTR: untranslated region. (B) Schematic of Mdv1p and Caf4p. The NH_2-terminal extension (NTE), coiled-coil, and WD40 regions are shown with percent identity. Overall identity is 37% and overall similarity is 57%.

Despite extensive efforts, however, there is no evidence that Fis1p can interact directly with Dnm1p. We speculated that there may be an additional component of the mitochondrial fission pathway required for the Fis1p-dependent assembly of Dnm1p puncta on mitochondria. Because a genome-wide screen for mitochondrial morphology mutants (Dimmer et al., 2002) did not yield obvious candidates, we used a biochemical approach to identify additional components of the mitochondrial fission machinery. Using immunopurification and mass spectrometry, we have identified the WD40 repeat protein Caf4p as a Fis1p-interacting protein. Caf4p localizes to mitochondria and associates with Fis1p, Mdv1p, and Dnm1p. Moreover, we show that *mdv1Δ* cells are only partially deficient in mitochondrial fission due to the redundant activity of Caf4p. Importantly, Caf4p mediates recruitment of Dnm1p puncta to mitochondria in *mdv1Δ* yeast. Inclusion of *CAF4* significantly clarifies the current models for mitochondrial fission.

Results

Caf4p is associated with Fis1p

To identify Fis1p-associated proteins by multidimensional protein identification technology (MudPIT) (Link et al., 1999; Graumann et al., 2004), we constructed a yeast strain containing endogenous Fis1p with an NH_2-terminal tandem affinity tag (Fig. 1 A). NH_2-terminal tagging is necessary because *FIS1* is nonfunctional when COOH-terminally tagged (unpublished data). We first designed a recombination cassette containing 9XMyc/TEV/*URA3*/TEV/His_8 modules (Fig. 1 A). After targeted integration into the *FIS1* locus, spontaneous and precise recombination between the flanking ~50-bp tobacco etch virus (TEV) protease sites excises *URA3*. This strategy was used to generate a yeast strain (DCY1557) that expresses a functional Fis1p with an NH_2-terminal 9XMyc/TEV/His_8 tag (M_9TH-Fis1p) from the endogenous locus.

Tandem affinity-purified M_9TH-Fis1p was subjected to MudPIT analysis in two independent experiments (see Materials and methods). Fis1p was identified in both experiments (61.3% coverage, 14 unique peptides; 58.7% coverage, 9 unique peptides). Mdv1p, a previously identified member of the mitochondrial fission pathway and a known Fis1p-interacting protein, was also identified in both experiments (22.1% coverage, 12 unique peptides; 10.2% coverage, 5 unique peptides). These data confirmed that our MudPIT procedure could preserve and identify Fis1p complexes relevant to mitochondrial fission. Dnm1p was not observed in either dataset, in agreement with previous immunoprecipitation experiments (Mozdy et al., 2000). The complete datasets are presented in Table S1 (available at http://www.jcb.org/cgi/content/full/jcb.200503148/DC1).

Interestingly, peptides derived from the WD40 repeat protein Caf4p were identified in both Fis1p MudPIT experiments (24.4% coverage, 9 unique peptides; 8.5% coverage, 3 unique peptides). *CAF4* (YKR036C) was first identified in a yeast two-hybrid screen for CCR4p-interacting proteins (Liu et al., 2001). CCR4p is a central component of the CCR4-NOT transcriptional regulator and cytosolic deadenylase complex (Denis and Chen, 2003). Caf4p is the nearest homologue of Mdv1p in *S. cerevisiae* (38% identity and 57% similarity), and the two proteins show extensive sequence identity throughout their lengths (Fig. 1 B). Both proteins share a unique NH_2-terminal extension (NTE) (25.3% identity), a central coiled-coil (CC) domain (19% identity) and a COOH-terminal WD40 repeat domain (44.4% identity). The Caf4p CC scores significantly more weakly (~0.3 probability) than the Mdv1p coiled coil (~1.0 probability) in the MultiCoil prediction program (Wolf et al., 1997).

Caf4p interacts with components of the mitochondrial fission machinery

We sought independent confirmation of the physical interaction between Fis1p and Caf4p. For immunoprecipitation experiments, Caf4p-HA or Mdv1p-HA were expressed from their endogenous promoters in strains carrying chromosomal M_3TH-*FIS1* (3XMyc/TEV/His_8-*FIS1*) and deleted for *CAF4* or *MDV1*, respectively. When M_3TH-Fis1p was immunoprecipitated, ~5% of both Caf4p-HA and Mdv1p-HA coprecipitated (Fig. 2 A, lanes 7 and 10).

Downloaded from www.jcb.org on April 13, 2006

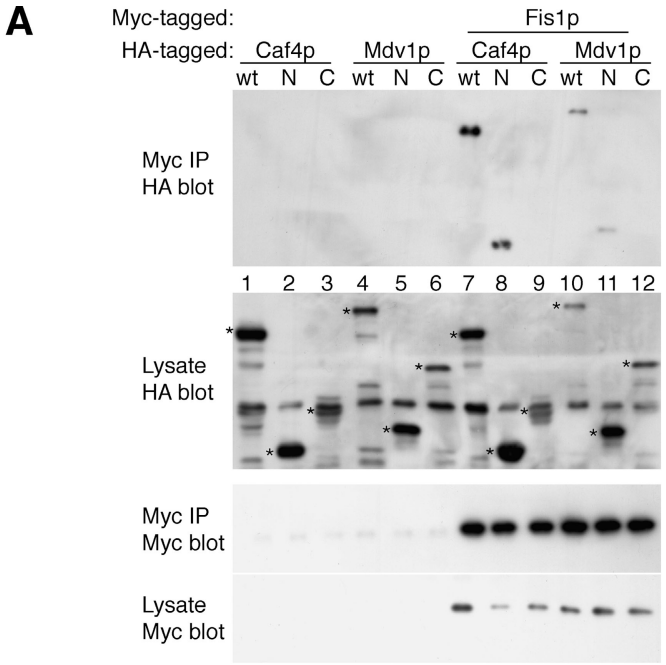

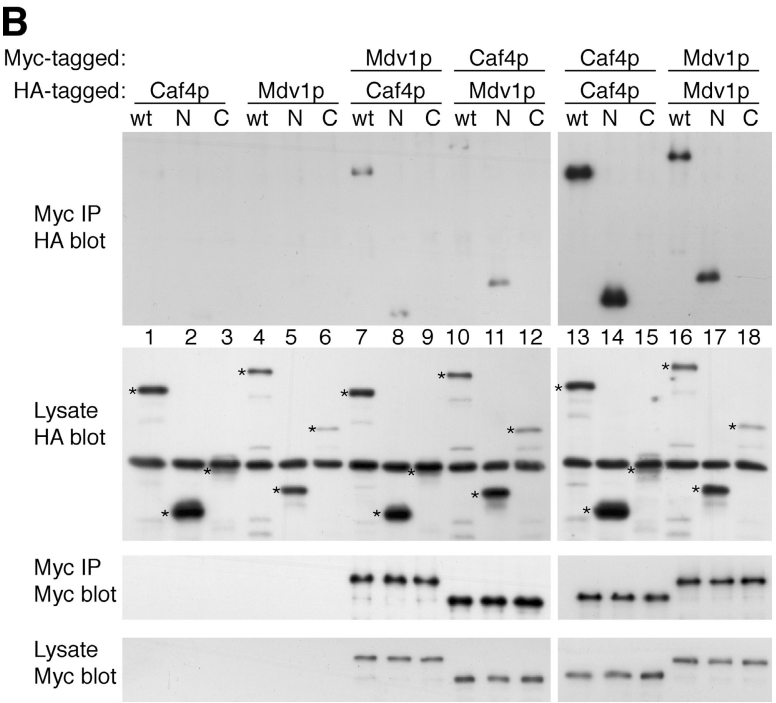

Figure 2. **Caf4p and Mdv1p coimmunoprecipitation experiments.** (A) Yeast carrying the indicated HA- and Myc-tagged constructs were lysed and immunoprecipitated with an anti-Myc antibody. Total lysates (labeled "Lysate") and immunoprecipitated samples (labeled "Myc IP") were analyzed by immunoblotting with anti-Myc (9E10) and anti-HA (12CA5) antibodies as indicated. The expression constructs were: Caf4p wt (residues 1–659), Caf4p N (residues 1–274), Caf4p C (residues 275–659), Mdv1 wt (residues 1–714), Mdv1p N (residues 1–300), and Mdv1p C (residues 301–714). The yeast backgrounds were: (A) wild-type, lanes 1–6; *caf4Δ* M_3TH-*FIS1*, lanes 7–9; *mdv1Δ* M_3TH-*FIS1*, lanes 10–12; (B) wild-type, lanes 1–6; *caf4Δ MDV1*-HTM, lanes 7–9; *mdv1Δ CAF4*-HTM, lanes 10–12; *CAF4*-HTM, lanes 13–15; *MDV1*-HTM, lanes 16–18. (B) Yeast carrying the indicated HA- and Myc-tagged constructs were immunoprecipitated and analyzed as in A. Immunoprecipitated samples were loaded at 10 (A) and 20 (B) equivalents of the lysate samples. HA-tagged proteins in the lysate are marked with an asterisk. The HA-tagged Caf4p C polypeptide comigrates with a background band in the total lysate blot probed with HA antibody.

Previous yeast two-hybrid analysis determined that the NTE/CC region of Mdv1p (residues 1–300) is responsible for its interaction with Fis1p (Tieu et al., 2002). We detected the same interaction by coimmunoprecipitation (Fig. 2 A, lane 11). Additionally, we found that the analogous region of Caf4p (residues 1–274) also interacted with Fis1p (Fig. 2 A, lane 8). A shorter Caf4p fragment lacking the majority of the predicted coiled coil (residues 1–250) interacted equally well with Fis1p (unpublished data). In contrast, Fis1p did not bind to the COOH-terminal regions of either Mdv1p or Caf4p (Fig. 2 A, lanes 9 and 12). These data suggest that both Caf4p and Mdv1p likely interact with Fis1p through a common mechanism involving the NTE domain.

We also used a yeast two-hybrid assay to analyze the interaction of Caf4p and Mdv1p with Fis1p and Dnm1p (Table I). Full-length Caf4p and an NTE/CC fragment of Caf4p interacted strongly with the cytosolic portion of Fis1p (residues 1–128), consistent with our immunoprecipitation data. Similar interactions were observed between Fis1p and both full-length Mdv1p and the NTE/CC region of Mdv1p, as has been previ-

Downloaded from www.jcb.org on April 13, 2006

Table I. **Caf4p and Mdv1p interact with Dnm1p and Fis1p in a yeast two-hybrid assay**

				Caf4p			Mdv1p		
		Fis1p	Dnm1p	wt	N	C	wt	N	C
Fis1p		−	−	+	+	−	+	+	−
Dnm1p		−	+	−	−	−	−	−	−
Caf4p	wt	+	−	−	−	−	−	weak	−
	N	+	−	−	−	−	−	−	−
	C	−	+	−	−	−	−	−	−
Mdv1p	wt	+	+	−	+	−	+	+	−
	N	+	−	−	+	−	+	+	−
	C	−	+	−	−	−	−	−	−

Caf4p, Mdv1p, Fis1p, and Dnm1p fragments were scored for growth (+), no growth (−), or poor growth (weak) on adenine-deficient plates. All constructs showed no growth when paired with empty activation domain or DNA-binding domain vector. Binding domain fusions are listed across the top of the table and activation domain fusions are listed down the left. Caf4p and Mdv1p N and C fragments are defined in Fig. 2.

ously reported (Tieu et al., 2002; Cerveny and Jensen, 2003). The WD40 domain of both Mdv1p and Caf4p interacted strongly with Dnm1p. However, full-length Mdv1p interacted more weakly and an interaction between full-length Caf4p and Dnm1p was not detected. These results suggest that the interaction of the WD40 domain with Dnm1p is regulated and may be inhibited by the NH_2-terminal region of Caf4p and Mdv1p.

We also detected homotypic and heterotypic interactions between Caf4p and Mdv1p. Approximately 5% of Caf4p-HA and Caf4p-N-HA (residues 1–274), but not Caf4-C-HA (residues 275–659), coimmunoprecipitate with full-length Caf4p-HTM (Fig. 2 B, lanes 13–15). A similar level of Mdv1p-HA and Mdv1p-N-HA (residues 1–300), but not Mdv1-C-HA (residues 301–714), coimmunoprecipitated with Mdv1p-HTM (Fig. 2 B, lanes 16–18). When Caf4p-HTM was precipitated, ~1% of Mdv1p-HA and Mdv1p-N-HA, but not Mdv1p-C-HA, coprecipitated (Fig. 2 B, lanes 10–12). Similarly, when Mdv1p-HTM was precipitated, ~1% of Caf4p-HA and Caf4p-N-HA, but not Caf4p-C-HA, coprecipitated (Fig. 2 B, lanes 7–9). Moreover, the NTE/CC regions of Caf4p and Mdv1p interact in the two-hybrid assay (Table I). Therefore, Caf4p interacts with all three members of the fission pathway, with the NH_2-terminal region mediating interactions with Fis1p, Mdv1p, and homotypic interactions with Caf4p.

Caf4p is involved in mitochondrial division

Given that Caf4p interacts with Fis1p, Mdv1p, and Dnm1p, we hypothesized that Caf4p, like Mdv1p, is a component of the mitochondrial division apparatus. *caf4Δ* yeast, however, display normal mitochondrial morphology, with tubular mitochondria evenly dispersed around the cell cortex (Fig. 3). Wild-type mitochondrial morphology was also observed at elevated temperatures and on carbon sources other than dextrose (glycerol or galactose; unpublished data). This observation is not surprising, given that *CAF4* was not identified in a genome-wide screen of deletion strains for mitochondrial morphology mutants (Dimmer et al., 2002).

We next tested whether *caf4Δ* cells show synthetic defects in mitochondrial morphology when other components of the

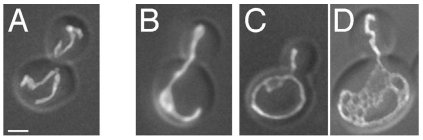

Genotype	Wild-type	Collapsed net	Spread net
Wild-type	100	0	0
caf4Δ	100	0	0
mdv1Δ	0	45.5	54.5
dnm1Δ	0	90	10
fis1Δ	0	92.5	7.5
mdv1Δ caf4Δ	0	91.5	8.5
mdv1Δ dnm1Δ	0	91.5	8.5

Figure 3. **CAF4 regulates mitochondrial morphology.** Strains expressing mitochondrially targeted GFP were grown in YP dextrose to mid-log phase and fixed. The percentage of cells (n = 400) with mitochondria having wild-type (A), collapsed net (B), or spread net morphology (C and D) is tabulated. The spread net phenotype encompasses a distribution of morphologies ranging from simple structures containing one or two loops (C) to complexly fenestrated mitochondria with dozens of loops (D). For both wild-type and *caf4Δ* strains, the wild-type category includes 1% fragmented cells. Bar, 1 μm.

fission machinery are deleted. Yeast defective in mitochondrial fission display net-like mitochondrial morphology due to unopposed mitochondrial fusion (Bleazard et al., 1999; Sesaki and Jensen, 1999). These mitochondrial nets can have a spread morphology (Fig. 3, C and D), or they can collapse to one side of the cell (Fig. 3 B). Although *FIS1*, *DNM1*, and *MDV1* are all involved in mitochondrial fission, we found that *mdv1Δ* cells have a distribution of mitochondrial profiles that can be readily distinguished from both *fis1Δ* and *dnm1Δ* cells (Fig. 3). In rich dextrose medium, almost all *fis1Δ* or *dnm1Δ* cells (93 and 90%, respectively) contain collapsed mitochondrial nets. In contrast, less than half of *mdv1Δ* cells contain collapsed nets, with the majority displaying a spread net morphology. The spread nets range in morphology from interconnected tubules with several loops (Fig. 3 C) to networks with complex fenestrations (Fig. 3 D). *mdv1Δ dnm1Δ* cells behave identically to *dnm1Δ* cells, with >90% collapsed nets in dextrose (Fig. 3). This observation indicates that the *dnm1Δ* collapsed net phenotype is epistatic to the *mdv1Δ* spread net phenotype. In rich galactose medium (unpublished data), a greater portion of all strains contain spread nets, but again *mdv1Δ* cells have a higher percentage of cells with spread nets (80%) compared with *fis1Δ* (45.5%), *dnm1Δ* (53%), or *mdv1Δdnm1Δ* cells (40.5%). These results agree with a previous report that *mdv1Δ* cells have more spread nets compared with *dnm1Δ* cells in galactose medium (Cerveny et al., 2001). However, this study found that the *mdv1Δ* spread net phenotype is epistatic to the *dnm1Δ* collapsed net phenotype (Cerveny et al., 2001). The reason for this discrepancy is unclear, but we note the *mdv1Δ* morphology is most distinct in dextrose cultures.

Most interestingly, we found that *mdv1Δ caf4Δ* cells have mitochondrial net distributions indistinguishable from

Downloaded from www.jcb.org on April 13, 2006

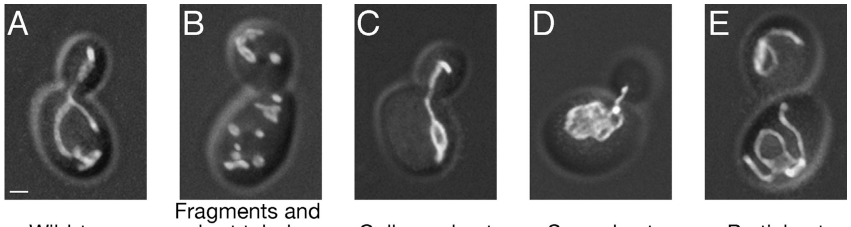

Genotype	LatA treatment	Wild-type	Fragments and short tubules	Collapsed net	Spread net	Partial net
Wild-type	-	95	5	0	0	0
	+	8	92	0	0	0
caf4Δ	-	95	4.5	0	0	0.5
	+	8.5	91.5	0	0	0
mdv1Δ	-	0	0	45.5	50.5	4
	+	0	0	5.5	14.5	80
dnm1Δ	-	0	0	96	3.5	0.5
	+	0	0	32.5	63.5	4
fis1Δ	-	0	0	96	4	0
	+	0	0	36.5	58.5	5
mdv1Δcaf4Δ	-	0	0	95	4	1
	+	0	0	38.5	57	4.5
mdv1Δdnm1Δ	-	0	0	95	4.5	0.5
	+	0	0	26	70.5	3.5

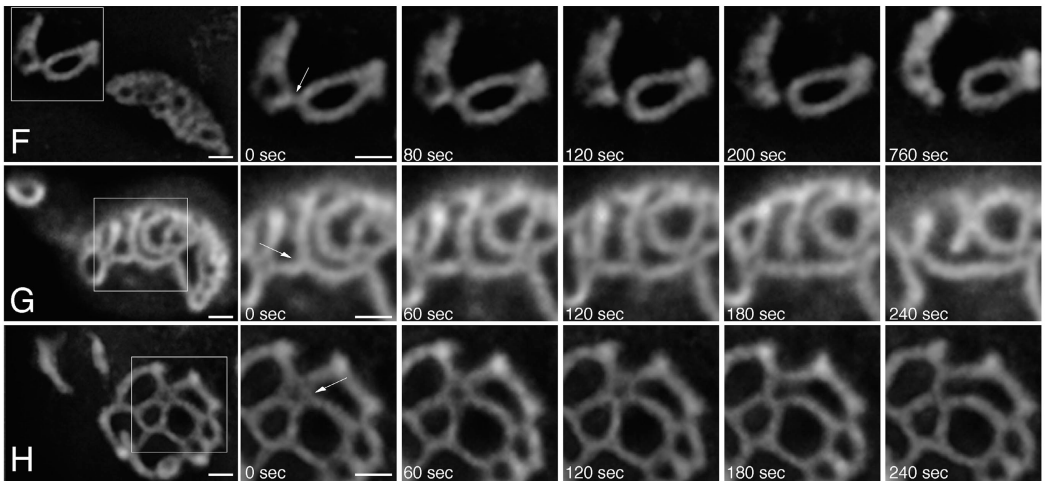

Figure 4. ***CAF4* mediates residual fission in *mdv1Δ* cells.** Top: mid-log cultures grown in YP dextrose were treated for 60 min with 200 μM latrunculin A (+) or vehicle (−). For each strain, 200 cells were scored into the following phenotypic categories: wild-type (A), fragments and short tubules (B), collapsed net (C), spread net (D), or partial net (E). Numbers shown are percentages. The fragments and short tubules category encompasses a range of morphologies from completely fragmented (as shown in B) to a mixture of fragments and short tubules. (F–H) Still images from time-lapse movies showing fission events in *mdv1Δ* yeast treated with 200 μM latrunculin A. The boxed area in the first frame is magnified in the subsequent sequence of five images. Arrows indicate fission events. Mitochondria were visualized with the outer membrane marker OM45-GFP. Bars, 1 μm.

either *dnm1Δ* cells or *fis1Δ* cells. Deletion of *CAF4* in *mdv1Δ* cells markedly shifts the distribution to one composed almost entirely of collapsed mitochondrial nets (>90% in dextrose, Fig. 3). Our results support a model in which partial reduction of mitochondrial fission results in predominantly spread mitochondrial nets, and complete loss of fission eventually results in collapse of the nets. That is, *mdv1Δ* cells retain residual mitochondrial fission, whereas *mdv1Δ caf4Δ* cells are devoid of fission, similar to *dnm1Δ*, *fis1Δ*, or *mdv1Δ dnm1Δ* cells. An analogous situation appears to exist in mammalian cells, in which weak Drp1 dominant-negative alleles cause the formation of spread nets, whereas strong dominant-negative alleles cause nets to collapse (Smirnova et al., 2001).

We tested this model by reanalyzing mitochondrial morphologies in the presence of latrunculin A, which disrupts the actin cytoskeleton. Disruption of the actin cytoskeleton leads to rapid fragmentation of the mitochondrial network due to ongoing mitochondrial fission (Boldogh et al., 1998; Jensen et al., 2000). Latrunculin A treatment rapidly resolves a fraction of collapsed nets into spread nets (Jensen et al., 2000; Cerveny et al., 2001), and allows a closer examination of the degree of connectivity in mitochondrial nets. Similarly, in mammalian cells, collapsed mitochondrial nets induced by overexpression of dominant-negative Drp1 can be spread by the microtubule-depolymerizing agent nocodazole (Smirnova et al., 2001). Both wild-type and *caf4Δ* yeast treated with latrunculin A show

Downloaded from www.jcb.org on April 13, 2006

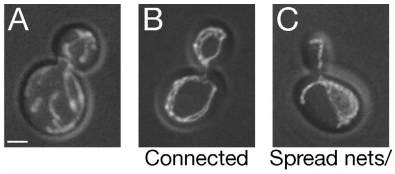

Plasmid		Wild-type	Connected tubules	Spread nets/ tubules
No Insert	Dex	99	1	0
	Gal	97	3	0
Caf4p-HA	Dex	97.5	2.5	0
	Gal	38.5	38	23.5
Caf4p-HA (aa1-250)	Dex	95	4	1
	Gal	58	33	9
Caf4p-HA (aa251-659)	Dex	99	1	0
	Gal	95.5	4.5	0

Figure 5. **Caf4p overexpression blocks mitochondrial fission.** Wild-type yeast (DCY1979) carrying the pRS416 GalL vector with no insert, full-length CAF4-HA, CAF4-HA N, or CAF4-HA C were grown in rich dextrose or galactose media for 180 min and fixed. Cells were scored into the following phenotypic categories: wild-type (A), connected tubules (B), or spread nets with tubules (C). Numbers shown are percentages (n = 200). Overexpression in galactose cultures was estimated to result in 20-fold greater expression than endogenous levels by Western blots of serially diluted lysates (not depicted). Bar, 1 μm.

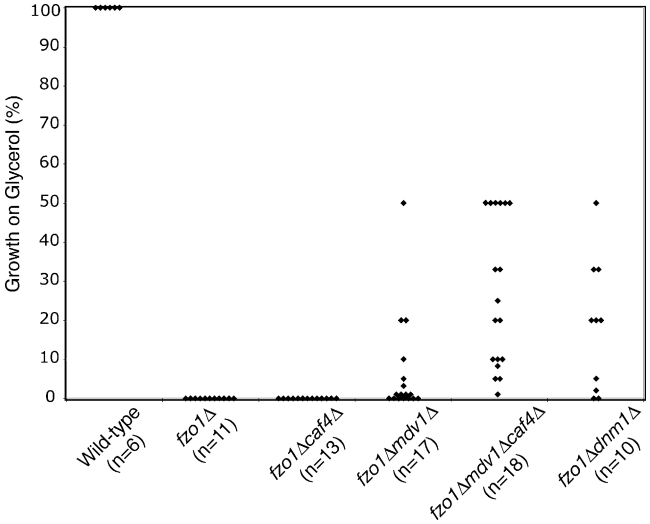

Figure 6. **Suppression of the glycerol growth defect of *fzo1Δ* cells.** Individual spores of the indicated genotypes were assayed by serial dilution on YP glycerol and YP dextrose plates to determine the percent survival on glycerol-containing medium. Each point represents the viability of an individual spore. For clarity, spores showing 1% or less survival were plotted as 1%.

mitochondrial fragmentation (Fig. 4). 80% of *mdv1Δ* cells treated with latrunculin A contain partial mitochondrial nets (Fig. 4 E, partial net) that are less interconnected and have fewer fenestrations than the collapsed or spread nets that predominate in latrunculin A–treated *dnm1Δ* or *fis1Δ* cells. 95% of latrunculin A–treated *mdv1Δ caf4Δ* cells show either collapsed nets or highly fenestrated spread nets, a profile indistinguishable from that in *dnm1Δ* or *fis1Δ* cells (Fig. 4). Thus, after disruption of the actin cytoskeleton, *mdv1Δ* yeast display a distribution of mitochondrial morphologies that suggest an incomplete defect in mitochondrial fission. In contrast, *mdv1Δ caf4Δ* yeast have mitochondrial morphologies similar to that in *fis1Δ* and *dnm1Δ* yeast. We conclude that *CAF4* mediates low levels of mitochondrial fission in *mdv1Δ* cells.

We next monitored the mitochondrial network in *mdv1Δ* cells by time-lapse microscopy to assess the levels of mitochondrial fission. In pilot experiments, we found that free mitochondrial ends produced by fission events in *mdv1Δ* cells were rapidly involved in fusion events, making unambiguous documentation of fission difficult. Because latrunculin A reduces the levels of fusion and thereby should prolong the presence of free mitochondrial ends, we monitored mitochondrial dynamics in latrunculin A–treated *mdv1Δ* cells carrying the outer membrane marker OM45-GFP. In 8 out of 10 *mdv1Δ* cells, we observed at least one fission event in a 30-min recording period (Fig. 4, F–H; Videos 1 and 2, available at http://www.jcb.org/cgi/content/full/jcb.200503148/DC1). Due to the complexity and rapid rearrangements of the mitochondrial networks in these cells (see Videos 1 and 2), these numbers likely underestimate the actual levels of fission. In contrast, no fission events were observed in 8 *mdv1Δ caf4Δ* cells. We conclude that the ability of *CAF4* to mediate mitochondrial fission events contributes significantly to the spread net morphology of *mdv1Δ* cells.

Mitochondrial fission is blocked by overexpression of Caf4p or Caf4p fragments

Because overexpression of Mdv1p or Mdv1p fragments inhibits mitochondrial fission (Cerveny and Jensen, 2003), we next tested the effects of Caf4p overproduction. Caf4p-HA under the control of the GalL promoter was expressed ~20 times above endogenous levels in rich galactose medium (unpublished data). Spread mitochondrial nets formed in 23.5% of cells (Fig. 5 C). An additional 38% of cells had an intermediate phenotype that we termed "connected tubules," consisting of a completely interconnected mitochondrial network in which no tubular ends were detected (Fig. 5 B). Overexpression of an NH_2-terminal fragment that interacts with Fis1p (residues 1–250; unpublished data) had a similar effect (9% spread nets, 33% connected tubules; Fig. 5), suggesting that the formation of mitochondrial net-like structures may result from a dominant-negative effect on Fis1p function. A similar distribution of mitochondrial phenotypes resulted from 20-fold overproduction of Mdv1p-HA (7.5% spread nets and 24.5% interconnected tubules) and an Mdv1p-HA NH_2-terminal fragment (5% spread nets and 39% interconnected tubules; unpublished data). These data confirm that Caf4p interacts with the mitochondrial fission apparatus.

Full bypass suppression of *fzo1Δ* requires loss of both *MDV1* and *CAF4*

Yeast fission mutants are able to suppress the glycerol growth defect of cells deficient in mitochondrial fusion (Bleazard et al., 1999). Indeed, *MDV1* was originally identified because of

Downloaded from www.jcb.org on April 13, 2006

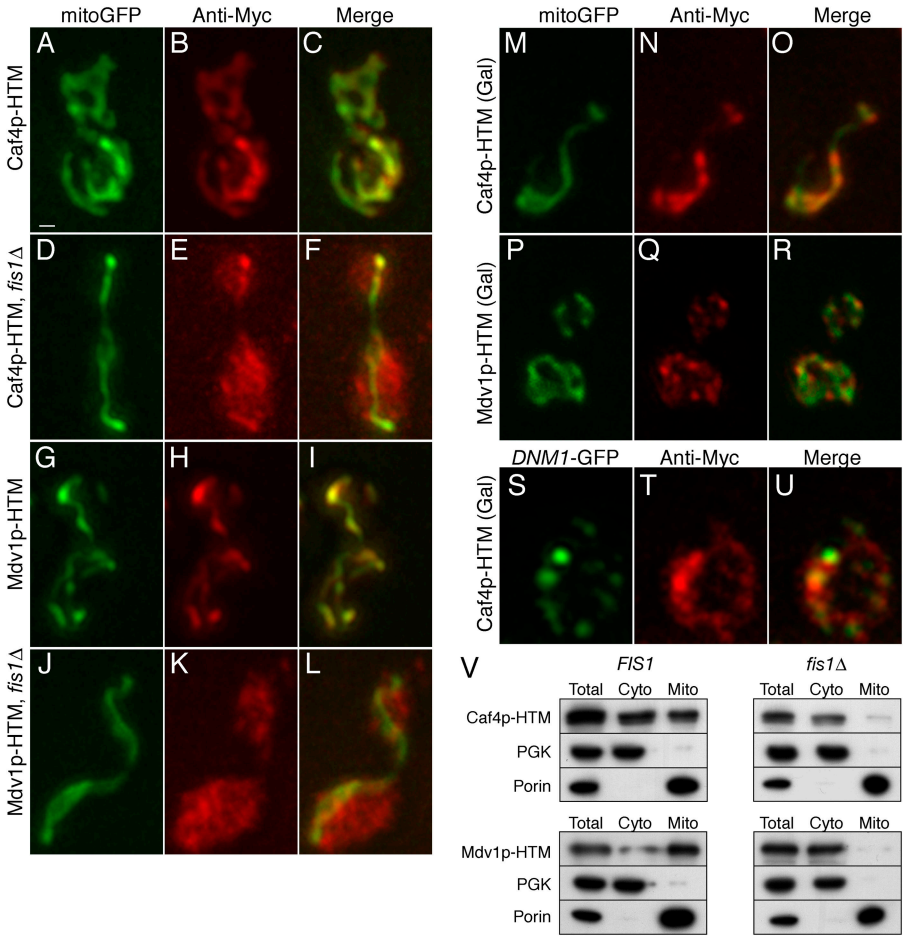

Figure 7. **Mitochondrial localization of Caf4p and Mdv1p requires Fis1p.** Immunofluorescence (red, middle panels) was used to localize Myc-tagged Caf4p (Caf4p-HTM; A–F and M–U) and Mdv1p (Mdv1p-HTM; G–L and P–R) in wild-type (A–C, G–I, and M–U) and *fis1Δ* cells (D–F and J–L). Caf4p-HTM and Mdv1p-HTM are expressed from the endogenous loci and are functional. Mitochondria were labeled with mitochondrially targeted GFP (A–R, left, green). The majority of Dnm1p-GFP puncta colocalize with Caf4p-HTM (S–U). Overlays of the two signals are shown in the merged images (right). Note that both Caf4p and Mdv1p localize to mitochondria in wild-type cells, but are diffusely cytosolic in *fis1Δ* cells. Cells were grown in YP dextrose (A–L) or YP galactose (M–U). Representative maximum intensity projections of deconvolved z-stacks are shown. Bar, 1 μm. (V) Caf4p-HTM and Mdv1p-HTM were analyzed by subcellular fractionation. The total cell lysate (Total), high-speed supernatant (Cyto), and mitochondrial pellet (Mito) were analyzed by Western blot with an anti-Myc antibody in wild-type (left) and *fis1Δ* (right) yeast. PGK (3-phosphoglycerate kinase) is a cytosolic marker, and porin is a mitochondrial outer membrane marker.

its ability to suppress the glycerol growth defect of strains carrying temperature-sensitive *fzo1* or *mgm1* alleles (Fekkes et al., 2000; Mozdy et al., 2000; Tieu and Nunnari, 2000; Cerveny et al., 2001). Deletion of *MDV1* has previously been reported to suppress the glycerol growth defect of *fzo1Δ* cells less efficiently than deletion of *DNM1* (Cerveny et al., 2001). To further test our hypothesis that *mdv1Δ* cells have only a partial loss of mitochondrial fission, we compared the efficiencies with which the *mdv1Δ* and *dnm1Δ* mutations suppress the glycerol growth defect of *fzo1Δ* cells. Diploids were sporulated, genotyped, and scored by serial dilution for their ability to grow on glycerol plates relative to dextrose plates (Fig. 6). As expected, all wild-type and no *fzo1Δ* spores grew on glycerol plates. Of 17 *mdv1Δ fzo1Δ* spores tested, 7 showed no detectable growth on glycerol and an additional 4 spores grew very poorly, with <1% cell survival on glycerol. Only 3 of the 6 remaining spores showed >20% survival on glycerol. More than half of *dnm1Δ fzo1Δ* spores grew robustly on glycerol plates, with between 20 and 50% cell survival. Most importantly, the triple mutant *mdv1Δ caf4Δ fzo1Δ* spores grew much more robustly than the *mdv1Δ fzo1Δ* spores, with all spores growing on glycerol and the majority between 20 and 50% cell survival. The markedly enhanced bypass suppression of *fzo1Δ* by *mdv1Δ caf4Δ* double mutations compared with the *mdv1Δ* mutation provides genetic evidence that *mdv1Δ* cells retain residual mitochondrial fission due to the activity of Caf4p.

Caf4p localizes to mitochondria in a Fis1p-dependent manner

We next sought to determine the subcellular localization of Caf4p. Caf4p was detected in highly purified mitochondrial preparations (Sickmann et al., 2003), and a Caf4p-GFP fusion generated in a genome-wide analysis localizes to mitochondria (Huh et al., 2003). We confirmed the mitochondrial localization of Caf4p-GFP, but did not study it further because the GFP fusion protein was not functional when expressed from the *CAF4* locus (unpublished data). We instead used immunofluorescence to localize Myc-tagged versions of Caf4p and Mdv1p (termed Caf4p-HTM and Mdv1p-HTM) that are expressed from the endogenous locus and are functional. Caf4p-HTM and Mdv1p-HTM showed clear mitochondrial localization (Fig. 7). When cells were grown in rich dextrose medium, both Caf4p-HTM and Mdv1p-HTM displayed a largely uniform mitochondrial distribution with occasional areas of increased intensity. In rich galactose medium, Caf4p-HTM and Mdv1p-HTM localize in a more punctate pattern on mitochondria (Fig. 7, M–R). Caf4p-HTM partially colocalizes with Dnm1-GFP puncta (Fig. 7, S–U). In *fis1Δ* cells grown in either dextrose or galactose media, both Caf4p-HTM and Mdv1p-HTM are found predominantly in the cytosol (Fig. 7, D–F and J–L). In some cells, however, low levels of residual localization to mitochondria could be discerned (e.g., Fig. 7, D–F). In *fis1* mutant yeast, overexpressed GFP-Mdv1p is dif-

Downloaded from www.jcb.org on April 13, 2006

fusely cytosolic but also retains some localization to mitochondria (Tieu and Nunnari, 2000; Tieu et al., 2002). Together, these data indicate that the normal mitochondrial localization of both Caf4p and Mdv1p depends largely on Fis1p, although some low levels of residual localization can occur in the absence of Fis1p.

We also evaluated the localization of Caf4p-HTM by subcellular fractionation. We found a significant portion of both Caf4p and Mdv1p in the mitochondrial pellet (Fig. 7 V). Mdv1p had previously been shown to be present in mitochondrial fractions (Fekkes et al., 2000; Tieu and Nunnari, 2000; Cerveny et al., 2001). However, in *fis1Δ* yeast both proteins behave as cytosolic proteins (Fig. 7 V). These data support our immunofluorescence studies and confirm that Mdv1p and Caf4p localize to mitochondria through their association with Fis1p.

Caf4p recruits Dnm1p-GFP to mitochondria

To understand the mechanism of mitochondrial fission, it is crucial to elucidate how Dnm1p is recruited to mitochondria. Given that Mdv1p associates with both Fis1p and Dnm1p, it is puzzling that Dnm1p assembly on mitochondria shows little or no dependence on Mdv1p (Fekkes et al., 2000; Mozdy et al., 2000; Tieu and Nunnari, 2000; Tieu et al., 2002; Cerveny and Jensen, 2003). With the identification of Caf4p as a component of the fission machinery, we reexamined this issue. We constructed a fully functional Dnm1p-GFP allele and analyzed its localization pattern using deconvolution microscopy (Table II). Similar to previous reports (Otsuga et al., 1998), Dnm1p-GFP is found predominantly in puncta associated with mitochondria (average 16.9 mitochondrial vs. 3.3 cytosolic puncta per cell) (Table II and Fig. 8, A–C). Deletion of *CAF4* or *MDV1* alone had little effect on this localization (15.4 mitochondrial vs. 5.2 cytosolic and 13.7 mitochondrial vs. 5.1 cytosolic per cell, respectively; Table II and Fig. 8, D–I). In all these strains, the Dnm1p puncta are relatively uniform in size and intensity.

In contrast, *fis1Δ* mutants showed dramatic defects, with the majority of the puncta now cytosolic (4.9 mitochondrial vs. 9.6 cytosolic) (Table II and Fig. 8, J–L). As has been previously noted, a small fraction of Dnm1p still localizes to mitochondria in *fis1Δ* cells (Tieu et al., 2002; Cerveny and Jensen, 2003), suggesting that Dnm1p may be recruited by a second pathway, perhaps through an intrinsic affinity for mitochondrial lipids or an unidentified mitochondrial binding partner. Importantly, a similar defect in Dnm1p localization was found in *mdv1Δ caf4Δ* cells (4.8 mitochondrial vs. 10.4 cytosolic per cell) (Table II and Fig. 8, M–O). In both *fis1Δ* and *mdv1Δ caf4Δ* cells, Dnm1p-GFP forms a few large aggregates and numerous less intense puncta. Similar results were obtained using immunofluorescence against a Dnm1p-HTM protein (unpublished data). These data clearly demonstrate that either Caf4p or Mdv1p is sufficient for effective recruitment of Dnm1p to mitochondria, and that Caf4p is essential for Mdv1p-independent recruitment of Dnm1p by Fis1p.

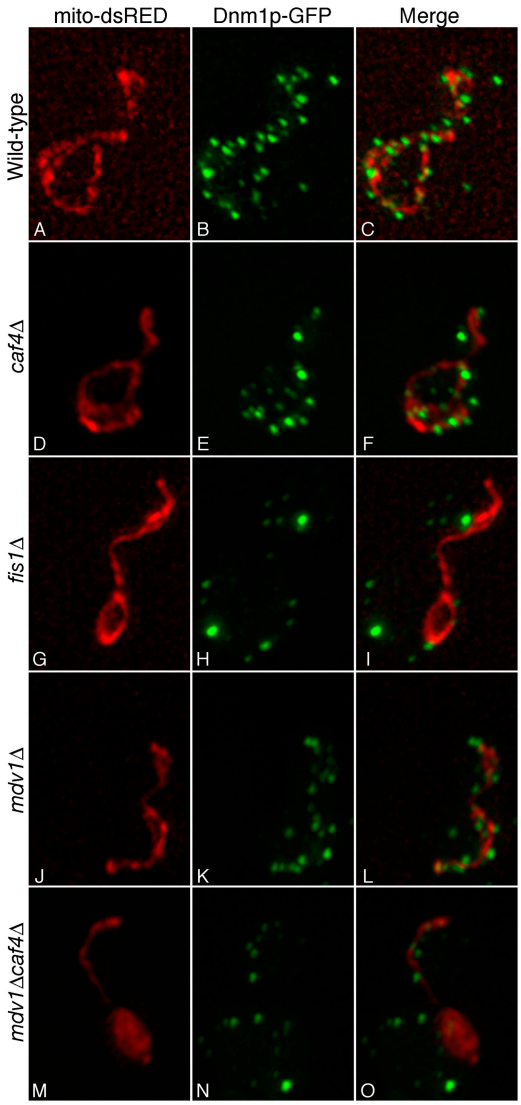

Figure 8. **Fis1p mediates Dnm1p-GFP localization through either Mdv1p or Caf4p.** The localization of Dnm1p-GFP (middle, green) was compared to mito-DsRed (left, red) in yeast of the indicated genotype. Merged images are shown on the right. Representative maximum intensity projections of deconvolved z-stacks are shown.

Discussion

CAF4 and *MDV1* perform similar functions in mitochondrial fission

By applying affinity purification and mass spectrometry to Fis1p, we have identified Caf4p as a novel component of the mitochondrial fission machinery. Our biochemical and genetic characterization indicate that *CAF4* functions in the same manner as *MDV1* in mitochondrial fission. Biochemically, both proteins interact with Fis1p and Dnm1p. Caf4p and Mdv1p share a common domain architecture comprised of an NTE, a central CC, and a COOH-terminal WD40 repeat. The NH_2-terminal regions mediate oligomerization and association with Fis1p, whereas the COOH-terminal WD40 regions mediate interactions with Dnm1p. In addition, both Caf4p and Mdv1p localize to mitochondria in a Fis1p-dependent manner.

Downloaded from www.jcb.org on April 13, 2006

Table II. **Quantification of Dnm1-GFP puncta localization**

	Mitochondrial	Cytosolic
Wild-type	16.9 (± 5.5)	3.3 (± 2.1)
caf4Δ	15.4 (± 5.2)	5.2 (± 2.6)
mdv1Δ	13.7 (± 5.0)	5.1 (± 3.0)
fis1Δ	4.9 (± 2.7)	9.6 (± 4.3)
mdv1Δ caf4Δ	4.8 (± 2.5)	10.4 (± 3.9)

Dnm1p puncta were scored for colocalization with mitochondrially localized DsRed in deconvolved images. For each genotype, 140 budded cells were analyzed by scoring Dnm1p-GFP spots in both the mother and bud, and the average is presented with the SD in parentheses.

Genetically, both *MDV1* and *CAF4* act positively in the mitochondrial fission pathway. *mdv1Δ* cells are dramatically compromised for mitochondrial fission, but a residual level of fission is mediated by *CAF4*. This residual fission activity is revealed by the observation that *mdv1Δ* yeast have a less severe mitochondrial morphology defect compared with *fis1Δ* or *dnm1Δ* yeast. In contrast, *mdv1Δ caf4Δ* yeast display predominantly collapsed mitochondrial nets, identical to those seen in *fis1Δ* and *dnm1Δ* cells. Time-lapse imaging of mitochondria in *mdv1Δ* cells indeed reveals a residual level of fission that is absent from *mdv1Δ caf4Δ* cells. These results directly support our conclusion that the morphology differences between *mdv1Δ* cells versus *mdv1Δ caf4Δ*, *fis1Δ*, and *dnm1Δ* cells are primarily due to differences in fission rates. It is also possible that the proposed role of Dnm1p in cortical distribution of mitochondria may contribute in part to the morphological differences (Otsuga et al., 1998). The *mdv1Δ* mutation acts as a weak suppressor of the glycerol growth defect in *fzo1Δ* cells. The *mdv1Δ caf4Δ* double mutation suppresses this phenotype much more efficiently. Based on these physical interaction and genetic data, we conclude that Caf4p likely acts in a similar manner to Mdv1p to promote mitochondrial fission.

Why are there two proteins that appear to perform similar and partially redundant roles in mitochondrial fission? This question is particularly intriguing because *caf4Δ* yeast have normal mitochondrial morphology, indicating that disruption of Caf4p does not cause a major loss of mitochondrial fission. First, *CAF4* may play a more important role in mitochondrial fission under conditions not yet tested. Second, the presence of two proteins mediating interactions between Fis1p and Dnm1p would increase the ability of cells to accurately regulate the rate of mitochondrial fission. The heterotypic and homotypic interactions between Caf4p and Mdv1p may provide an additional layer of regulation. Finally, Caf4p may have an additional function in another pathway. Previous two-hybrid studies have implicated Caf4p in the CCR4-NOT complex, which is thought to be involved in regulation of transcription and/or mRNA processing (Liu et al., 2001).

A revised model for mitochondrial fission

The current models for mitochondrial fission propose that Mdv1p acts late in the fission pathway. One model proposes a two-step pathway in which Fis1p first recruits Dnm1p, in an Mdv1p-independent manner. Mdv1p then acts as a molecular adaptor at a post-recruitment step, along with Fis1p, to promote fission by Dnm1p (Shaw and Nunnari, 2002; Tieu et al., 2002; Osteryoung and Nunnari, 2003). A second model also proposes that Mdv1p acts after Dnm1p recruitment to organize an active fission complex (Cerveny and Jensen, 2003).

Our study reveals a new role for Mdv1p and Caf4p early in mitochondrial fission. Fis1p recruits Dnm1p to mitochondrial fission complexes through Mdv1p or Caf4p, which act as molecular adaptors. This revised model is strongly supported by our demonstration that Dnm1p recruitment in *mdv1Δ* yeast depends on Caf4p function. In the absence of both Mdv1p and Caf4p, Fis1p is unable to recruit Dnm1p.

Although Mdv1p and Caf4p clearly act early in the fission pathway, there is evidence that at least Mdv1p has a subsequent role in the activation of fission, as previously proposed (Shaw and Nunnari, 2002; Tieu et al., 2002; Cerveny and Jensen, 2003). In *caf4Δ* cells, Mdv1p recruits Dnm1p to fission complexes, and fission occurs at apparently normal levels. However, in *mdv1Δ* cells, Caf4p is similarly able to recruit Dnm1p to fission complexes, but mitochondrial fission is severely compromised. Therefore, Mdv1p and Caf4p can independently recruit Dnm1p, but complexes recruited by Mdv1p appear to be more highly active. These observations suggest that Dnm1p recruitment by itself is insufficient for fission to occur. Indeed, studies of Dnm1p dynamics indicates that most Dnm1p puncta do not result in fission (Legesse-Miller et al., 2003). Our identification of Caf4p as part of the fission machinery clarifies the early steps in mitochondrial fission. Future studies will need to define the additional steps beyond Dnm1p recruitment necessary for fission.

Materials and methods

Media and yeast genetic techniques

Yeast strains are listed in Table S1. Standard genetic techniques and yeast media were used. SC and YP media supplemented with either 2% dextrose, 3% glycerol, 2% raffinose, or 2% galactose were prepared as described previously (Guthrie and Fink, 1991). YJG12 and DCY1557 are in the w303 background. All other strains are in the S288C background. *fis1::KanMX6*, *mdv1::KanMX6*, *caf4::KanMX6*, and *dnm1::KanMX6* are derived from the *MATa* deletion library (Open Biosystems).

Plasmid construction

The M_9TH cassette was generated as follows. Primers Eg258 (see Table S3, available at http://www.jcb.org/cgi/content/full/jcb.200503148/DC1) and Eg259 were used to amplify *URA3* from pRS416 (Stratagene). Eg260 and Eg4, an *FZO1* reverse primer, were used to amplify a TEV/His_8 module from EG704 (pRS414 + 9XMyc/TEV/His_8-*FZO1*). The 3′ end of the *URA3* product overlaps by 18 bp with the 5′ end of the TEV/His_8 product. This overlap allows them to anneal together and be amplified in a second PCR with the primers Eg258 and Eg4. The *URA3*/TEV/His_8 product was cloned into pRS403 as an EcoRV/SalI fragment (which removes all *FZO1* sequence), resulting in EG928. 9xMyc/TEV was amplified with Eg256 and Eg260 from EG704 and fused to the 5′ end of *URA3* (Eg258/259 product) by mixing and amplifying with Eg256 and Eg259. The resulting product was cloned into EG928 as an EcoRV/EcoRI fragment, yielding EG940 (pRS403+9xMyc/TEV/*URA3*/TEV/His_8). EG940 was converted to pRS403+3xMyc/TEV/*URA3*/TEV/His_8 by digesting with Xba1, yielding EG957.

To construct HA-tagged versions of *CAF4* and *CAF4* fragments, *CAF4* sequences were PCR amplified from *end3Δ* genomic DNA (Open Biosystems). First, the *CAF4* 3′ untranslated region (UTR) was amplified with the primers Eg313 and Eg314 and cloned as a KpnI/SalI fragment into pRS416, resulting in pRS416 + *CAF4* 3′ UTR. 3XHA was amplified with Eg327 and Eg328 and cloned as a SalI/XhoI fragment into the SalI site to generate pRS416 + 3XHA/*CAF4* 3′ UTR. The *CAF4* 5′ UTR was cloned as a SacI/SpeI fragment using Eg312 and Eg317, resulting in pRS416 + *CAF4* 5′ UTR/3XHA/3′ UTR. Full-length *CAF4* was amplified

Downloaded from www.jcb.org on April 13, 2006

with Eg316 and Eg315 and cloned as a SpeI/XhoI fragment into the SpeI/SalI sites, resulting in EG1041. *CAF4* N (residues 1–274) and C (residues 275–659) were amplified with Eg316/Eg353 and Eg315/Eg352, respectively, and cloned as SpeI/XhoI fragments, resulting in EG1045 and EG1043. Four independent clones encoded glutamine at residue 110 and arginine at residue 111. Full-length *CAF4-HA* was able to complement *caf4Δ* in *caf4Δ mdv1Δ* yeast, indicating that it is functional.

To construct HA-tagged versions of *MDV1* and *MDV1* fragments, *MDV1* sequences were amplified by PCR from *end3Δ* genomic DNA. First, the *MDV1* 3′ UTR was amplified with the primers Eg323 and Eg324 and cloned as a SacI/SalI fragment into pRS416. A 3XHA cassette was added as described for *CAF4-HA*, resulting in the plasmid pRS416 + *3XHA-MDV1* 3′ UTR. The *MDV1* 5′ UTR was amplified with primers Eg320 and Eg322 and cloned as a SacII/SpeI fragment, resulting in pRS416 + *MDV1* 5′ UTR/3XHA/3′ UTR. Full-length *MDV1* was amplified using primers Eg109 and Eg321 and cloned as a SpeI/XhoI fragment into the SpeI/SalI sites, resulting in EG1047. *MDV1* N (residues 1–300) and C (residues 301–714) were amplified with Eg323/Eg326 and Eg321/325, respectively, and cloned as SpeI/XhoI fragments, resulting in EG1051 and EG1049. Full-length *MDV1*-HA complemented the mitochondrial morphology defects in *mdv1Δ* cells.

The galactose-inducible Caf4p expression vectors EG1133 (Caf4p-HA), EG1135 (Caf4p-HA, residues 251–659), and EG1136 (Caf4p-HA, residues 1–250) were generated by replacing the *CAF4* 5′ UTR in EG1041, EG1043, and EG1045 with a SacI/ClaI GalL promoter fragment from p413 GalL (Mumberg et al., 1994) containing a start codon inserted between the XbaI and EcoRI sites.

pRS403 + GPD/mito-GFP (EG686) was generated by first cloning the GPD promoter from p413 GPD (Mumberg et al., 1995) as a SacI (blunt)/SpeI fragment into the SmaI/SpeI sites of pRS403 (Stratagene), yielding EG128. Next, a HindIII (blunt)/NotI mito-GFP fragment from pYES-mtGFP (Westermann and Neupert, 2000) was inserted into EG128 linearized with SpeI (blunt)/NotI. pRS403 + GPD/mito-DsRed (EG823) was generated by subcloning DsRed into the BamHI and NotI sites of EG686, replacing GFP with DsRed. OM45 was PCR amplified with primers Eg151 and Eg154 and cloned as an XhoI/XbaI fragment with an XbaI/BamHI GFP fragment into the XhoI/BamHI sites of pRS416, yielding pRS416 + OM45-GFP (EG252).

Yeast strain construction

An M_9TH-*FIS1* strain was generated by amplifying the 9XMyc/TEV/*URA3*/TEV/His_8 cassette from EG943 (pRS403-9XMyc/TEV/*URA3*/TEV/His_8) with the *FIS1*-targeting primers Eg261 and Eg262 and transforming YJG12. *URA3*+ transformants were screened by PCR for correct integration (2 out of 8 positive), grown overnight in YPD to allow for loss of *URA3*, and plated on 5-FOA plates. Colonies were screened by Western blotting for expression of M_9TH-Fis1p (9 out of 16 positive). This strain displayed wild-type morphology in 64% of cells and moderate defects in the remaining cells. The same strategy was used to generate M_3TH-*FIS1* from the pRS403-3XMyc/TEV/*URA3*/TEV/His_8 template (EG957) for subsequent experiments in the S288C background. This strain (DCY2192) displayed wild-type morphology in 89% of cells and mild defects in the remaining cells. DCY2192 was crossed to *mdv1Δ* and *caf4Δ* strains (Open Biosystems *MATa* deletion library) and sporulated to generate M_3TH-*FIS1 mdv1Δ* (DCY2302) and M_3TH-*FIS1 caf4Δ* (DCY2305).

fzo1::HIS5 was generated by transformation with a *HIS5* (*Saccharomyces kluyveri*) fragment amplified with the *FZO1* targeting primers Eg9 and Eg10. mito-GFP was integrated to the *leu2Δ0* locus by transformation with NarI-digested EG686 (pRS403 + GPD/mito-GFP). mito-DsRed was integrated to the *leu2Δ0* locus by transformation with HpaI-digested EG823 (pRS403 + GPD/mito-DsRed). *dnm1Δ::HIS5* was generated by transformation with a *HIS5* (*S. kluyveri*) fragment amplified with the *DNM1*-targeting primers Eg57 and Eg58.

Chromosomal *CAF4*-HTM was generated by transformation of DCY1979 with a His_8/2TEV/9XMyc/*HIS5* cassette (Seol et al., 1999) amplified with the *CAF4* targeting primers Eg284 and Eg285. Chromosomal *MDV1*-HTM was generated transformation with the same cassette amplified with *MDV1* targeting primers Eg80 and Eg81. Both *CAF4*-HTM and *MDV1*-HTM are functional because 70% of *CAF4*-HTM *mdv1Δ* yeast display spread mitochondrial nets and 95% of *MDV1*-HTM yeast cells display wild-type mitochondrial morphology.

DNM1-GFP was generated by amplifying GFP/*HIS5* from pKT128 (Sheff and Thorn, 2004) with Eg342 and Eg343. This product was transformed into DCY1626 (wild-type yeast with mito-DsRed) to generate DCY2370. DCY2370 was crossed to *fis1Δ* and *mdv1Δ caf4Δ* strains to generate DCY2404 (*DNM1*-GFP *fis1Δ*), DCY2414 (*DNM1*-GFP *caf4Δ*), DCY2417 (*DNM1*-GFP *mdv1Δ*), and DCY2418 (*DNM1*-GFP *mdv1Δ caf4Δ*).

Tandem affinity purification MudPIT

Pellets from 2-l cultures (OD_{600} ~1.5) grown in YPD were prepared essentially as described previously for HPM tag Dual-Step affinity purification (Graumann et al., 2004), with the following modifications. Fungal protease inhibitors were used (Sigma-Aldrich) and lysates were cleared at 20 kg for 15 min. Cleavage from 9E10 beads was performed with GST-TEV protease for 3 h at RT. The second affinity step was performed with 40 μl Magne-His beads (Promega). Samples were proteolytically digested and analyzed by multidimensional chromatography in-line with a Deca XP ion trap mass spectrometer (ThermoElectron) as described previously (Mayor et al., 2005). Samples were released stepwise from the strong cation exchanger phase of the triphasic capillary columns as reported previously (Graumann et al., 2004).

Immunoprecipitation

CAF4-HA (EG1041), *CAF4*-HA residues 1–274 (EG1043), and *CAF4*-HA residues 275–659 (EG1045) were expressed in strains DCY1979 (wild-type) and DCY2305 (M_3TH-*FIS1 caf4Δ*). *MDV1*-HA (EG1047), *MDV1*-HA residues 1–300 (EG1049), and *MDV1*-HA residues 301–714 (EG1051) were expressed in DCY1979 or DCY2302 (M_3TH-*FIS1 mdv1Δ*). Cultures were grown in selective SD media and harvested at OD_{600} ~0.8. 20 OD_{600} units of cells were lysed with glass beads (40 s with a vortex mixer, 4 times) in 500 μl ice-cold lysis buffer (50 mM Tris, pH 7.4, 150 mM NaCl, 0.1 mM EDTA, and 0.2% Triton X-100) in the presence of Fungal protease inhibitors (Sigma-Aldrich). Lysates were cleared by centrifuging 5 min at 5 krpm and 15 min at 14 krpm. At this point, a total lysate sample was taken. 400 μl of cleared lysate was mixed with a 20-μl bead volume of 9E10-conjugated protein A–Sepharose beads (Sigma-Aldrich) for 90 min. Beads were washed four times with 1-ml washes of lysis buffer. Precipitate was eluted with 100 μl SDS buffer at 95°C for 5 min. SDS-PAGE Western blotting was performed with 9E10 hybridoma supernatant (anti-Myc) or 12CA5 ascites fluid (anti-HA).

Yeast two-hybrid assay

pGAD vectors were transformed into PJ69-4α. pGBDU vectors were transformed into PJ69-4a (James et al., 1996). Indicated vectors were mated on YPD plates using two transformants for each vector (totaling four matings per combination). Diploids were selected by replica plating to SD-leu-ura plates. Interactions were assayed by replica plating to SD-leu-ura-lys-ade and incubating for 4 d at 30°C.

Mitochondrial morphology analysis

Mitochondrially targeted GFP (mito-GFP) was used to monitor mitochondrial morphology. DCY1979 (wild-type), DCY1945 (*caf4Δ*), DCY1984 (*caf4Δ mdv1Δ*), DCY2009 (*fis1Δ*), DCY2128 (*mdv1Δ*), DCY2155 (*mdv1Δ dnm1Δ*), and DCY2312 (*dnm1Δ*) were grown overnight, diluted 1:20 into fresh medium, and grown for 4 h at 30°C. Cultures were fixed by adjusting cultures to 3.7% formaldehyde and incubated 10 min at 30°C. Cells were washed 4 times with 1 ml PBS and scored for mitochondrial morphology. For *CAF4* overexpression studies, plasmids p416 GalL/*CAF4*-HA (EG1133), p416 GalL/*CAF4*-HA residues 251–659 (EG1135), or p416 GalL/*CAF4*-HA residues 1–250 (EG1137) were transformed into DCY1979. Cultures were grown overnight in selective SRaff and diluted 1:20 in fresh YPD or YPGal and grown 3 h at 30°C. Samples were taken for Western analysis and the remaining culture was fixed as described above.

For latrunculin A treatment, overnight YPD cultures were diluted 1:20 in fresh YPD and grown for 3 h. Cultures were then treated for 1 h at 30°C with 200 μM latrunculin A in or with an equivalent amount of vehicle (DMSO). Cultures were then fixed as described above.

For time-lapse imaging, overnight SGal cultures were diluted 1:20 in fresh YPGal and grown for 3 h. Cells were pelleted, resuspended in fresh media, and embedded in 1% low melting point agarose containing 200 μM latrunculin A.

Bypass suppression assay

DCY2002 and DCY2343 were sporulated and dissected onto YPD plates. Spores were picked, grown overnight in 3 ml YPD at 30°C, pelleted, and resuspended to OD_{600} ~1.0 in YP. 3 μl of 1:5 serial dilutions were spotted on YPD and YPGlycerol and grown at 30°C for 2 and 4 d, respectively, to determine the fraction of cells that grow on glycerol. Genotypes were determined by PCR.

Downloaded from www.jcb.org on April 13, 2006

Differential centrifugation

Yeast strains *CAF4*-HTM (DCY2055), *CAF4*-HTM *fis1Δ* (DCY2094), *MDV1*-HTM (DCY2053), and *MDV1*-HTM *fis1Δ* (DCY2097) were grown in YPD and harvested at OD_{600} ~1.2. 100 OD units of cells were spheroplasted with zymolyase and lysed in a small clearance Dounce homogenizer (0.6 M sorbitol and 10 mM Tris, pH 7.4). The lysate was spun twice at 2.9 krpm for 5 min. An aliquot of the second supernatant was saved as the total lysate sample. The second supernatant was spun at 10 krpm for 10 min, and an aliquot of the supernatant was saved as the cytosol sample. The pellet was resuspended and spun again at 10 krpm for 10 min. An aliquot of the final pellet was saved as the mitochondrial pellet. Equal cell equivalents were loaded for Western blot analysis. The difference in porin intensity between the total and mitochondrial fractions most likely results from fewer obscuring proteins in the mitochondrial fraction.

Imaging

Images were acquired on a microscope (Axiovert 200M; Carl Zeiss MicroImaging, Inc.) using a 100× Plan-Apochromat, NA 1.4, oil-immersion objective. Z-stack images (between 0.1- and 0.2-μm intervals for still images and between 0.3- and 0.4-μm intervals for time-lapse images) were collected at RT with an ORCA-ER camera (Hamamatsu), controlled by AxioVision 4.2 software. Images were collected at either 30- or 40-s intervals for 30 min for time-lapse experiments. Iterative deconvolutions were performed with Axiovision 4.2 and maximum intensity projections were generated with AxioVision 4.2 for still images and Image J for time-lapse images. Fluorescent images in Figs. 3–5 were overlaid with differential interference contrast images (set at 50% opacity) in Adobe Photoshop CS.

Immunofluorescence

Cells were processed for immunofluorescence essentially as described previously (Guthrie and Fink, 1991) with the following modifications. Cultures were fixed for 15 min with 3.7% formaldehyde. Tween 20 (0.5%) was included in blocking buffer (PBS, 1% BSA) during a 15-min block step. Cells were stained with 9E10 hybridoma supernatant and a Cy3-conjugated anti–mouse secondary antibody. Washes after primary and secondary incubations were 5 min with blocking buffer, 5 min with blocking buffer containing 0.5% Tween 20, and two 5-min washes with blocking buffer. All incubations were performed at RT. GelMount (Biomeda) was used as mounting medium to preserve fluorescence.

Online supplemental material

Table S1 lists proteins identified in MudPIT experiments with M_9TH-Fis1p. Table S2 shows yeast strains. Table S3 lists primer sequences. Videos 1 and 2 show mitochondrial fission in *mdv1Δ* yeast. Mitochondria were monitored by the mitochondrial outer membrane marker OM45-GFP. Arrows highlight a subset of fission events. Online supplemental material available at http://www.jcb.org/cgi/content/full/jcb.200503148/DC1.

We thank T.R. Suntoke, S.A. Detmer, and H. Chen for helpful comments on the manuscript; and L. Lytle for technical assistance. J. Copeland constructed some of the two-hybrid plasmids. We thank Dr. Ray Deshaies for stimulating discussions on mass spectrometry.

E.E. Griffin was supported by a National Institutes of Health training grant (NIH GM07616) and a Ferguson fellowship. MudPIT analysis was performed in the mass spectrometry facility of the laboratory of R.J. Deshaies (Investigator, Howard Hughes Medical Institute, Caltech). This facility is supported by the Beckman Institute at Caltech and by a grant from the Department of Energy to R.J. Deshaies and B.J. Wold. J. Graumann is supported by R.J. Deshaies through Howard Hughes Medical Institute funds. D.C. Chan is a Bren Scholar and Beckman Young Investigator. This research was supported by the National Institutes of Health (GM62967).

Submitted: 25 March 2005
Accepted: 9 June 2005

References

Bleazard, W., J.M. McCaffery, E.J. King, S. Bale, A. Mozdy, Q. Tieu, J. Nunnari, and J.M. Shaw. 1999. The dynamin-related GTPase Dnm1 regulates mitochondrial fission in yeast. *Nat. Cell Biol.* 1:298–304.

Boldogh, I., N. Vojtov, S. Karmon, and L.A. Pon. 1998. Interaction between mitochondria and the actin cytoskeleton in budding yeast requires two integral mitochondrial outer membrane proteins, Mmm1p and Mdm10p. *J. Cell Biol.* 141:1371–1381.

Cerveny, K.L., and R.E. Jensen. 2003. The WD-repeats of Net2p interact with Dnm1p and Fis1p to regulate division of mitochondria. *Mol. Biol. Cell.* 14:4126–4139.

Cerveny, K.L., J.M. McCaffery, and R.E. Jensen. 2001. Division of mitochondria requires a novel DMN1-interacting protein, Net2p. *Mol. Biol. Cell.* 12:309–321.

Denis, C.L., and J. Chen. 2003. The CCR4-NOT complex plays diverse roles in mRNA metabolism. *Prog. Nucleic Acid Res. Mol. Biol.* 73:221–250.

Dimmer, K.S., S. Fritz, F. Fuchs, M. Messerschmitt, N. Weinbach, W. Neupert, and B. Westermann. 2002. Genetic basis of mitochondrial function and morphology in *Saccharomyces cerevisiae*. *Mol. Biol. Cell.* 13:847–853.

Fannjiang, Y., W.-C. Cheng, S.J. Lee, B. Qi, J. Pevsner, J.M. McCaffery, R.B. Hill, G. Basanez, and J.M. Hardwick. 2004. Mitochondrial fission proteins regulate programmed cell death in yeast. *Genes Dev.* 18:2785–2797.

Fekkes, P., K.A. Shepard, and M.P. Yaffe. 2000. Gag3p, an outer membrane protein required for fission of mitochondrial tubules. *J. Cell Biol.* 151: 333–340.

Frank, S., B. Gaume, E.S. Bergmann-Leitner, W.W. Leitner, E.G. Robert, F. Catez, C.L. Smith, and R.J. Youle. 2001. The role of dynamin-related protein 1, a mediator of mitochondrial fission, in apoptosis. *Dev. Cell.* 1:515–525.

Graumann, J., L.A. Dunipace, J.H. Seol, W.H. McDonald, J.R. Yates III, B.J. Wold, and R.J. Deshaies. 2004. Applicability of tandem affinity purification MudPIT to pathway proteomics in yeast. *Mol. Cell. Proteomics.* 3:226–237.

Guthrie, C., and G. Fink. 1991. Guide to Yeast Genetics and Molecular Biology. Academic Press, San Diego, CA. 933 pp.

Huh, W.K., J.V. Falvo, L.C. Gerke, A.S. Carroll, R.W. Howson, J.S. Weissman, and E.K. O'Shea. 2003. Global analysis of protein localization in budding yeast. *Nature.* 425:686–691.

Jagasia, R., P. Grote, B. Westermann, and B. Conradt. 2005. DRP-1-mediated mitochondrial fragmentation during EGL-1-induced cell death in *C. elegans*. *Nature.* 433:754–760.

James, P., J. Halladay, and E.A. Craig. 1996. Genomic libraries and a host strain designed for highly efficient two-hybrid selection in yeast. *Genetics.* 144:1425–1436.

Jensen, R.E., A.E. Hobbs, K.L. Cerveny, and H. Sesaki. 2000. Yeast mitochondrial dynamics: fusion, division, segregation, and shape. *Microsc. Res. Tech.* 51:573–583.

Legesse-Miller, A., R.H. Massol, and T. Kirchhausen. 2003. Constriction and Dnm1p recruitment are distinct processes in mitochondrial fission. *Mol. Biol. Cell.* 14:1953–1963.

Link, A.J., J. Eng, D.M. Schieltz, E. Carmack, G.J. Mize, D.R. Morris, B.M. Garvik, and J.R. Yates III. 1999. Direct analysis of protein complexes using mass spectrometry. *Nat. Biotechnol.* 17:676–682.

Liu, H.Y., Y.C. Chiang, J. Pan, J. Chen, C. Salvadore, D.C. Audino, V. Badarinarayana, V. Palaniswamy, B. Anderson, and C.L. Denis. 2001. Characterization of CAF4 and CAF16 reveals a functional connection between the CCR4-NOT complex and a subset of SRB proteins of the RNA polymerase II holoenzyme. *J. Biol. Chem.* 276:7541–7548.

Mayor, T., J.R. Lipford, J. Graumann, G.T. Smith, and R.J. Deshaies. 2005. Analysis of polyubiquitin conjugates reveals that the rpn10 substrate receptor contributes to the turnover of multiple proteasome targets. *Mol. Cell. Proteomics.* 4:741–751.

Mozdy, A.D., J.M. McCaffery, and J.M. Shaw. 2000. Dnm1p GTPase-mediated mitochondrial fission is a multi-step process requiring the novel integral membrane component Fis1p. *J. Cell Biol.* 151:367–380.

Mumberg, D., R. Muller, and M. Funk. 1994. Regulatable promoters of *Saccharomyces cerevisiae*: comparison of transcriptional activity and their use for heterologous expression. *Nucleic Acids Res.* 22:5767–5768.

Mumberg, D., R. Muller, and M. Funk. 1995. Yeast vectors for the controlled expression of heterologous proteins in different genetic backgrounds. *Gene.* 156:119–122.

Osteryoung, K.W., and J. Nunnari. 2003. The division of endosymbiotic organelles. *Science.* 302:1698–1704.

Otsuga, D., B.R. Keegan, E. Brisch, J.W. Thatcher, G.J. Hermann, W. Bleazard, and J.M. Shaw. 1998. The dynamin-related GTPase, Dnm1p, controls mitochondrial morphology in yeast. *J. Cell Biol.* 143:333–349.

Praefcke, G.J., and H.T. McMahon. 2004. The dynamin superfamily: universal membrane tubulation and fission molecules? *Nat. Rev. Mol. Cell Biol.* 5:133–147.

Seol, J.H., R.M. Feldman, W. Zachariae, A. Shevchenko, C.C. Correll, S. Lyapina, Y. Chi, M. Galova, J. Claypool, S. Sandmeyer, et al. 1999. Cdc53/cullin and the essential Hrt1 RING-H2 subunit of SCF define a ubiquitin ligase module that activates the E2 enzyme Cdc34. *Genes Dev.* 13:1614–1626.

Sesaki, H., and R.E. Jensen. 1999. Division versus fusion: Dnm1p and Fzo1p antagonistically regulate mitochondrial shape. *J. Cell Biol.* 147:699–706.

Downloaded from www.jcb.org on April 13, 2006

Shaw, J.M., and J. Nunnari. 2002. Mitochondrial dynamics and division in budding yeast. *Trends Cell Biol.* 12:178–184.

Sheff, M.A., and K.S. Thorn. 2004. Optimized cassettes for fluorescent protein tagging in *Saccharomyces cerevisiae*. *Yeast.* 21:661–670.

Sickmann, A., J. Reinders, Y. Wagner, C. Joppich, R. Zahedi, H.E. Meyer, B. Schonfisch, I. Perschil, A. Chacinska, B. Guiard, et al. 2003. The proteome of *Saccharomyces cerevisiae* mitochondria. *Proc. Natl. Acad. Sci. USA.* 100:13207–13212.

Smirnova, E., L. Griparic, D.L. Shurland, and A.M. van der Bliek. 2001. Dynamin-related protein Drp1 is required for mitochondrial division in mammalian cells. *Mol. Biol. Cell.* 12:2245–2256.

Tieu, Q., and J. Nunnari. 2000. Mdv1p is a WD repeat protein that interacts with the dynamin-related GTPase, Dnm1p, to trigger mitochondrial division. *J. Cell Biol.* 151:353–366.

Tieu, Q., V. Okreglak, K. Naylor, and J. Nunnari. 2002. The WD repeat protein, Mdv1p, functions as a molecular adaptor by interacting with Dnm1p and Fis1p during mitochondrial fission. *J. Cell Biol.* 158:445–452.

Westermann, B., and W. Neupert. 2000. Mitochondria-targeted green fluorescent proteins: convenient tools for the study of organelle biogenesis in *Saccharomyces cerevisiae*. *Yeast.* 16:1421–1427.

Wolf, E., P.S. Kim, and B. Berger. 1997. MultiCoil: a program for predicting two- and three-stranded coiled coils. *Protein Sci.* 6:1179–1189.

Downloaded from www.jcb.org on April 13, 2006

Table S3. **Primer sequences**

Primer	Sequence
Eg4	GGTACGGTCATCAGTTACTCC
Eg9	TATCTGATATCACGGATAGAGGCAAAACGGTAGGCTCATTTAACGAGATTGTACTG AGAGTGCAC
Eg10	TTATGTATATTGATTTGAAAAGACCTCATATATTTACAAGAATATCTGTGCGGTATT TCACACCG
Eg57	CATTAAGTAGCTACCAGCGAATCTAAATACGACGGATAAAGAAGATTGTACTGAGA GTGCAC
Eg58	CAATGTTGAAGTAAGATCAAAAATGAGATGAATTATGCAACTGTGCGGTATTTCAC ACCG
Eg80	GGTTGAGGGTCGTGAAAATGGGGACGTAAATATTTGGGCCGTAGGTGGCAGCCATC ACCACCATC
Eg81	CCATCCAAGGTATTGACGATACTTTATTTACATTCCAGAACGGCGTTAGTATCGAAT CGAC
Eg109	GCACTCGAGTACGGCCCAAATATTTACGTC
Eg151	GCGTCTAGAGTCCTTTTTCGAGCTC
Eg154	GCGCTCGAGCAGGAGCACAAGCTCGCC
Eg256	GCAGAATTCGCCACCATGGTCGAGGGA
Eg259	TCCGGATCCCTGTGCGGTATTTCAC
Eg260	TACCGCACAGGGATCCGGAGAAGGC
Eg261	CGGCACATAGAAGCACAGATCAGAGCACAGCCATACAACATAAGTCGCCACCATGG TCGAGGG
Eg262	GTTCGTATGCGTCCTTAAGAGTTGGCCAAAAATCTACTTTGGTCATGCCGCCATGAT GATGATG
Eg284	GATCAATGGGCACAACGATGGAGACATCAATGTATGGACACTTGGTGGCAGCCATC ACCACCATC
Eg285	GTTATGTATGTATGACCACATATGCTGTACATAAATTGTATACGCGTTAGTATCGAA TCGAC
Eg312	GCAGAGCTCAAGAATAGATATTTCCTTTG
Eg313	GCAGGTACCGTTCATCATTACGTTTCCAG
Eg314	GCAGTCGACTAGGAAGGAAAAAGATTAT
Eg315	GCACTCGAGAAGTGTCCATACATTGATGT
Eg316	GCAACTAGTCATTCATGGTTAGTTTTT
Eg317	GCAACTAGTCATTCATGGTTAGTTTTT
Eg320	GCACCGCGGTGAGGGTATAAGATACCG
Eg321	GCAACTAGTTCAGTGAACGACCAAATAAC
Eg322	GCAACTAGTCATTATTTGTCATTATTTGC
Eg323	GCAGTCGACTGATAGGCATTGCATTGCAA
Eg324	CGCCACTTAAATATTAATCAT
Eg325	GCAACTAGTTTGGAGGTGATCGAAGCTAAT
Eg326	GCACTCGAGTCCGTACTCTTCTAAAAAG
Eg327	CGAGCTCGGTGTCGACCTTGGTTACCC
Eg328	GCGGTTTAAACTTCTCGAGAGCGTAGTC
Eg342	GGAGTTTATAAAAAGGCTGCAACCCTTATTAGTAATATTCTGGGTGACGGTGCTGGT TTA
Eg343	GCACATTTGAAATCATCAACTGAGTAAAGGAATAAACACTGACCTTCGATGAATTC GAGCTCG
Eg352	GCAACTAGTTTCACGCAAAATGAAGAA
Eg353	GCACTCGAGGGACGACGCTTCAGATGA

Table S1. **Proteins Identified in MudPIT Experiments with M_9TH-Fis1p.**

Experiment #1

Systematic Name	Descriptive Name	Unique Peptides	Total Peptides	Sequence Coverage
YAL005C	SSA1	9	13	19.30%
YAL035W	FUN12	2	2	4.10%
YAL038W	CDC19	4	7	12.80%
YAL060W	BDH1	2	3	3.90%
YAR073W	IMD1	3	4	14.10%
YBL075C	SSA3	4	6	9.60%
YBR030W	YBR030W	4	4	9.60%
YBR118W	TEF2	14	20	31.00%
YBR127C	VMA2	4	5	14.30%
YBR221C	PDB1	7	9	28.10%
YBR263W	SHM1	2	2	4.80%
YCL028W	RNQ1	2	2	9.90%
YCL037C	SRO9	4	4	14.80%
YCL067C	HMLALPHA2	2	39	7.10%
YCR039C	MATALPHA2	2	39	7.10%
YDL055C	PSA1	4	5	19.70%
YDL131W	LYS21	2	2	7.50%
YDL182W	LYS20	2	2	7.70%
YDL229W	SSB1	12	16	23.70%
YDR120C	TRM1	9	12	22.80%
YDR170C	SEC7	2	3	2.00%
YDR371W	CTS2	6	7	18.60%
YER103W	SSA4	3	5	7.20%
YER165W	PAB1	5	6	14.20%
YER178W	PDA1	7	9	21.00%
YGL068W	YGL068W	2	2	16.50%
YGL245W	YGL245W	2	2	3.70%
YGR032W	GSC2	2	2	1.30%
YGR054W	YGR054W	2	2	6.10%
YGR086C	PIL1	5	8	28.60%
YGR162W	TIF4631	3	4	5.80%
YGR192C	TDH3	3	8	17.80%
YHL007C	STE20	2	5	3.30%
YHR020W	YHR020W	4	6	9.30%
YHR196W	UTP9	2	3	5.60%
YHR216W	IMD2	5	7	18.40%
YIL065C	FIS1	14	50	61.30%
YJL109C	UTP10	2	2	1.80%
YJL112W	MDV1	12	18	22.10%
YJL130C	URA2	10	12	8.40%
YJL206C	YJL206C	3	3	8.30%

YJR009C	TDH2	2	2	10.50%
YKL025C	PAN3	2	2	4.10%
YKR036C	CAF4	9	15	24.40%
YLL024C	SSA2	9	12	19.20%
YLR044C	PDC1	2	2	6.20%
YLR150W	STM1	8	16	32.20%
YLR197W	SIK1	4	5	12.30%
YLR342W	FKS1	2	2	1.80%
YLR362W	STE11	1	13	2.90%
YLR432W	IMD3	6	8	21.40%
YML010W	SPT5	2	2	2.80%
YML056C	IMD4	5	7	17.70%
YML085C	TUB1	2	2	7.60%
YML123C	PHO84	2	2	6.30%
YMR012W	CLU1	3	3	4.00%
YMR108W	ILV2	5	5	11.80%
YMR229C	RRP5	4	4	3.90%
YNL071W	LAT1	5	7	13.50%
YNL132W	KRE33	3	3	4.30%
YNL209W	SSB2	12	16	25.00%
YOR142W-A	YOR142W-A	2	2	2.30%
YOR204W	DED1	6	9	16.70%
YPL004C	LSP1	3	3	13.80%
YPR080W	TEF1	14	20	31.00%
YPR171W	BSP1	6	13	15.80%

Experiment #2

Systematic Name	Descriptive Name	Unique Peptides	Total Peptides	Sequence Coverage
YAL005C	SSA1	10	25	18.70%
YAL035W	FUN12	9	11	13.10%
YAL038W	CDC19	29	66	61.00%
YAR073W	IMD1	3	7	14.10%
YBL003C	HTA2	2	3	17.40%
YBL075C	SSA3	4	16	6.90%
YBL076C	ILS1	3	3	4.40%
YBR030W	YBR030W	3	6	12.10%
YBR072W	HSP26	3	5	26.60%
YBR079C	RPG1	5	6	8.60%
YBR084W	MIS1	4	5	9.00%
YBR118W	TEF2	28	72	57.90%
YBR127C	VMA2	11	13	31.90%
YBR143C	SUP45	4	4	15.30%
YBR221C	PDB1	10	18	44.30%
YBR263W	SHM1	8	11	23.00%
YCL037C	SRO9	5	5	15.70%
YCR009C	RVS161	2	3	12.80%
YCR028C-A	RIM1	2	2	30.40%
YCR030C	SYP1	2	2	4.70%
YDL014W	NOP1	2	5	8.60%
YDL051W	LHP1	2	2	16.70%
YDL055C	PSA1	2	2	9.10%
YDL143W	CCT4	4	8	17.00%
YDL185W	TFP1	3	6	4.90%
YDL208W	NHP2	2	2	16.20%
YDL229W	SSB1	15	25	30.70%
YDR037W	KRS1	3	3	7.80%
YDR074W	TPS2	2	2	6.60%
YDR091C	RLI1	2	2	4.10%
YDR170C	SEC7	2	2	2.50%
YDR172W	SUP35	2	2	3.20%
YDR214W	AHA1	2	2	9.10%
YDR225W	HTA1	2	3	17.40%
YDR237W	MRPL7	2	2	11.00%
YDR238C	SEC26	2	2	4.20%
YDR251W	PAM1	2	2	5.30%
YDR342C	HXT7	2	3	4.00%
YDR343C	HXT6	2	3	4.00%
YDR371W	CTS2	5	6	12.90%
YDR388W	RVS167	3	3	7.90%
YDR432W	NPL3	7	15	25.40%
YEL026W	SNU13	2	5	19.00%

YEL034W	HYP2	3	3	42.70%
YEL051W	VMA8	2	2	14.80%
YEL060C	PRB1	2	2	4.90%
YEL071W	DLD3	2	2	6.70%
YER025W	GCD11	10	10	29.60%
YER036C	YER036C	5	8	11.10%
YER103W	SSA4	4	8	8.10%
YER165W	PAB1	5	5	15.60%
YER178W	PDA1	15	17	37.90%
YFL022C	FRS2	2	2	8.50%
YFL037W	TUB2	2	7	8.80%
YFL039C	ACT1	7	7	28.80%
YFR030W	MET10	4	4	7.50%
YGL008C	PMA1	5	9	10.50%
YGL049C	TIF4632	5	5	9.60%
YGL068W	YGL068W	2	5	10.80%
YGL105W	ARC1	2	2	8.80%
YGL171W	ROK1	2	2	7.40%
YGL173C	KEM1	2	2	2.90%
YGL245W	YGL245W	5	5	8.60%
YGR032W	GSC2	6	7	5.90%
YGR054W	YGR054W	7	10	21.30%
YGR090W	UTP22	2	2	2.50%
YGR094W	VAS1	2	2	3.40%
YGR103W	NOP7	2	2	7.40%
YGR128C	UTP8	2	2	5.90%
YGR159C	NSR1	6	6	23.70%
YGR162W	TIF4631	6	8	11.40%
YGR185C	TYS1	2	2	5.60%
YGR192C	TDH3	11	19	60.20%
YGR193C	PDX1	4	5	17.10%
YGR234W	YHB1	2	2	7.80%
YGR240C	PFK1	5	5	8.40%
YGR254W	ENO1	4	5	24.70%
YGR285C	ZUO1	12	20	39.00%
YHL034C	SBP1	5	6	24.10%
YHR019C	DED81	6	6	17.00%
YHR020W	YHR020W	5	7	12.90%
YHR052W	CIC1	3	3	14.10%
YHR064C	SSZ1	16	52	45.60%
YHR089C	GAR1	3	4	16.60%
YHR121W	YHR121W	2	2	16.00%
YHR174W	ENO2	3	4	22.00%
YHR193C	EGD2	4	4	28.70%
YHR216W	IMD2	5	14	17.40%
YIL065C	FIS1	9	19	58.70%

YIL078W	THS1	2	3	4.40%
YJL008C	CCT8	2	2	9.50%
YJL052W	TDH1	4	4	18.70%
YJL080C	SCP160	3	5	4.00%
YJL095W	BCK1	2	2	3.00%
YJL109C	UTP10	3	3	2.80%
YJL112W	MDV1	5	5	10.20%
YJL130C	URA2	19	25	14.20%
YJL206C	YJL206C	4	5	9.90%
YJR007W	SUI2	3	3	16.80%
YJR009C	TDH2	6	11	22.90%
YKL009W	MRT4	2	2	14.40%
YKL054C	DEF1	4	4	14.00%
YKL081W	TEF4	3	5	12.90%
YKL182W	FAS1	9	9	8.80%
YKR036C	CAF4	3	4	8.50%
YLL018C	DPS1	5	9	16.30%
YLL024C	SSA2	11	26	22.40%
YLR044C	PDC1	2	2	8.20%
YLR058C	SHM2	3	4	15.60%
YLR150W	STM1	13	29	51.30%
YLR153C	ACS2	3	6	10.40%
YLR192C	HCR1	3	10	15.50%
YLR197W	SIK1	9	14	28.80%
YLR249W	YEF3	11	14	19.40%
YLR342W	FKS1	8	9	8.80%
YLR432W	IMD3	9	19	29.60%
YML056C	IMD4	7	14	20.80%
YML085C	TUB1	4	4	17.40%
YML123C	PHO84	2	2	7.00%
YML124C	TUB3	3	3	12.80%
YMR012W	CLU1	6	6	8.90%
YMR049C	ERB1	4	6	8.60%
YMR108W	ILV2	9	9	19.80%
YMR146C	TIF34	10	15	41.20%
YMR186W	HSC82	5	10	9.80%
YMR229C	RRP5	16	27	17.40%
YMR290C	HAS1	2	2	10.10%
YMR295C	YMR295C	2	2	27.40%
YMR308C	PSE1	2	2	3.60%
YMR309C	NIP1	12	16	21.90%
YNL007C	SIS1	5	5	25.00%
YNL071W	LAT1	12	24	29.30%
YNL085W	MKT1	4	5	8.30%
YNL112W	DBP2	3	10	11.00%
YNL138W	SRV2	4	4	8.60%

YNL209W	SSB2	14	20	28.50%
YNL248C	RPA49	2	3	11.30%
YOL010W	RCL1	2	2	7.10%
YOL086C	ADH1	3	3	16.10%
YOL123W	HRP1	2	2	6.70%
YOL139C	CDC33	2	2	12.20%
YOL145C	CTR9	2	3	3.00%
YOR153W	PDR5	2	2	2.50%
YOR164C	YOR164C	2	2	11.20%
YOR198C	BFR1	21	29	37.20%
YOR204W	DED1	15	17	38.40%
YOR298C-A	MBF1	3	3	46.60%
YOR310C	NOP58	5	5	14.10%
YOR341W	RPA190	2	2	2.60%
YOR347C	PYK2	2	2	2.00%
YOR361C	PRT1	4	12	9.70%
YPL004C	LSP1	2	2	13.20%
YPL012W	RRP12	4	4	8.30%
YPL032C	SVL3	3	3	5.80%
YPL036W	PMA2	5	9	10.10%
YPL037C	EGD1	6	7	48.40%
YPL085W	SEC16	2	2	2.70%
YPL119C	DBP1	2	2	3.70%
YPL226W	NEW1	2	2	3.20%
YPL231W	FAS2	2	2	1.60%
YPL237W	SUI3	5	5	29.80%
YPL240C	HSP82	5	10	9.70%
YPR010C	RPA135	2	3	5.50%
YPR033C	HTS1	5	5	14.50%
YPR080W	TEF1	28	72	57.90%
YPR110C	RPC40	2	2	11.60%
YPR144C	UTP19	4	4	13.90%
YPR158W-B	YPR158W-B	3	3	5.20%
YPR171W	BSP1	7	9	16.10%

Ribosomal and Ty transposon ORFs have been filtered out.

Table S2. **Yeast strains**

Strain	Genotype
YJG12	*MATa, can1-100, leu2-3, -112, his3-11, -15, trp1-1, ura3-1, ade2-1, pep4::*TRP1, *bar1*::hisG
DCY1979	*MATα, his3-, leu2Δ200, met15Δ0, ura3Δ0, leu2::*GPD mito-GFP-*LEU2*
DCY1945	*MATα, his3-, leu2Δ200, met15Δ0, ura3Δ0, leu2::*GPD mito-GFP-*LEU2*, *caf4Δ::KanMX6*
DCY2128	*MATα, his3-, leu2Δ200, met15Δ0, ura3Δ0, leu2::*GPD mito-GFP-*LEU2*, *mdv1Δ::KanMX6*
DCY1984	*MATα, his3-, leu2Δ200, met15Δ0, ura3Δ0, leu2::*GPD mito-GFP-*LEU2*, *caf4Δ::KanMX6, mdv1Δ::KanMX6*
DCY2009	*MATα, his3-, leu2Δ200, met15Δ0, ura3Δ0, leu2::*GPD mito-GFP-*LEU2*, *fis1Δ::KanMX6*
DCY2312	*MATa, his3-, leu2Δ200, met15Δ0, ura3Δ0, leu2::*GPD mito-GFP-*LEU2*, *dnm1Δ::KanMX6*
DCY2155	*MATa, his3-, leu2Δ200, met15Δ0, ura3Δ0, leu2::*GPD mito-GFP-*LEU2*, *mdv1Δ::KanMX6, dnm1::HIS5*
DCY1557	*MATa, can1-100, leu2-3, -112, his3-11, -15, trp1-1, ura3-1, ade2-1, pep4::*TRP1, *bar1*::hisG, M_9TH-*FIS1*
DCY1626	*MATα, his3Δ200, leu2Δ200, met15Δ0, ura3Δ0, trp1Δ63, leu2::*GPD mito-DsRed-*LEU2*
DCY2002	*MATa/α, his3-/his3Δ1, ade2-/ADE2*, *trp1Δ63/*TRP1*, met15Δ0/met15Δ0, ura3Δ0/ura3Δ0, leu2Δ0/leu2::*GPD mito-GFP-*LEU2*, CAF4/*caf4Δ::KanMX6,* MDV1/*mdv1Δ::KanMX6, FZO1/fzo1Δ::HIS5*
DCY2343	*MATa/α, his3-/his3Δ1, ade2-/ADE2 trp1Δ63/*TRP1*, met15Δ0/met15Δ0, ura3Δ0/ura3Δ0, leu2Δ0/leu2::*GPD mitoGFP-*LEU2*, CAF4/*caf4Δ::KanMX6,* DNM1/*dnm1Δ::KanMX6, FZO1/fzo1Δ::HIS5*
DCY2053	*MATα, his3-, leu2Δ200, met15Δ0, ura3Δ0, leu2::*GPD mito-GFP-*LEU2*, *MDV1-HTM::HIS5*
DCY2055	*MATα, his3-, leu2Δ200, met15Δ0, ura3Δ0, leu2::*GPD mito-GFP-*LEU2*, *CAF4-HTM::HIS5*
DCY2090	*MATα, his3-, leu2Δ200, met15Δ0, ura3Δ0, leu2::*GPD mito-GFP-*LEU2*, *CAF4-HTM::HIS5, mdv1Δ::KanMX6*
DCY2094	*MATα, his3-, leu2Δ200, met15Δ0, ura3Δ0, leu2::*GPD mito-GFP-*LEU2*, *CAF4-HTM::HIS5, fis1Δ::KanMX6*
DCY2097	*MATα, his3-, leu2Δ200, met15Δ0, ura3Δ0, leu2::*GPD mito-GFP-*LEU2*, *MDV1-HTM::HIS5, fis1Δ::KanMX6*
DCY2099	*MATα, his3-, leu2Δ200, met15Δ0, ura3Δ0, leu2::*GPD mito-GFP-*LEU2*, *MDV1-HTM::HIS5, caf4Δ::KanMX6*
DCY2370	*MATα, hisΔ200, leu2Δ0, met15Δ0, trp1Δ63, ura3Δ0, leu2::*GPD mito-DsRed-*LEU2*, *DNM1-GFP-spHIS5*
DCY2404	*MATa, his1-, met15Δ0, ura3Δ0, leu2::*GPD mitoGFP-*LEU2*, *DNM1-GFP-spHIS5, fis1Δ::KanMX6*
DCY2414	*MATα, his1-, met15Δ0, ura3Δ0, leu2::*GPD*, ade2-,* mitoGFP-*LEU2*, *DNM1-GFP-spHIS5, caf4Δ::KanMX6*
DCY2417	*MATa, his1-, met15Δ0, ura3Δ0, leu2::*GPD*,* mitoGFP-*LEU2*, *DNM1-GFP-spHIS5, mdv1Δ::KanMX6*
DCY2418	*MATa, his1-, met15Δ0, ura3Δ0, leu2::*GPD*, ade2-,* mitoGFP-*LEU2*, *DNM1-GFP-spHIS5, caf4Δ::KanMX6, mdv1::KanMX6*
DCY2192	*MATα, leu2::*GPD mitoGFP-*LEU2*, *his-, leu2Δ0, met15Δ0, ura3Δ0,* M_3TH-*FIS1*
DCY2302	*MATα, leu2::*GPD mitoGFP-*LEU2*, *his-, leu2Δ0, met15Δ0, ura3Δ0,* M_3TH-*FIS1, mdv1Δ::KanMX6*
DCY2305	*MATα, leu2::*GPD mitoGFP-*LEU2*, *his-, leu2Δ0, met15Δ0, ura3Δ0,* M_3TH-*FIS1, caf4Δ::KanMX6*
PJ69-4a	*MATa, ura3-52, leu2-3,-113, his3Δ200, trp1-901, gal4Δ, gal80Δ, GAL2-ADE2, LYS2::GAL1-HIS3, met2::GAL7-lacZ*
PJ69-4α	*MATα, ura3-52, leu2-3,-113, his3Δ200, trp1-901, gal4Δ, gal80Δ, GAL2-ADE2, LYS2::GAL1-HIS3, met2::GAL7-lacZ*

Chapter 3

Domain interactions within Fzo1p oligomers are essential for mitochondrial fusion

Erik E. Griffin and David C. Chan

The paper has been accepted for publication by the
Journal of Biological Chemistry, 2006

Domain interactions within Fzo1 oligomers are essential for mitochondrial fusion*

Erik E. Griffin and David C. Chan

From the Division of Biology, California Institute of Technology, Pasadena, CA 91125

Running Title: Domain interactions required for Fzo1 function

Address correspondence to: David C. Chan, Division of Biology, California Institute of Technology, 1200 E. California Blvd, MC114-96, Pasadena, CA 91125. Tel: (626) 395-2670; Fax: (626) 395-8826; E-Mail: dchan@caltech.edu

Mitofusins are conserved GTPases essential for the fusion of mitochondria. These mitochondrial outer membrane proteins contain a GTPase domain and two or three regions with hydrophobic heptad repeats, but little is known about how these domains interact to mediate mitochondrial fusion. To address this issue, we have analyzed the yeast mitofusin Fzo1p and find that mutation of any of the three heptad repeat regions (HRN, HR1, and HR2) leads to a null allele. Specific pairs of null alleles show robust complementation, indicating that functional domains need not exist on the same molecule. Biochemical analysis indicates that this complementation is due to Fzo1p oligomerization mediated by multiple domain interactions. Moreover, we find that two non-overlapping protein fragments, one consisting of HRN/GTPase and the other consisting of HR1/HR2, can form a complex that reconstitutes Fzo1p fusion activity. Each of the null alleles disrupts the interaction of these two fragments, suggesting that we have identified a key interaction involving the GTPase domain and heptad repeats essential for fusion.

The balance between fusion and fission maintains mitochondria as a dynamic tubular reticulum. In the absence of fusion, ongoing fission results in complete fragmentation of the

mitochondrial network. Fragmentation leads to a loss of mtDNA and respiratory incompetence in yeast (1–2) and accumulation of poorly functional mitochondria in mammals (3). Mice deficient for mitochondrial fusion die during midgestation (4), and mutations in the mitochondrial fusion genes *Mfn2* and *OPA1* cause the neurodegenerative diseases Charcot-Marie-Tooth Disease Type 2A and Dominant Optic Atrophy, respectively (5–9). Importantly, the mitochondrial fusion machinery is dedicated solely to mitochondrial fusion and does not include SNARE proteins or NSF, which mediate most other intracellular membrane fusion events. Thus, mitochondrial fusion likely involves a unique mechanism.

There are three essential components of the fusion pathway in yeast. The yeast mitofusin Fzo1p is a 98 kilodalton transmembrane GTPase uniformly distributed in the mitochondria outer membrane (1–2). Both the N- and C-terminal portions of Fzo1p are oriented towards the cytosol, in position to mediate important steps during fusion (1–2). Mgm1p is a dynamin-related protein in the mitochondrial intermembrane space (10–12). It remains unclear if Mgm1p possesses the membrane severing activity of other dynamin family members, and if so, how this activity relates to its requirement for fusion. The third component of the fusion pathway is Ugo1p, a 58 kilodalton protein that spans the outer membrane once and interacts with both Fzo1p and Mgm1p (10,12–14). In this capacity, Ugo1p may anchor a fusion complex that coordinates the mitochondrial outer and inner membranes during fusion.

Fzo1p is the best candidate to directly mediate fusion of the mitochondrial outer membrane. Unlike Mgm1p, it is positioned in the outer membrane and unlike Ugo1p its requisite role is conserved from yeast to mammals. In addition, Fzo1p has three hydrophobic heptad repeat (HR)[1] regions that are predicted to form coiled-coils. Heptad repeat regions are directly involved in SNARE and Class I viral membrane fusion. In both cases, membrane fusion is driven when a *trans* complex that spans both membranes undergoes a structural transition to a highly

stable fusogenic conformation. These fusogenic structures use coiled-coil like helical bundles to position the two membranes in close apposition, leading to fusion (15–18).

Given these similarities, it is likely that the heptad repeat regions form interactions critical for mitochondrial fusion. Indeed, the mammalian mitofusins Mfn1 and Mfn2 form homotypic and heterotypic complexes, and several intermolecular interactions have been identified. Mfn1 HR2 is known to form a *trans* anti-parallel, dimeric coiled-coil that tethers mitochondria together (19). There is also evidence that Mfn1 HR1 and HR2 interact with each other (20). Moreover, Fzo/mitofusins have similarity to dynamins, a family of large membrane-associated GTPases characterized by oligomerization-stimulated GTP hydrolysis and multiple inter- and intramolecular interactions (21). It has not been established if Fzo1p forms similar intermolecular interactions that contribute to mitochondrial fusion.

In this study, we show that Fzo1p functions as an oligomer during mitochondrial fusion. We demonstrate that each of the Fzo1p heptad repeats is essential, and that the GTPase domains and heptad repeats from different Fzo1p molecules within an oligomer function together to mediate fusion. Finally, we define a novel interaction between the HRN/GTPase and HR1/HR2 regions of Fzo1p that is essential for mitochondrial fusion.

EXPERIMENTAL PROCEDURES

Media and yeast genetic techniques— Standard genetic techniques and media were used. SD and YP media supplemented with either 2% dextrose (YPD) or 3% glycerol (YPG) were prepared as described previously (22).

DCY538 (*MATa*, *ura3-52*, *his3Δ200*, *leu2Δ1*, *trp1Δ63*, *lys2Δ202*, *fzo1*::HIS3, *leu2*::GPD-mitoGFP-*LEU2*, pRS416-*FZO1)* was derived from JSY2287 (kindly provided by J. Shaw)

(1) by integration of BstEII-linearized EG686 (pRS405 + mito-GFP) into the *leu2D1* locus. DCY328 (*MATa*, *ura3-52*, *his3Δ200*, *leu2Δ1*, *trp1Δ63*, *fzo1*::HIS3, rho^0) was derived from JSY2793 (1) by selecting for the loss of pRS414-*fzo1-1*.

Because the loss of mtDNA in *fzo1Δ* yeast is a non-revertible phenotype, a plasmid shuffle strategy was used to generate yeast strains for structure-function and intragenic allelic complementation analysis. Briefly, DCY538, a *rho*$^+$ yeast strain containing a chromosomal deletion of *FZO1* covered by an *FZO1*-expressing plasmid (pRS416-*FZO1*), was transformed with a plasmid encoding a *FZO1* under *TRP1* selection (structure-function experiments) or two *FZO1* plasmids under *TRP1* and *LYS2* selection (intragenic complementation experiments). The transformation plates were replica-plated, and the pRS416-*FZO1* plasmid was removed by counterselection with 5-fluoroorotic acid. The resulting yeast colonies were replica-plated onto YPD and YPG plates. The glycerol growth phenotype was reproducibly evident after three days of growth. In the intragenic complementation experiments, for example, all colonies showed growth on YPG plates when a pair of null alleles complemented. For quantitative serial dilution and morphological analysis, representative colonies were isolated and reanalyzed. The possibility of recombination events was excluded by the presence of many non-complementing pairs of alleles [for example, *fzo1(V172P)* and *fzo1(L819P)*], the robust complementation between non-overlapping fragments (Fzo1p-HRN/GTPase + Fzo1p-HR1/HR2), and the reproducibility of the glycerol growth phenotype among all colonies at the replica–plating stage. In addition, in the complementation experiment involving Fzo1p-HRN/GTPase and Fzo1p-HR1/HR2, Western blot analysis confirmed the expression of the proper fragments.

Mitochondrial morphology and glycerol growth analysis— Yeast strains expressing the indicated *FZO1* constructs were generated through a plasmid shuffle strategy and grown at 30°C in appropriate SD medium overnight. Cultures were diluted 1:20 in fresh YPD medium and counted

live during logarithmic growth. For glycerol growth assays, cultures grown overnight in SD medium were pelleted, resuspended at a density of 1 OD_{600} units/mL and diluted 1:5 six times in YP. 3 μL of the dilutions were spotted to plates and grown for 2 days (YPD) or 4 days (YPG) at 30°C.

Plasmid Construction— pRS414 + 9XMyc-*FZO1* (EG36) was constructed as follows: The *FZO1* terminator was amplified from genomic DNA using the oligonucleotides Eg5 (CTCTATACGAAGGAACCGTGGCTC) and Eg6 (GCAGAATTCTTGTTGTCTTTTAAATGGAG) and cloned as a ClaI/EcoRI fragment. The *FZO1* coding sequence was cloned as a SalI and ClaI fragment using the *FZO1* forward primer Eg3 (ACCATGGTCGACTCTGAAGGAAAACAACAATTC) to engineer a SalI restriction site following the initiator ATG. The *FZO1* 5'UTR was amplified using the primers Eg1 (GCAGGTACCAAGGAGTTTGTGTCGTTTTTCAC) and Eg2 (CAGAGTCGACCATGGTCGTTAAATGAGCCTACCGTTTTGCC) and cloned as a KpnI/SalI fragment. These fragments were all subcloned into pRS414 (Stratagene) to yield pRS414 + *FZO1* (EG32). Next, a 9XMyc cassette was cloned into the SalI site to yield pRS414 + 9XMyc-*FZO1* (EG36). The entire 9XMyc-*FZO1* cassette was moved as a KpnI (blunted)/EcoRI fragment into SmaI and EcoRI sites of pRS317 to generate pRS317 + 9XMyc-*FZO1* (EG197). The 9XMyc cassette in EG36 was replaced with a 6XHA cassette (XhoI/SalI fragment) to generate pRS414 + 6XHA-*FZO1* (EG594). The entire 6XHA-*FZO1* fragment was moved as a KpnI/EcoRI fragment into pRS416, resulting in pRS416 + 6XHA-*FZO1* (EG600).

pRS416 + 6XHA-*FZO1-HR1/HR2* (residues 416-855) was generated using the primer Eg253 (GCAGTCGACCATTATCATAATGAAAATG). pRS414 + 9XMyc-*FZO1-HRN/GTPase* (1-415) was generated with the primer Eg226 (GCAATCGATTGGCAATTCATCTCCGTT). Mutations were initially generated in the pRS414 + 9XMyc-*FZO1* vector with the QuickChange

site-directed mutagenesis kit (Stratagene) or by subcloning PCR products containing the indicated mutations. Primer sequences are available upon request.

Mating Assay— The indicated yeast strains were grown overnight in the appropriate SD medium, mixed by gently centrifuging together and incubated in YPD at 30°C for 5 hours. The cells were then fixed for 10 minutes with 3.7% formaldehyde and washed four times with 1 mL PBS. Large budded zygotes were scored for the complete overlap of the mito-GFP and mito-DsRed signals. Plasmids were expressed in DCY1440 (*MATα*, *his3Δ200*, *met15Δ0*, *trp1Δ63*, *ura3Δ0*, *dnm1*::HIS5, *fzo1*::KANMX6, *lue2*::GPD mito-DsRed-*LEU2*) and DCY1553 (*MATa*, *his3Δ200*, *met15Δ0*, *trp1Δ63*, *ura3Δ0*, *dnm1*::*HIS5*, *fzo1*::KANMX6, *leu2*:: GPD mito-GFP-*LEU2*). DCY1451 (*MATα*, *his3Δ200*, *met15Δ0*, *trp1Δ63*, *ura3Δ0*, *dnm1*::*HIS5*, *leu2*::GPD mito-DsRed-*LEU2*) and DCY2312 (*MATa*, *his3-*, *met15Δ0*, *ura3Δ0*, *dnm1*::kanMX6, *leu2*:: GPD mito-GFP-*LEU2*) were used for the two *FZO1 dnm1*Δ strains.

Immunoprecipitations— 9XMyc- and 6XHA-tagged Fzo1p constructs were expressed in a rho^0 *fzo1Δ* strain (EG328). The use of a rho^0 strain eliminated differences in mtDNA levels supported by functional and null alleles of *FZO1*. Overnight cultures were grown in the appropriate SD medium, diluted into YPD and harvested at OD_{600}~1.5. Approximately 50 OD_{600} units of cells were disrupted by glass bead lysis (40s with a vortex mixer, four times) in 500 μL lysis buffer (50mM Tris, pH7.4, 150mM NaCl, 0.5mM EDTA, 0.2% Triton X-100) supplemented with fungal protease inhibitors (Sigma-Aldrich). Lysates were cleared by centrifugation at 5 krpm for 5 minutes and 14 krpm for 15 minutes at 4°C. A total lysate sample was taken, and 400 μL of the remaining lysate was incubated with to 20 μL (bead volume) of 9E10-conjugated protein A Sepharose beads (Sigma-Aldrich) for 90 minutes at 4°C. The beads were then washed four times with 1 mL lysis buffer and eluted in SDS gel loading buffer for 5 min at 95°C. Western blot

analysis was performed with 9E10 hybridoma supernatant (anti-Myc) or 12CA5 ascites fluid (anti-HA).

Immunofluorescence— The indicated 9XMyc-Fzo1p constructs were introduced in DCY538 by a plasmid shuffle. YPD cultures at ~1.5 OD_{600} were fixed for 10 minutes with 3.7% formaldehyde. The cells were washed four times with water and spheroplasted with Zymolyase 100T (ICN). Spheroplasts were permeabilized for 10 minutes in blocking buffer (PBS containing 1% bovine serum albumin and 1% Tween-20) and incubated for one hour with 9E10 hybridoma diluted 1:1 in blocking buffer. After four 5-minute washes with blocking buffer, the cells were incubated with a Cy3-conjugated anti-mouse secondary antibody for one hour. After four 5-minute washes, Gel Mount (BioMedia) was added to preserve fluorescence. All incubations were performed at room temperature.

Imaging— Images were acquired on a Axiovert 200M microscope (Carl Zeiss MicroImaging, Inc.) equipped with a 100X Plan-Apochromat, NA 1.4 oil-immersion objective and controlled by the Axiovision 4.2 software. Z-stacks were collected at 100 µm to 200 µm intervals with an ORCA-ER camera (Hamamatsu) at room temperature. Iterative deconvolutions and maximun intensity projections were performed using Axiovision 4.2. Fluorescent images were overlaid with differential interference contrast images set at 50% opacity (Figure 1) using Adobe Photoshop CS.

RESULTS

Identification of essential Fzo1p domains— Fzo1p has a bipartite transmembrane domain that resides in the mitochondrial outer membrane and divides the protein into N- and C-terminal regions, both of which face towards the cytosol (Fig. 1*A*) (1,2,23). The N-terminal region contains a GTPase domain that is required for fusion (1). Fzo1p also contains three domains with hydrophobic heptad repeats. Like other mitofusins, including the mammalian Mfn1 and Mfn2, Fzo1p contains the hydrophobic heptad repeat regions HR1 and HR2, which flank the transmembrane domain. (Fig. 1*A*). However, Fzo1p also contains an additional heptad repeat region near the N-terminus that we term HRN. Because the role of these heptad repeats in Fzo1p-mediated mitochondrial fusion has not previously been assessed, we performed a structure-function analysis of Fzo1p HRN, HR1, and HR2. Our analysis made use of the fact that loss of Fzo1p function causes complete fragmentation of the mitochondrial reticulum due to ongoing mitochondrial fission (1,24). In addition, because mitochondrial fragmentation leads to a secondary loss of mitochondrial DNA, fusion mutants can grow on the fermentable carbon source dextrose but not the non-fermentable carbon source glycerol (1). Thus, we assessed the function of Fzo1p mutants by monitoring mitochondrial morphology and growth on glycerol plates.

HR1 is 64 residues long (residues 484–547 as predicted by COILS) and lies between the GTPase domain and transmembrane domain (Fig. 1*A*) (25). We substituted proline residues along HR1 to disrupt the predicted coiled-coil structure (Y490P, L518P, M525P, and K538P). Proline residues impose a kink in the protein backbone and are often incompatible with a helical fold, although sometimes such substitutions can be tolerated by local distortions in backbone geometry. The mutant *fzo1(M525P)* retained significant function, while *fzo1(Y490P)*, *fzo1(L518P), and fzo1(K538P)* were strong loss-of-function alleles, incapable of supporting growth on glycerol plates or rescuing fragmentation of the mitochondrial network (Fig. 1*B* and *C)*. In addition, we substituted alanine for leucine at two *a* and *d* positions, L501 and L504. Bulky hydrophobic residues at the *a* and *d* positions of the heptad repeat (*abcdefg*) form a stable

hydrophobic interface between the interacting helices of a coiled coil; their substitution by the smaller residue alanine is predicted to destabilize this interface. Individually, *fzo1(L501A)* and *fzo1(L504A)* behaved as mild loss-of-function alleles. However, the double mutant *fzo1(L501A, L504A)* behaved as a null allele, showing no growth on glycerol and completely fragmented mitochondrial morphology (Fig. 1*B* and *C*). Taken together, our mutagenesis of HR1 generated an allelic series and demonstrated that HR1 is essential for Fzo1p function.

In mammalian Mfn1, HR2 forms an anti-parallel dimer that tethers mitochondria together at an early step in fusion (19). Proline substitutions in Mfn1 HR2 prevent mitochondrial tethering and block mitochondrial fusion (19). Proline substitutions at residues L776, L794, and L802 of Fzo1p HR2 (residues 764–826) were tolerated with only modest effects on *FZO1* function (Fig. 1*B* and *C*). However, proline substitutions at positions Y769, L773, and L819 in HR2 caused a complete loss of function and resulted in no growth on glycerol plates and mitochondrial fragmentation (Fig. 1*B* and *C*). Thus, like Mfn1 HR2, Fzo1p HR2 is essential for mitochondrial fusion.

HRN (residues 91–190) is also required for *FZO1* function. Initial experiments showed that N-terminal truncations that spared HRN had little effect on *FZO1* activity, whereas truncations that deleted portions of HRN behaved as null alleles[2]. In addition, *fzo1(L98P)* had only slight loss of function, whereas *fzo1(V172P)* behaved as a null allele (Fig. 1*B* and *C*). Taken together, these results indicate that like HR1 and HR2, HRN is essential for Fzo1p activity.

We made several further observations in our structure-function analysis. First, consistent with previous reports, mutations in the GTPase domain of *FZO1* [*fzo1(K200A), fzo1(S201N), fzo1(T221A)*] all caused complete fragmentation of the mitochondrial reticulum (1). Second, in several of the null mutants [including *fzo1(V172P)*, *fzo1(T221A)*, *fzo1(Y490P)*, and *fzo1(L518P)*] the mitochondrial fragments frequently formed loose aggregates (Fig. 1*C*). The basis of this aggregation is unclear, but may reflect the trapping of tethered intermediates. Finally, the

charged residues present in the bipartite transmembrane domain are not essential for fusion. Fzo1p has three lysines (K727, K735, and K736) in the region of the transmembrane domain thought to form a U-turn in the intermembrane space. The triple mutant *fzo1(K727A, K735A, K736A)* was highly functional (Fig. 1*B* and *C*). Thus, although the loop residing in the intermembrane space is important for Fzo1p function (23), its charged nature is not essential.

Intragenic complementation between FZO1 null alleles— Mammalian mitofusins have been shown to form higher order complexes (4,26) and Fzo1p has been shown to be present in a high molecular weight complex in yeast (2). In unusual cases, proteins that self-assemble can show intragenic complementation, a genetic phenomenon that results from formation of a functional complex from individually nonfunctional subunits (27). To test whether yeast Fzo1p could exhibit intragenic complementation, we used a plasmid shuffle strategy to construct *fzo1Δ* strains co-expressing two null *fzo1* alleles. The function of the co-expressed null alleles was evaluated by growth on glycerol plates and mitochondrial morphology. Based on our results above, we used *fzo1(V172P)*, *fzo1(L501A, L504A)*, and *fzo1(L819P)* as representative null alleles with mutations in HRN, HR1, and HR2, respectively (Fig. 2*A*). These mutants were tested along with the three GTPase mutants.

With these six mutants, we constructed 15 pairwise combinations, and intragenic complementation was reproducibly observed in six cases (Table 1 and Fig. 2). Co-expression of either of two GTPase mutants with a heptad repeat (HR) mutant restored Fzo1p function. In repeated trials, the GTPase mutants *fzo1(K200A)* or *fzo1(T221A)* showed strong complementation with either *fzo1(V172P)*, *fzo1(L501A, L504A)* or *fzo1(L819P),* resulting in tubular mitochondrial morphology that corresponded with a restored ability to grow on glycerol plates (Fig. 2*B* and *C*). Thus, Fzo1p activity can occur when the function of the GTPase and heptad repeat regions reside

on different Fzo1p molecules. These complementation data also indicate that the null mutations do not have global effects on Fzo1p structure.

In contrast, many pairs of alleles failed to complement. The GTPase mutant *fzo1(S201N)* did not complement any of the heptad repeat mutants (see next section). No complementation was observed when an HR1 mutant [*fzo1(L501A, L504A)*] was co-expressed with an HR2 mutant [*fzo1(L819P)*] or an HRN mutant [*fzo1(V172P)*] (Fig. 2*B* and *C*). In addition, when an HRN mutant was co-expressed with an HR2 mutant, *FZO1* activity was not restored (Fig. 2*B* and *C*). Finally, co-expression of any two GTPase mutants did not restore mitochondrial fusion.

The simplest interpretation of these data is that Fzo1p functions as an oligomer in which GTPase and heptad repeat activity can be donated by different molecules. However, it is also possible that the GTPase and heptad repeat regions act independently (for example, sequentially) at different steps in the fusion pathway. We sought to distinguish these possibilities by testing directly for Fzo1p oligomerization.

Fzo1p functions as an oligomer— We sought evidence for Fzo1p oligomerization by using a co-immunoprecipitation assay. In these experiments, HA-Fzo1p and Myc-Fzo1p were co-expressed at endogenous levels in *fzo1Δ* cells. When Myc-Fzo1p was immunoprecipitated, approximately 10% of HA-Fzo1p co-immunoprecipitated (Fig. 3, *lane 3*). Similarly, the mammalian orthologs Mfn1 and Mfn2 have previously been shown to form homotypic and heterotypic complexes (4). Taken in conjunction with our intragenic complementation results, these interaction data strongly suggest that Fzo1p functions as an oligomer during mitochondrial fusion.

If intragenic complementation is due to oligomerization between mutant Fzo1p molecules, we would expect complementing mutant pairs to co-immunoprecipitate. Indeed, the Fzo1p GTPase mutants *fzo1(T221A)* and *fzo1(K200A)* interacted with each of the heptad repeat mutants *fzo1(V172P)*, *fzo1(L501A, L504A)*, and *fzo1(L819P)* (Fig. 3, *lanes 4-6, 10–12*). In

contrast, *fzo1(S201N)* interacted weakly with all the heptad repeat mutants (Fig. 3, *lanes 7–9*) and was unable to complement (Table 1, Fig. 2), suggesting efficient oligomerization is necessary for intragenic complementation.

Surprisingly, all of our null mutants retained the ability to form homotypic interactions. Mutations in HRN, HR1, HR2 or in both HR1 and HR2 had little effect on Fzo1p self-assembly (Fig. 4, *lanes 7–10*). More of an effect was seen with the GTPase mutants, most notably S201N, which displayed the lowest levels of interaction (Fig. 4, *lanes 4–6*). Given that mutations in no single domain completely disrupt Fzo1p interactions, we conclude that oligomerization of Fzo1p likely involves interactions between multiple domains, and that the null phenotypes of the heptad repeat and GTPase mutants are not a result of Fzo1p dissociation.

Interaction between Fzo1p-HRN/GTPase and Fzo1p-HR1/HR2—Because several domains likely work in concert to stabilize full-length Fzo1p oligomerization, we attempted to develop a simplified system for examining domain interactions. We tested whether fragments of Fzo1p could physically interact with each other. We analyzed an N-terminal Fzo1p fragment containing HRN and the GTPase domain (Fzo1p-HRN/GTPase, residues 1–415) and a C-terminal fragment that includes HR1, the TM and HR2 (Fzo1p-HR1/HR2, residues 416–855). Fzo1p-HR1/HR2, like full-length Fzo1p, interacted efficiently with full-length Fzo1p (Fig. 5, *lanes 3 and 10*). A weaker interaction was also seen between two Fzo1p-HR1/HR2 fragments (Fig. 5, *lane 11*). Most interestingly, the non-overlapping Fzo1p-HRN/GTPase and Fzo1p-HR1/HR2 fragments interacted with each other as efficiently as the full-length Fzo1p/Fzo1p interaction (Fig. 5, *lane 12*). Thus, Fzo1p-HR1/HR2 has at least two modes of interaction; a homotypic interaction with itself and a heterotypic interaction with Fzo1p-HRN/GTPase.

We confirmed the interaction between Fzo1p-HRN/GTPase and Fzo1p-HR1/HR2 by showing that Fzo1p-HR1/HR2 can recruit Fzo1p-HRN/GTPase to mitochondria. Full-length

Myc-Fzo1p (n=200, Fig. 5, *B-D*) and Fzo1p-HR1/HR2 (data not shown) displayed a uniform mitochondrial localization pattern in all cells. In contrast, Myc-Fzo1p-HRN/GTPase localization was non-mitochondrial and probably cytosolic in all cells (n=200, Fig. 5, *E-G*). However, co-expression with the mitochondrial HA-Fzo1p-HR1/HR2 caused redistribution of Myc-Fzo1p-HRN/GTPase to mitochondria in 41% (7% completely mitochondrial, 34.5% mitochondrial and cytosolic) of cells (n=200, Fig. 5, *H-J*). These data confirm the physical interaction between Fzo1p-HRN/GTPase and Fzo1p-HR1/HR2 and indicate that this interaction occurs on mitochondria.

Having identified an interaction between these two Fzo1p fragments, we tested whether this interaction is functionally important. The null mutations identified previously were tested for their effect on the binding of Fzo1p-HRN/GTPase to Fzo1p-HR1/HR2. When mutations in either HR1 or HR2 were introduced into Fzo1p-HR1/HR2, its interaction with Fzo1p-HRN/GTPase was completely abolished (Fig. 6, *lanes 11–13*). Similarly, when mutations in HRN or the GTPase domain were introduced into Fzo1p-HRN/GTPase, its interaction with Fzo1p-HR1/HR2 was abolished (Fig. 6, *lanes 7–10*). Therefore, our null alleles indicate that the interaction of Fzo1p-HRN/GTPase with Fzo1p-HR1/HR2 is essential for fusion.

Functional complementation between Fzo1p-HRN/GTPase and Fzo1p-HR1/HR2— Given their physical interaction on mitochondria, we tested if co-expression of Fzo1p-HRN/GTPase and Fzo1p-HR1/HR2 could restore mitochondrial fusion. When expressed individually, neither fragment supported growth on glycerol or rescued mitochondrial morphology (Fig. 7 *A* and *B*). Remarkably, the co-expression of Fzo1p-HRN/GTPase and Fzo1p-HR1/HR2 was sufficient to restore fusion. These cells grew robustly on glycerol plates, and displayed largely tubular mitochondria (Fig. 7 *A* and *B*). Moreover, cells co-expressing the Fzo1p fragments show significant mitochondrial fusion in the zygotic fusion assay (Table 2) (28). These data indicate

that Fzo1p-HRN/GTPase and Fzo1p-HR1/HR2 form a complex competent to support mitochondrial fusion.

DISCUSSION

In this study, we show that Fzo1p functions as an oligomer during mitochondrial fusion. In support of this conclusion, Fzo1p forms homotypic oligomers detectable by co-immunoprecipitation. In addition, specific pairs of *fzo1* null alleles are capable of intragenic complementation. Intragenic complementation can occur between pairs of mutants if each mutant affects a different domain of an oligomerized multi-domain protein. Within the oligomer, different functional domains are donated from distinct molecules, resulting in the restoration of activity (27). An alternative senario for intragenic complementation is that the GTPase and heptad repeat domains are not required on the same molecule because they act at different steps in the fusion reaction. While we cannot formally exclude this latter explanation, the observation that Fzo1p molecules physically associate strongly favors the former model.

Our intragenic complementation data provide insight into the requirements for the activity of different domains on Fzo1p molecules within these oligomers. Within an Fzo1p oligomer, one molecule must possess the activity of all three heptad repeats (for example, a GTPase mutant). A second molecule must possess GTPase activity but not necessarily full heptad repeat activity (for example, an HRN, HR1 or HR2 mutant). Thus co-expression of Fzo1p molecules with heptad repeat activity and Fzo1p molecules with GTPase activity restores fusion, while co-expression of two heptad repeat mutants or two GTPase mutants does not restore fusion. Because Fzo1p is required on adjacent mitochondria to support fusion (29), an interesting question that remains to be addressed is whether the intragenic complementation we observe occurs in *cis* (in a complex formed on one mitochondrion) or in *trans* (in a complex that spans two mitochondria prior to fusion). In principle, this issue could be determined using an *in vitro*

fusion assay, but unfortunately the available assay does not work for mitochondria isolated from yeast that are incompetent for respiration (29).

We have also identified binding of Fzo1p-HRN/GTPase to Fzo1p-HR1/HR2 as an interaction critical for mitochondrial fusion. First, co-expression of Fzo1p-HRN/GTPase and Fzo1p-HR1/HR2 supports mitochondrial fusion. Second, these Fzo1p fragments physically interact with each other. Finally, mutations in the GTPase domain or heptad repeat regions block this interaction and cause complete loss of mitochondrial fusion activity.

Future work will help to resolve the complex interactions occurring between Fzo1p molecules. Fzo1p is a large membrane-associated GTPase with some similarities to the dynamin family of mechanochemical membrane severing enzymes. Dynamins are characterized by their oligomerization-dependent stimulation of GTP hydrolysis. Thus, it will be interesting to test the possibility that intermolecular interactions within an Fzo1p oligomer regulate its GTPase activity. Given that co-expression of a functional GTPase domain on one Fzo1p molecule and functional heptad repeat regions on another molecule is sufficient to support fusion, it is possible that the heptad repeats could play a role in regulating GTPase activity. For example, based on its location near the C-terminus, it has been suggested HR2 could function analogously to the GTPase Effector Domain (GED) of dynamin (21). *In vitro* characterization of recombinant Fzo1p fragments can be used to address this possibility. Ultimately, structural information will be required to fully understand the nature of the Fzo1p oligomer.

REFERENCES

1. Hermann, G. J., Thatcher, J. W., Mills, J. P., Hales, K. G., Fuller, M. T., Nunnari, J., and Shaw, J. M. (1998) *J Cell Biol* **143**(2), 359–373

2. Rapaport, D., Brunner, M., Neupert, W., and Westermann, B. (1998) *J Biol Chem* **273**(32), 20150–20155

3. Chen, H., Chomyn, A., and Chan, D. C. (2005) *J Biol Chem* **280**(28), 26185–26192

4. Chen, H., Detmer, S. A., Ewald, A. J., Griffin, E. E., Fraser, S. E., and Chan, D. C. (2003) *J Cell Biol* **160**(2), 189–200

5. Alexander, C., Votruba, M., Pesch, U. E., Thiselton, D. L., Mayer, S., Moore, A., Rodriguez, M., Kellner, U., Leo-Kottler, B., Auburger, G., Bhattacharya, S. S., and Wissinger, B. (2000) *Nat Genet* **26**(2), 211–215

6. Delettre, C., Lenaers, G., Griffoin, J. M., Gigarel, N., Lorenzo, C., Belenguer, P., Pelloquin, L., Grosgeorge, J., Turc-Carel, C., Perret, E., Astarie-Dequeker, C., Lasquellec, L., Arnaud, B., Ducommun, B., Kaplan, J., and Hamel, C. P. (2000) *Nat Genet* **26**(2), 207–210

7. Kijima, K., Numakura, C., Izumino, H., Umetsu, K., Nezu, A., Shiiki, T., Ogawa, M., Ishizaki, Y., Kitamura, T., Shozawa, Y., and Hayasaka, K. (2005) *Hum Genet* **116**(1-2), 23–27

8. Lawson, V. H., Graham, B. V., and Flanigan, K. M. (2005) *Neurology* **65**(2), 197–204

9. Zuchner, S., Mersiyanova, I. V., Muglia, M., Bissar-Tadmouri, N., Rochelle, J., Dadali, E. L., Zappia, M., Nelis, E., Patitucci, A., Senderek, J., Parman, Y., Evgrafov, O., Jonghe, P. D., Takahashi, Y., Tsuji, S., Pericak-Vance, M. A., Quattrone, A., Battaloglu, E., Polyakov, A. V., Timmerman, V., Schroder, J. M., and Vance, J. M. (2004) *Nat Genet* **36**(5), 449–451

10. Sesaki, H., Southard, S. M., Yaffe, M. P., and Jensen, R. E. (2003) *Mol Biol Cell* **14**(6), 2342–2356

11. Wong, E. D., Wagner, J. A., Gorsich, S. W., McCaffery, J. M., Shaw, J. M., and Nunnari, J. (2000) *J Cell Biol* **151**(2), 341–352

12. Wong, E. D., Wagner, J. A., Scott, S. V., Okreglak, V., Holewinske, T. J., Cassidy-Stone, A., and Nunnari, J. (2003) *J Cell Biol* **160**(3), 303–311

13. Sesaki, H., and Jensen, R. E. (2001) *J Cell Biol* **152**(6), 1123–1134

14. Sesaki, H., and Jensen, R. E. (2004) *J Biol Chem* **279**(27), 28298–28303

15. Bonifacino, J. S., and Glick, B. S. (2004) *Cell* **116**(2), 153–166

16. Eckert, D. M., and Kim, P. S. (2001) *Annu Rev Biochem* **70**, 777–810

17. Skehel, J. J., and Wiley, D. C. (1998) *Cell* **95**(7), 871–874

18. Ungar, D., and Hughson, F. M. (2003) *Annu Rev Cell Dev Biol* **19**, 493–517

19. Koshiba, T., Detmer, S. A., Kaiser, J. T., Chen, H., McCaffery, J. M., and Chan, D. C. (2004) *Science* **305**(5685), 858–862

20. Rojo, M., Legros, F., Chateau, D., and Lombes, A. (2002) *J Cell Sci* **115**(Pt 8), 1663–1674

21. Praefcke, G. J., and McMahon, H. T. (2004) *Nat Rev Mol Cell Biol* **5**(2), 133–147

22. Gunthrie, C., and Fink, G. (1991) *Guide to Yeast Genetics and Molecular Biology*, Academic Press, San Diego, CA

23. Fritz, S., Rapaport, D., Klanner, E., Neupert, W., and Westermann, B. (2001) *J Cell Biol* **152**(4), 683–692

24. Sesaki, H., and Jensen, R. E. (1999) *J Cell Biol* **147**(4), 699–706

25. Lupas, A., Van Dyke, M., and Stock, J. (1991) *Science* **252**(5010), 1162–1164

26. Eura, Y., Ishihara, N., Yokota, S., and Mihara, K. (2003) *J Biochem (Tokyo)* **134**(3), 333–344

27. Zhang, Y., Billington, C. J., Jr., Pan, D., and Neufeld, T. P. (2006) *Genetics* **172**(1), 355–362

28. Nunnari, J., Marshall, W. F., Straight, A., Murray, A., Sedat, J. W., and Walter, P. (1997) *Mol Biol Cell* **8**(7), 1233–1242

29. Meeusen, S., McCaffery, J. M., and Nunnari, J. (2004) *Science* **305**(5691), 1747–1752

FOOTNOTES

[*] Supported by National Institutes of Health grant GM62967 (to D.C.C.). D. Chan is a Beckman Young Investigator and Bren Scholar.

[1] The abbreviations used are: HR, heptad repeat; SD, synthetic media with 2% dextrose; YP, yeast extract peptone; mito-GFP, mitochondrially targeted green fluorescent protein; mito-DsRed, mitochondrially targeted red fluorescent protein from *Discosoma*; mtDNA, mitochondrial DNA.

[2] E. Griffin and D. Chan, unpublished results.

ACKNOWLEDGMENTS

We thank Janet Shaw for stimulating discussions on allelic complementation.

FIGURE LEGENDS

Fig. 1. Identification of critical regions of Fzo1p. *A*, Schematic of Fzo1p including HRN (residues 91–190), the GTPase domain (residues 194–373), HR1 (residues 484–547), the bipartite transmembrane (TM) domain (residues 717–750), and HR2 (residues 769–831). The point mutations analyzed are indicated below. *B*, A serial dilution growth assay to analyze *fzo1Δ* yeast expressing the indicated alleles of *FZO1*. Growth on rich dextrose (YPD) and glycerol (YPG) plates are shown. These strains were generated through a plasmid shuffle strategy in which pRS416 + *FZO1* is replaced by a pRS414 + 9XMyc-*FZO1* plasmid containing the indicated mutations. Null alleles analyzed further in the paper are indicated in bold. *C*, Summary of mitochondrial morphologies in yeast expressing the indicated *fzo1* mutant. Examples of the morphology classes are shown in the images above. Two hundred live cells were analyzed during log phase growth in minimal selective media; percentages are indicated.

Fig. 2. Allelic complementation between null alleles of *FZO1*. *A*, Schematic of the null mutations used for allelic complementation analysis. Asterisks are used to indicate the mutations in HRN (V172P), HR1 (L501A, L504A) and HR2 (L819P) in (*B*). *B*, Serial dilution assay for growth on dextrose and glycerol plates. The assays were performed as in Fig. 1, except that the null *FZO1* alleles were co-expressed from pRS414 + 9XMyc-*FZO1* and pRS317 + 9XMyc-*FZO1*

plasmids. A schematic of the different co-expressed alleles is indicated on the left. *C*, Summary of mitochondrial morphologies in yeast expressing the indicated alleles. Two hundred live cells were counted for each strain; percentages are indicated.

Fig. 3. Self-association of Fzo1p. Lysates (labeled "Lysate") from yeast expressing the indicated HA-Fzo1p and Myc-Fzo1p alleles were immunoprecipitated with anti-Myc antibodies (labeled "Myc IP") and analyzed by western blotting with anti-Myc (9E10) and anti-HA (12CA5) antibodies. The immunoprecipitate samples are loaded at 10 equivalents of the lysate samples.

Fig. 4. Fzo1p null mutants form homotypic oligomers. Co-immunoprecipitations were performed as in Fig. 3. Yeast strains contained Myc- and HA-tagged alleles of Fzo1p as indicated. HRN: V172P; HR1: L501A, L504A; HR2: L819P; HR1/2: L501A, L504A, L819P.

Fig. 5. Two interacting fragments of Fzo1p. *A*, Co-immunoprecipitations were performed as in Fig. 3. Fzo1p-HRN/GTPase (residues 1-415) is referred to as 'N' and Fzo1p-HR1/HR2 (residues 416-855) is referred to as 'C'. wt: full-length Fzo1p. *B-J*, Immunofluorescence (red, middle panels) was used to localize Myc-tagged full-length Fzo1p (Myc-Fzo1p, panels *B-D*), Myc-Fzo1p-HRN/GTPase (panels *E-G*), and Myc-Fzo1p-HRN/GTPase when co-expressed with HA-Fzo1p-HR1/HR2 (panels *H-J*) in *fzo1Δ* cells. Mitochondria were labeled with mito-GFP (left panels). Overlays of the two signals are shown in the merged images (right panels). Bar, 1 μm.

Fig. 6. The GTPase and heptad repeat regions are required for the interaction between Fzo1p-HRN/GTPase and Fzo1p-HR1/HR2. Co-immunoprecipitations were performed and labeled as in Fig. 3. The indicated mutations were present in either Fzo1p-HRN/GTPase (HRN: V172P;

K200A; S201N; T221A) or HA-Fzo1p-HR1/HR2 (HR1: L501A,L504A, HR2: L819P). FL: full-length wild-type Fzo1p.

Fig. 7. Co-expression of the Fzo1p-HRN/GTPase and Fzo1p-HR1/HR2 fragments of Fzo1p complements *fzo1Δ*. *A*, Serial dilution assay for growth on glycerol was performed as described in Fig. 1. *B*, Percentage of cells displaying the indicated mitochondrial morphologies during log phase growth in selective minimal dextrose media (images of the morphological classes are provided in Fig. 1). Two hundred live cells were counted for each strain.

Table 1.

	K200A	S201N	T221A	V172P	L501A,504A	L819P
K200A		-	-	+	+	+
S201N	-		-	-	-	-
T221A	-	-		+	+	+
V172P	+	-	+		-	-
L501A,504A	+	-	+	-		-
L819P	+	-	+	-	-	

Table 1. Summary of intragenic complementation data presented in Figure 2. For simplicity, each data point is presented twice. "+" indicates growth on glycerol plates and tubular mitochondrial morphology. "-" indicates failure to grow on glycerol plates and fragmented mitochondrial morphology.

Table 2

Strains Mated	**Mitochondrial Fusion**
FZO1 dnm1Δ x *FZO1 dnm1Δ*	96%
fzo1Δ dnm1Δ x *fzo1Δ dnm1Δ*	0%
fzo1Δ dnm1Δ + pRS414-*9XMYC-FZO1* x *fzo1Δ dnm1Δ* + pRS414-*9XMYC-FZO1*	86%
fzo1Δ dnm1Δ + pRS414-*9XMYC-FZO1(HRN/GTPase)* + pRS416-6XHA-*FZO1(HR1/HR2)* x *fzo1Δ dnm1Δ* + pRS414-*9XMYC-FZO1(HRN/GTPase)* + pRS416-6XHA-*FZO1(HR1/HR2)*	38.5%

Table 2. Yeast expressing mito-GFP and mito-DsRed were mated in YPD for 5 hours.

Following fixation, 200 large-budded zygotes were scored for mitochondrial fusion.

Figure 1

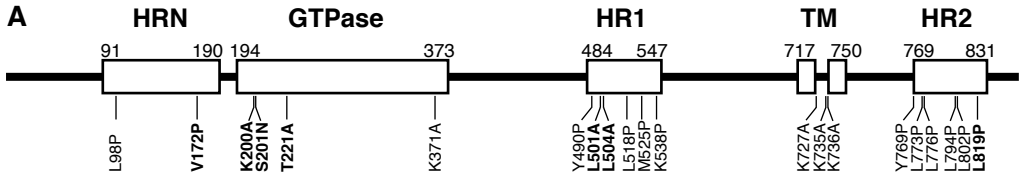

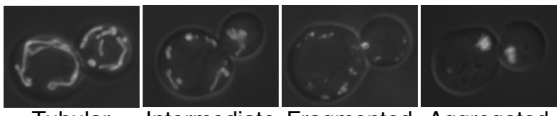

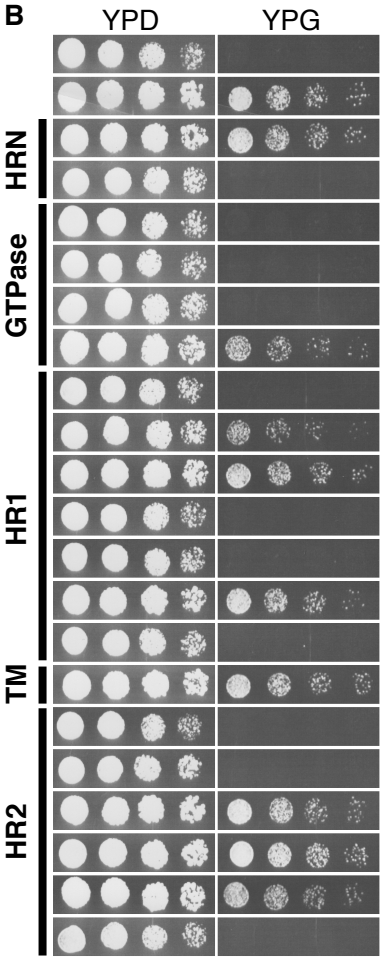

		Tubular	Intermediate	Fragmented	Aggregated
	*fzo1*Δ	0	5	88.5	6.5
	WT	74.5	9.5	5.5	10.5
HRN	L98P	65.5	9	15	10.5
HRN	**V172P**	0	12	42	46
GTPase	**K200A**	0	10	80	10
GTPase	**S201N**	0	10.5	81	8.5
GTPase	**T221A**	0	8	52.5	39.5
GTPase	K371A	37.5	28	29	5.5
HR1	Y490P	0	8	37	55
HR1	L501A	33.5	22	25.5	19
HR1	L504A	42	16.5	28.5	13
HR1	**L501A, L504A**	0	5.5	80.5	14
HR1	L518P	0	4.5	48.5	47
HR1	M525P	45	15.5	24	15.5
HR1	K538P	3	13	74	10
TM	K727A, K735A, K736A	44.5	17.5	26	12
HR2	Y769P	0	10	81.5	8.5
HR2	L773P	0	16.5	71	12.5
HR2	L776P	50.5	15	20	14.5
HR2	L794P	44	19.5	25	11.5
HR2	L802P	35.5	19.5	27	18
HR2	**L819P**	0	9	69.5	21.5

Figure 2

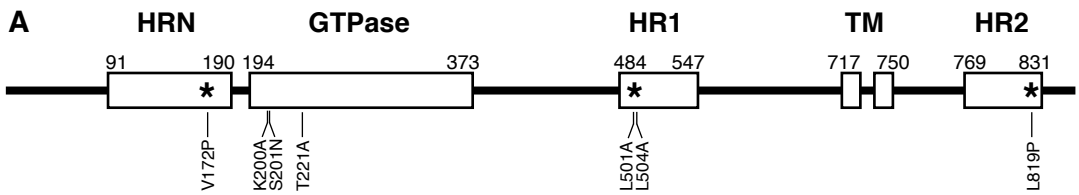

B

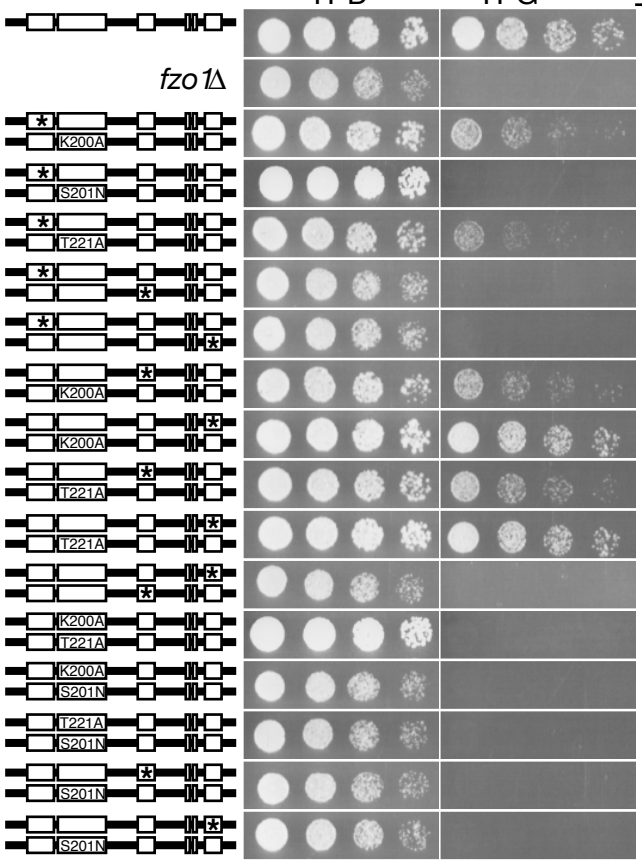

C

	Tubular	Intermediate	Fragmented	Aggregated
	76	12.5	8.5	3
fzo1Δ	0	7.5	85.5	7
K200A	31	29.5	29	10.5
S201N	0	8.5	55.5	36
T221A	10.5	44	18.5	27
	0	19	42.5	38.5
	0	7.5	51	41.5
K200A	19.5	38.5	23	19
K200A	69.5	12.5	15.5	2.5
T221A	18	35	15	32
T221A	41	13.5	28.5	17
	1	16	49.5	33.5
K200A T221A	0	12	47.5	40
K200A S201N	0.5	17	75.5	7
T221A S201N	0	14.5	65	20.5
S201N	0	18.5	48	33.5
S201N	0	16.5	70.5	13

Figure 3

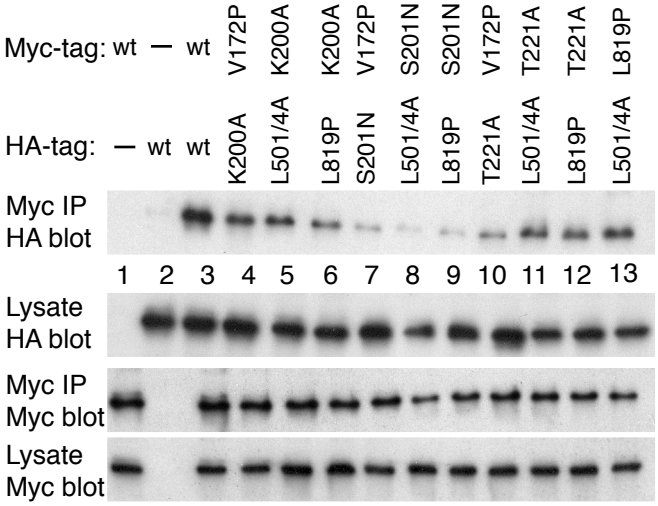
Myc-tag: wt — wt V172P K200A K200A V172P S201N S201N V172P T221A T221A L819P
HA-tag: — wt wt K200A L501/4A L819P S201N L501/4A L819P T221A L501/4A L819P L501/4A
Myc IP
HA blot
1 2 3 4 5 6 7 8 9 10 11 12 13
Lysate
HA blot
Myc IP
Myc blot
Lysate
Myc blot

Figure 4

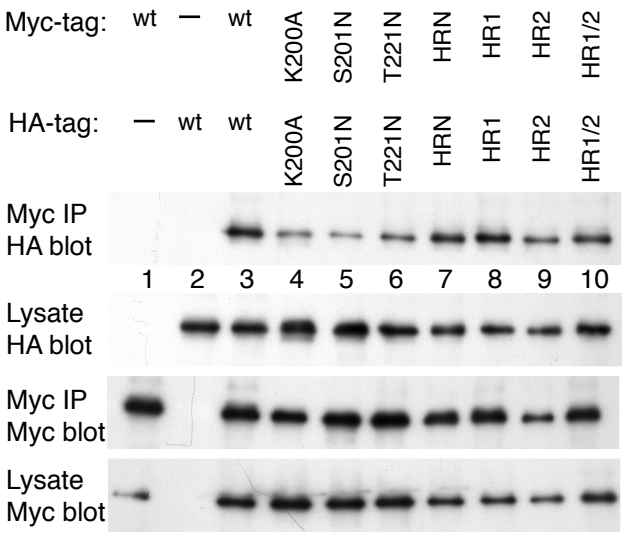
Myc-tag:
wt
—
wt
K200A
S201N
T221N
HRN
HR1
HR2
HR1/2
HA-tag:
—
wt
wt
K200A
S201N
T221N
HRN
HR1
HR2
HR1/2
Myc IP
HA blot
1 2 3 4 5 6 7 8 9 10
Lysate
HA blot
Myc IP
Myc blot
Lysate
Myc blot

Figure 5

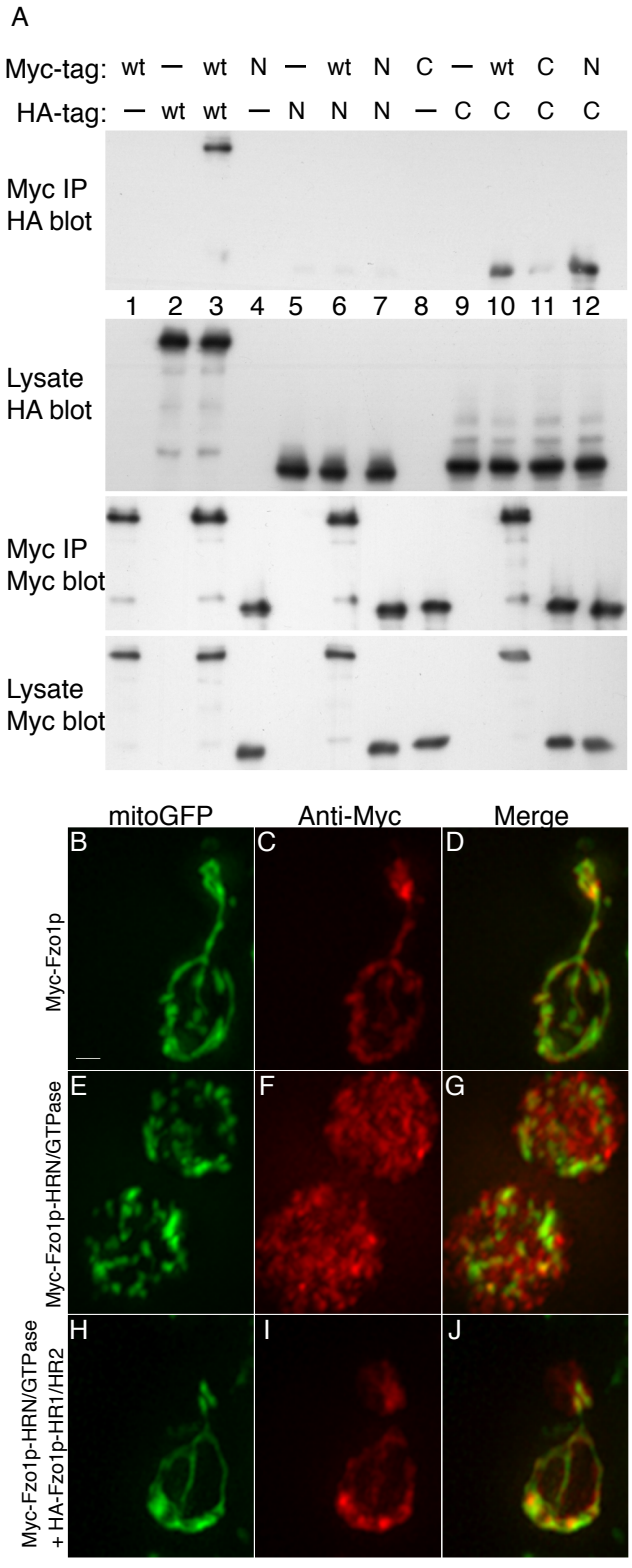
A
Myc-tag: wt — wt N — wt N C — wt C N
HA-tag: — wt wt — N N N — C C C C
Myc IP
HA blot
1 2 3 4 5 6 7 8 9 10 11 12
Lysate
HA blot
Myc IP
Myc blot
Lysate
Myc blot
mitoGFP
Anti-Myc
Merge
B
C
D
Myc-Fzo1p
E
F
G
Myc-Fzo1p-HRN/GTPase
H
I
J
Myc-Fzo1p-HRN/GTPase
+ HA-Fzo1p-HR1/HR2

Figure 6

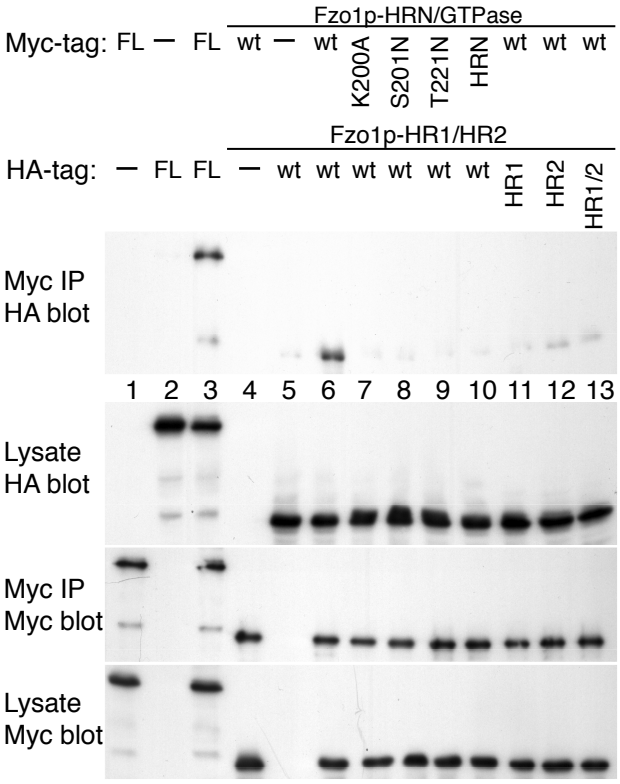
Fzo1p-HRN/GTPase
Myc-tag: FL — FL wt — wt K200A S201N T221N HRN wt wt wt
Fzo1p-HR1/HR2
HA-tag: — FL FL — wt wt wt wt wt wt HR1 HR2 HR1/2
Myc IP
HA blot
1 2 3 4 5 6 7 8 9 10 11 12 13
Lysate
HA blot
Myc IP
Myc blot
Lysate
Myc blot

Figure 7

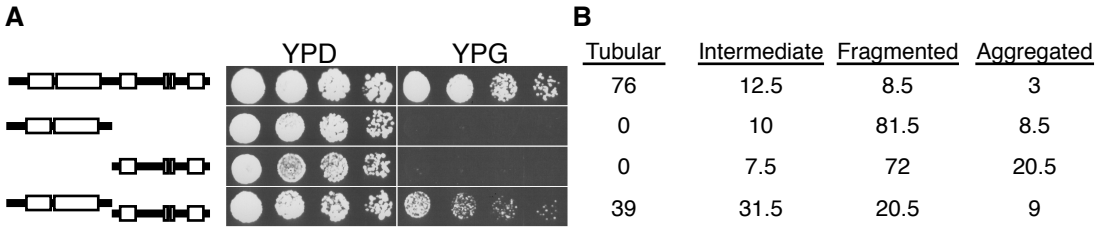
A
YPD
YPG
B
Tubular
Intermediate
Fragmented
Aggregated
76
12.5
8.5
3
0
10
81.5
8.5
0
7.5
72
20.5
39
31.5
20.5
9

Chapter 4: Om14p interacts with Fzo1p and Ugo1p and negatively regulates mitochondrial fusion

Erik Griffin, Johannes Graumann, and David Chan

Johannes Graumann is a graduate student in Ray Deshaies' lab at Caltech where he performed the MudPIT analysis described in this paper.

Abstract

We have identified Om14p as a novel glycerol-induced regulator of mitochondrial morphology. Om14p is a mitochondrial outer membrane protein that physically interacts with two proteins that mediate mitochondrial fusion: Fzo1p and Ugo1p. *om14Δ* cells have a simplified mitochondrial morphology, which suggests an increase in mitochondrial fusion. Additionally, *om14Δ* partially rescues a hypomorphic *fzo1* allele by increasing mitochondrial fusion. Based on these data, we propose *OM14* is the first negative regulator of mitochondrial fusion.

Introduction

Mitochondria are dynamic organelles that maintain a tubular morphology through balanced levels of fusion and fission (Nunnari et al., 1997; Sesaki and Jensen, 1999). Mitochondrial morphology is responsive to energetic, developmental, and apoptotic cues. For example, in yeast, the shift from dextrose fermentation to glycerol respiration results in dramatic elaboration of the mitochondrial reticulum (Egner et al., 2002). Interestingly, mitochondria isolated from respiring cells are more active in an *in vitro* fusion assay than mitochondria isolated from fermenting cells (Meeusen et al., 2004), suggesting the morphological changes may result from regulation of mitochondrial fusion. Understanding how mitochondrial dynamics are regulated may contribute to understanding the basis for diseases that result from imbalances between fusion and fission (Alexander et al., 2000; Zuchner et al., 2004).

Three proteins are required for mitochondrial fusion in yeast. The transmembrane GTPase Fzo1p mediates mitochondrial outer membrane fusion (Hermann et al., 1998;

Rapaport et al., 1998). Mgm1p is a dynamin-related protein in the intermembrane space required for outer, and potentially inner membrane fusion (Sesaki and Jensen, 2004; Wong et al., 2003). Ugo1p is an outer membrane protein that interacts with both Fzo1p and Mgm1p and may coordinate inner and outer membrane fusion (Sesaki and Jensen, 2004; Wong et al., 2003). Very little is understood about how these proteins mediate membrane fusion or how their activities are regulated.

In this study, we used a proteomics-based approach to identify the mitochondrial outer membrane protein Om14p as a new Fzo1p and Ugo1p binding partner. Om14p is required for wild-type mitochondrial morphology in respiring cultures. *om14Δ* cells support increased mitochondrial fusion, suggesting Om14p may be the first inhibitor of mitochondrial fusion.

Materials and Methods

Yeast Strains

The yeast strains used in this study are listed in Table 1. 9XMyc/TEV/His_8-*FZO1* (DCY1624) was generated in the same manner as described previously for M9TH-*FIS1* (DCY1557) except the *FZO1* targeting oligos Eg265 (gatatcacggatagaggcaaaacggtaggctcatttaacgatggtcgagggatcc) and Eg266 (cggtttattgctgtctttgaattgttgttttccttcagacatgccgccatgatgatgatg) were used (Griffin et al., 2005). *UGO1*-His_8/TEV/3XMyc (DCY2139) was generated by amplifying a His_8/TEV/3XMyc/*HIS5* cassette from EG1005 using the primers Eg142 (caaatgatgaataaagttgatatcaacatggaacaagagaagttcggtggcagccatcaccaccatc) and Eg143 (caaaaattgtggagaaaaagggccactggaataccatgggcgaacgcgttagtatcgaatcgac). DCY2766 was

derived from the *MATa* haploid deletion library (Open Biosystems) by transformation of NarI linearized EG686 (Griffin et al., 2005). DCY2869 and DCY2871 are two clones derived from JSY2793 (Hermann et al., 1998) obtained by deleting replacing *yBR230c* with a kanamycin cassette using the primers Eg396 (attccaacaattagaaacataacatctacctccagcatctcataatagattgtactgagagtgcac) and Eg397 (gtgagtgtgtgagtgtgtgaaaggatgttattaaatagtatgttactgtgcggtatttcacaccg).

Zygotic mitochondrial fusion assay

DCY1440, DCY1553, DCY2789, and DCY2834 expressing a temperature sensitive allele of *FZO1* (EG1210; pRS416 + *fzo1-1*) were grown to log phase in selective SGE at room temperature. Matings were initiated by mixing two strains and pelleting them at 5 krpm for 30 seconds. Pellets were gently resuspended in YPGE and incubated at the indicated temperatures until large budded zygotes had formed (~ 8 hours). Cells were fixed for 10 minutes with pre-warmed 37% formaldehyde, washed four times with 1 ml PBS and large budded zygotes were scored for complete colocalization of mito-GFP and mito-DsRed.

Coimmumoprecipitations

Indicated strains were harvested from YP media supplemented with the indicated carbon source at OD_{600} ~1.0. ~ 50 OD units of cells were lysed with glass beads in 500 µl ice cold YLB (50 mM Tris, 150 mM NaCl, 0.5 mM EDTA, 0.2% Triton X-100, pH 7.4) supplemented with Fungal Protease inhibitors (Sigma-Aldrich) using a vortex mixer 4 times for 40 seconds. Lysates were cleared by centrifuging at 5 krpm for 5 minutes then

14 krpm for 15 minutes. At this point, a total lysate sample was taken. The remaining lysate was added to 20 μl IgG Sepharose beads (Amersham Biosciences) and incubated at 4°C for 90 minutes. Beads were washed four times with 1 ml YLB and brought to 150 μl with YLB. 50 μl were saved as the TAP-IP sample and analyzed by SDS-PAGE Western blot using anti-HA (12CA5) and anti-TAP (Open Biosystems) antibodies.

Miscellaneous

Mitochondrial morphology was analyzed in live cells by growing the yeast strains in YP media supplemented with the indicated carbon source to log phase at 30°C. Microscopy was performed as described (Griffin et al., 2005).

DCY2573 (yBR230c-TAP) was grown in the indicated YP media and harvested at OD_{600} ~1.0. ~ 10 OD units of cells were subjected to glass bead lysis in SDS sample buffer lacking dye. Protein levels loaded for Western blot analysis were normalized using the RC DC Protein Assay (BioRad).

In order to determine growth on glycerol, JSY2793, JSY2287 (kind gift of Janet Shaw, Hermann et al., 1998), DCY2869 and DCY2871 were grown at ~25°C in YPGlycerol + ethanol. Cultures were resuspended in YP at OD_{600} ~1.0, diluted 1:5 six times in YP, and 3 μl were spotted on YPDextrose and YPGlycerol plates. Plates were incubated at 25°C and 37°C for 3 days (YPDextrose) and 6 days (YPGlycerol).

TAP-MudPIT was performed as previously described (Griffin et al., 2005) except cultures were grown in YPGlycerol instead of YPDextrose.

Results

In order to identify Fzo1p and Ugo1p binding partners, we first generated strains expressing 9XMyc/TEV/His_8-*FZO1* and *UGO1*-His_8/TEV/3XMyc from their endogenous promoters. These strains were grown as respiring cultures (rich glycerol medium) because these conditions support more mitochondrial fusion (Meeusen et al., 2004). Tandem affinity purified 9XMyc/TEV/His_8-Fzo1p and Ugo1p-His_8/TEV/3XMyc were subjected to MudPIT analysis and the results are presented in Tables 8 and 9 of the Appendix (Graumann et al., 2004; Griffin et al., 2005; Link et al., 1999).

Om14p physically interacts with Fzo1p and Ugo1p

Om14p was selected for further analysis because it co-purified with both Fzo1p and Ugo1p, it localizes to the mitochondrial outer membrane, and has not been functionally characterized (Burri et al., 2006; Huh et al., 2003; Sickmann et al., 2003). We first sought to verify the interaction between Om14p and Fzo1p and Ugo1p using a coimmunoprecipitation assay. When yeast were grown in rich glycerol or galactose media, both 6XHA-Fzo1p and Ugo1p-3XHA coimmunoprecipitated with an epitope-tagged version of Om14p (Om14p-TAP) (Fig. 1, lanes 2–3, and 6–7). In contrast, when cultures were grown in rich dextrose media, Ugo1p-3XHA failed coimmunoprecipitated with Om14p-TAP (Fig. 1, lanes 5). These data indicate that Om14p interacts with Fzo1p and Ugo1p and the interaction with Ugo1p is more robust in glycerol and galactose than in dextrose media.

We observed higher Om14p-TAP expression levels in glycerol and galactose than in dextrose during our coimmunoprecipitation experiments. To assess Om14p expression

levels more rigorously, we monitored porin, PGK, and Om14p-TAP levels in yeast grown in rich dextrose, glycerol, and galactose media. Om14p-TAP is repressed in dextrose and increases several fold in galactose and glycerol media, similar to previous reports (Fig. 2) (Burri et al., 2006; Ohlmeier et al., 2004). The mitochondrial marker porin is similarly repressed in dextrose while the cytosolic protein PGK is unchanged in the different growth conditions (Fig. 2). Thus, Om14p is upregulated in respiring cultures and its interaction with Ugo1p may be regulated at the level of Om14p expression.

om14Δ cells have a simplified mitochondrial morphology

Having identified Om14p as a glycerol induced Fzo1p and Ugo1p interacting protein, we next asked if *om14Δ* yeast had a mitochondrial morphology defect. Mutations in the mitochondrial fusion machinery result in fragmentation of the tubular mitochondrial reticulum due to ongoing fission (Hermann et al., 1998; Sesaki and Jensen, 1999). Defects in mitochondrial fission cause the formation of interconnected networks of mitochondrial due to ongoing fusion (Bleazard et al., 1999; Sesaki and Jensen, 1999). In dextrose media, *om14Δ* yeast have wild-type mitochondrial morphology (Fig. 3), indicating Om14p is not required for normal mitochondrial dynamics under conditions where Om14p expression is repressed.

In conditions in which Om14p is highly expressed, *om14Δ* cells display a mitochondrial morphology defect. When grown in glycerol, the majority of wild-type cells display a tubular reticulum of increased complexity relative to dextrose conditions (93.5%, Fig 3). In contrast, the majority of *om14Δ* cells grown in glycerol have simple

mitochondrial networks with reduced tubule ends and mitochondrial branch points (62%; Fig. 3C). In galactose media, 24% of *om14Δ* cells had simple networks compared to 10.5% of wild-type cells. The simplified, overly fused, mitochondrial morphology in *om14Δ* cells is consistent with a higher rate of mitochondrial fusion relative to fission.

Om14p negatively regulates mitochondrial fusion

Given the morphological defect in *om14Δ*, we next asked whether *OM14* interacted genetically with the mitochondrial fusion pathway. A secondary consequence of mitochondrial fragmentation in fusion mutants is the loss of mtDNA and an inability to grow on non-fermentable carbon sources such as glycerol (Hermann et al., 1998). Yeast expressing *FZO1* grew on glycerol plates at both 25°C and 37°C, whereas yeast expressing a temperature-sensitive allele of *FZO1*, *fzo1-1*, failed to grow on glycerol plates at 37°C (Fig. 4) (Hermann et al., 1998). Interestingly, *om14Δ* partially rescued the *fzo1-1* glycerol growth defect (Fig. 4), indicating *om14Δ* is a suppressor of *fzo1-1*. Two possible classes of *fzo1-1* suppressors include mitochondrial fission mutants that bypass the requirement for mitochondrial fusion (Fekkes et al., 2000; Mozdy et al., 2000; Tieu and Nunnari, 2000). A second class of suppressors could increase the mitochondrial fusion activity of *fzo1-1*.

We next asked whether *OM14* is a component of the mitochondrial fission pathway. *DNM1* is required for mitochondrial fission. If the mitochondrial morphology defect in *om14Δ* resulted from reduced mitochondrial fission, then we would expect *dnm1Δ om14Δ* cells to be indistinguishable from *dnm1Δ* cells. However, if mitochondrial fusion were improperly regulated in *om14Δ* cells, this would persist in

dnm1Δ cells. In this scenario, we would expect a morphological difference between *dnm1Δ* and *dnm1Δ om14Δ* cells. In 87% of *dnm1Δ* cells, mitochondria form elaborate nets spread throughout the cell. In contrast, in 74% of *dnm1Δ om14Δ* cells, the mitochondria form tight nets that are more compact than those seen in *dnm1Δ* cells (Fig 3b). This difference in the mitochondrial morphology of *dnm1Δ* and *dnm1Δ om14Δ* cells suggest *OM14* does not act positively in the mitochondrial fission pathway. Rather, the morphology of *om14Δ* and *dnm1Δ om14Δ* suggests increased mitochondrial fusion.

Given these morphological data and the physical interaction between Om14p and Fzo1p and Ugo1p, we next tested whether *OM14* could regulate mitochondrial fusion. We tested the temperature-sensitive allele of *FZO1*, *fzo1-1*, in a zygotic mitochondrial fusion assay (Hermann et al., 1998). At 30°C, mitochondrial fusion occurred in almost all cells (96% of *fzo1-1 dnm1Δ* cells and 97% of *fzo1-1 dnm1Δ om14Δ* = 97% cells). *fzo1-1* activity was almost completely blocked at 34.5°C, and mitochondrial fusion occurred in only 9% of *fzo1-1 dnm1Δ* and 13% of *fzo1-1 dnm1Δ om14Δ* cells (Fig. 5). However, at the semi-permissive temperatures of 32°C, 33°C and 34°C, there was consistently more mitochondrial fusion *fzo1-1 dnm1Δ om14Δ* cells than *fzo1-1 dnm1Δ* cells (Fig. 5). For example, at 34°C, 18% of *fzo1-1 dnm1Δ* zygotes had fused mitochondria while 41% of *fzo1-1 dnm1Δ om14Δ* had fused mitochondria. Thus, deletion of *OM14* increased the mitochondrial fusion supported by *fzo1-1*, indicating Om14p is a negative regulator of mitochondrial fusion.

Discussion

We have identified Om14p as a novel glycerol-induced regulator of mitochondrial morphology. We provide four lines of evidence that Om14p negatively regulates mitochondrial fusion. First, Om14p physically associates with two components of the mitochondrial fusion machinery, Fzo1p and Ugo1p. Second, *om14Δ* yeast have a mitochondrial morphology defect that is consistent with an increase in mitochondrial fusion. Third, the overly fused morphology persists in *dnm1Δ om14Δ* cells, indicating that Om14p is not involved in mitochondrial fission. Finally, the level of mitochondrial fusion supported by a hypomorphic *FZO1* allele is increased in *om14Δ* cells.

If mitochondrial fusion activity is high in respiring cultures, why would a negative regulator of fusion be upregulated? We speculate there may also be an activating signal that is upregulated in respiring cultures. In this scenario, Om14p could modulate the activation of fusion induced in glycerol. Close homologs of *OM14* are evident in all of the species of budding yeast that have been sequenced (Burri et al., 2006), suggesting its contribution to the adaptation of mitochondrial morphology to different growth conditions is conserved in budding yeast.

An important goal of future work is to determine how Om14p inhibits mitochondrial fusion. Given the physical interaction with Ugo1p and Fzo1p, it is likely these molecules are the target of Om14p inhibition. For example, Om14p could regulate the interactions between Fzo1p, Ugo1p and Mgm1p (Sesaki and Jensen, 2004; Wong et al., 2003) or intermolecular Fzo1p interactions ((Koshiba et al., 2004) and Chapter 3). Alternatively, Om14p could regulate the GTPase activity of Fzo1p, which is required for mitochondrial fusion (Chen et al., 2003; Hales and Fuller, 1997; Hermann et al., 1998).

This work demonstrates that inhibition of fusion is an important regulator of mitochondrial dynamics in yeast and raises the possibility of similar regulation in mammals.

Table 1: Yeast strains

DCY1440	*MATα*, *his3Δ200*, *met15Δ0*, *trp1Δ63*, *ura3Δ0*, *dnm1*::HIS5, *fzo1*::KANMX6, *lue2*::GPD mito-DsRed-*LEU2*
DCY1553	*MATa*, *his3Δ200*, *met15Δ0*, *trp1Δ63*, *ura3Δ0*, *dnm1*::HIS5, *fzo1*::KANMX6, *lue2*::GPD mito-GFP-*LEU2*
DCY2789	*MATa*, *his3-*, *met15Δ0*, *trp1Δ63*, *ura3Δ0*, *dnm1*::HIS5, *fzo1*::KANMX6, *yBR230c*::KANMX6, *lue2*::GPD mito-DsRed-*LEU2*
DCY2834	*MATα*, *his3-*, *met15Δ0*, *ura3Δ0*, *dnm1*::HIS5, *fzo1*::KANMX6, *yBR230c*::KANMX6, *lue2*::GPD mito-GFP-*LEU2*
DCY2869	*MATα*, *ura3-52*, *his3Δ200*, *leu2Δ1*, *trp1Δ63*, *fzo1*::*HIS3*, *yBR230c*::KANMX6, pRS414-*fzo1-1*
DCY2871	*MATα*, *ura3-52*, *his3Δ200*, *leu2Δ1*, *trp1Δ63*, *fzo1*::*HIS3*, *yBR230c*::KANMX6, pRS414-*fzo1-1*
DCY1624	*MATa*, can1-100, *leu2-3, -112*, *his3-11,-15*, *trp1-1*, *ura3-1*, *ade2-1*, *pep4*::*TRP1*, bar1::hisG, 9XMyc/TEV/His_8-*FZO1*
DCY2139	*MATa*, can1-100, *leu2-3, -112*, *his3-11,-15*, *trp1-1*, *ura3-1*, *ade2-1*, *pep4*::*TRP1*, bar1::hisG, *UGO1*-His_8/TEV/3XMyc
DCY2766	*MATa*, *his3-1*, *lue2*::GPD mito-GFP-*LEU2*, *met15Δ0*, *ura3Δ0*, *yBR230c*::KANMX6
DCY2827	*his3-1*, *lue2*::GPD mito-GFP-*LEU2*, *met15Δ0*, *ura3Δ0*, *yBR230c*::KANMX6, *dnm1*::*HIS5*

References

Alexander, C., M. Votruba, U.E. Pesch, D.L. Thiselton, S. Mayer, A. Moore, M. Rodriguez, U. Kellner, B. Leo-Kottler, G. Auburger, S.S. Bhattacharya, and B. Wissinger. 2000. OPA1, encoding a dynamin-related GTPase, is mutated in autosomal dominant optic atrophy linked to chromosome 3q28. *Nat Genet*. 26:211–5.

Bleazard, W., J.M. McCaffery, E.J. King, S. Bale, A. Mozdy, Q. Tieu, J. Nunnari, and J.M. Shaw. 1999. The dynamin-related GTPase Dnm1 regulates mitochondrial fission in yeast. *Nat Cell Biol*. 1:298–304.

Burri, L., K. Vascotto, I.E. Gentle, N.C. Chan, T. Beilharz, D.I. Stapleton, L. Ramage, and T. Lithgow. 2006. Intergral membrane proteins in the mitochondrial outer membrane of *Saccharomyces cerevisiae*. *The FEBS Journal*. 273:1507–1515.

Chen, H., S.A. Detmer, A.J. Ewald, E.E. Griffin, S.E. Fraser, and D.C. Chan. 2003. Mitofusins Mfn1 and Mfn2 coordinately regulate mitochondrial fusion and are essential for embryonic development. *J Cell Biol*. 160:189–200.

Egner, A., S. Jakobs, and S.W. Hell. 2002. Fast 100-nm resolution three-dimensional microscope reveals structural plasticity of mitochondria in live yeast. *Proc Natl Acad Sci U S A*. 99:3370–5.

Fekkes, P., K.A. Shepard, and M.P. Yaffe. 2000. Gag3p, an outer membrane protein required for fission of mitochondrial tubules. *J Cell Biol*. 151:333–40.

Graumann, J., L.A. Dunipace, J.H. Seol, W.H. McDonald, J.R. Yates, 3rd, B.J. Wold, and R.J. Deshaies. 2004. Applicability of tandem affinity purification MudPIT to pathway proteomics in yeast. *Mol Cell Proteomics*. 3:226–37.

Griffin, E.E., J. Graumann, and D.C. Chan. 2005. The WD40 protein Caf4p is a component of the mitochondrial fission machinery and recruits Dnm1p to mitochondria. *J Cell Biol*. 170:237–48.

Hales, K.G., and M.T. Fuller. 1997. Developmentally regulated mitochondrial fusion mediated by a conserved, novel, predicted GTPase. *Cell*. 90:121–9.

Hermann, G.J., J.W. Thatcher, J.P. Mills, K.G. Hales, M.T. Fuller, J. Nunnari, and J.M. Shaw. 1998. Mitochondrial fusion in yeast requires the transmembrane GTPase Fzo1p. *J Cell Biol*. 143:359–73.

Huh, W.K., J.V. Falvo, L.C. Gerke, A.S. Carroll, R.W. Howson, J.S. Weissman, and E.K. O'Shea. 2003. Global analysis of protein localization in budding yeast. *Nature*. 425:686–91.

Koshiba, T., S.A. Detmer, J.T. Kaiser, H. Chen, J.M. McCaffery, and D.C. Chan. 2004. Structural basis of mitochondrial tethering by mitofusin complexes. *Science*. 305:858–62.

Link, A.J., J. Eng, D.M. Schieltz, E. Carmack, G.J. Mize, D.R. Morris, B.M. Garvik, and J.R. Yates, 3rd. 1999. Direct analysis of protein complexes using mass spectrometry. *Nat Biotechnol*. 17:676–82.

Meeusen, S., J.M. McCaffery, and J. Nunnari. 2004. Mitochondrial fusion intermediates revealed in vitro. *Science*. 305:1747–52.

Mozdy, A.D., J.M. McCaffery, and J.M. Shaw. 2000. Dnm1p GTPase-mediated mitochondrial fission is a multi-step process requiring the novel integral membrane component Fis1p. *J Cell Biol*. 151:367–80.

Nunnari, J., W.F. Marshall, A. Straight, A. Murray, J.W. Sedat, and P. Walter. 1997. Mitochondrial transmission during mating in *Saccharomyces cerevisiae* is determined by mitochondrial fusion and fission and the intramitochondrial segregation of mitochondrial DNA. *Mol Biol Cell.* 8:1233–42.

Ohlmeier, S., A.J. Kastaniotis, J.K. Hiltunen, and U. Bergmann. 2004. The yeast mitochondrial proteome, a study of fermentative and respiratory growth. *J Biol Chem.* 279:3956–79.

Rapaport, D., M. Brunner, W. Neupert, and B. Westermann. 1998. Fzo1p is a mitochondrial outer membrane protein essential for the biogenesis of functional mitochondria in *Saccharomyces cerevisiae*. *J Biol Chem.* 273:20150–5.

Sesaki, H., and R.E. Jensen. 1999. Division versus fusion: Dnm1p and Fzo1p antagonistically regulate mitochondrial shape. *J Cell Biol.* 147:699–706.

Sesaki, H., and R.E. Jensen. 2004. Ugo1p links the Fzo1p and Mgm1p GTPases for mitochondrial fusion. *J Biol Chem.* 279:28298–303.

Sickmann, A., J. Reinders, Y. Wagner, C. Joppich, R. Zahedi, H.E. Meyer, B. Schonfisch, I. Perschil, A. Chacinska, B. Guiard, P. Rehling, N. Pfanner, and C. Meisinger. 2003. The proteome of *Saccharomyces cerevisiae* mitochondria. *Proc Natl Acad Sci U S A.* 100:13207–12.

Tieu, Q., and J. Nunnari. 2000. Mdv1p is a WD repeat protein that interacts with the dynamin-related GTPase, Dnm1p, to trigger mitochondrial division. *J Cell Biol.* 151:353–66.

Wong, E.D., J.A. Wagner, S.V. Scott, V. Okreglak, T.J. Holewinske, A. Cassidy-Stone, and J. Nunnari. 2003. The intramitochondrial dynamin-related GTPase, Mgm1p,

is a component of a protein complex that mediates mitochondrial fusion. *J Cell Biol*. 160:303–11.

Zuchner, S., I.V. Mersiyanova, M. Muglia, N. Bissar-Tadmouri, J. Rochelle, E.L. Dadali, M. Zappia, E. Nelis, A. Patitucci, J. Senderek, Y. Parman, O. Evgrafov, P.D. Jonghe, Y. Takahashi, S. Tsuji, M.A. Pericak-Vance, A. Quattrone, E. Battaloglu, A.V. Polyakov, V. Timmerman, J.M. Schroder, and J.M. Vance. 2004. Mutations in the mitochondrial GTPase mitofusin 2 cause Charcot-Marie-Tooth neuropathy type 2A. *Nat Genet*. 36:449–51.

Figure Legends

Figure 1. Om14p interacts with Ugo1p and Fzo1p.

Yeast expressing the indicated proteins were harvested from rich dextrose, galactose, or glycerol cultures. Cells were lysed and Om14p-TAP was immunoprecipitated with IgG beads. Total lysate and immunoprecipitate samples were analyzed by immunoblotting with anti-HA (12CA5) or anti-TAP (anti-CBP) antibodies. TAP-IP samples are loaded at ten equivalents of the lysate samples.

Figure 2. Om14p is upregulated in glycerol and galactose cultures.

Lysates were generated from DCY2537 grown to log phase in rich media supplemented with dextrose, galactose, or glycerol. An equivalent amount of protein was loaded in each lane and analyzed by Western blotting against Om14p-TAP (anti-TAP antibody), the mitochondrial marker porin, or the cytosolic marker PGK.

Figure 3. Mitochondrial morphology defect in *om14Δ* cells.

A. Wild-type (DCY1979), *om14Δ* (DCY2766) yeast were grown to log phase in rich media supplemented with dextrose, galactose, or glycerol and scored for tubular mitochondria (*B*) or simple mitochondrial networks (*C*). Simple networks are distinguished from tubular mitochondria by the decrease in tubule ends and the decrease in mitochondrial branch points. *B*. *dnm1Δ* and *dnm1Δ om14Δ* were grown to log phase in rich glycerol media and scored for the presence of spread mitochondrial nets (*E*) or

compact nets (*F*). The percentage of cells (n=200) displaying the indicated morphologies are shown.

Figure 4. *om14Δ* is an *fzo1-1* suppressor.

fzo1Δ yeast expressing a plasmid encoding *FZO1* (JSY2287) or a temperature-sensitive allele of *fzo1*, *fzo1-1* (JSY2793) and two *fzo1Δ om14Δ* strains expressing *fzo1-1* (DCY2869 and DCY2871) were serially diluted and spotted on YPDextrose and YPGlycerol plates. Plates were grown at 25°C or 37°C for 3 days (YPDextrose) and 6 days (YPGlycerol).

Figure 5. *om14Δ* suppresses *fzo1-1* by increasing mitochondrial fusion. *fzo1Δ dnm1Δ* (DVY1440 and DCY1553; *fzo1-ts*) and *fzo1Δ dnm1Δ om14Δ* (DCY2789 and DCY2834; *fzo1-ts, om14Δ*) expressing *fzo1-1* and either mito-GFP or mito-DsRed were mated in YPGlycerol/Ethanol at the indicated temperatures. Large budded zygotes were scored for the complete overlap of mito-GFP and mito-DsRed.

Figure 1.

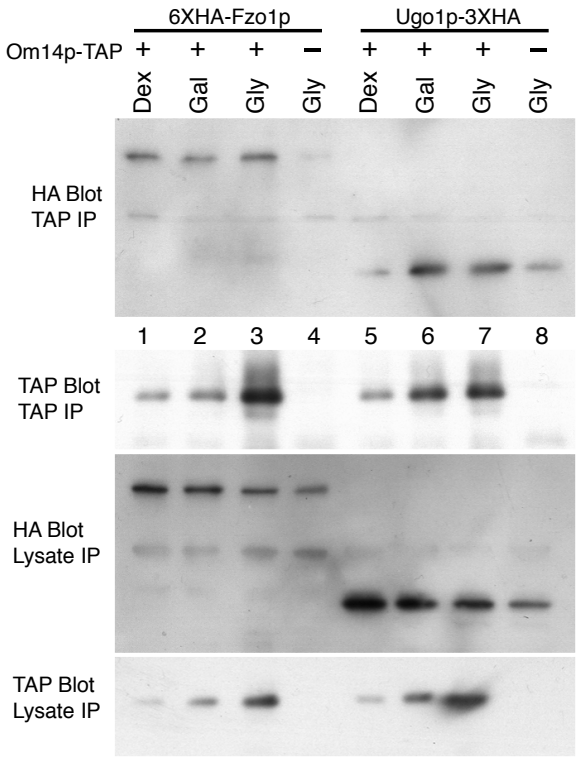
6XHA-Fzo1p
Ugo1p-3XHA
Om14p-TAP + + + − + + + −
Dex Gal Gly Gly Dex Gal Gly Gly
HA Blot
TAP IP
1 2 3 4 5 6 7 8
TAP Blot
TAP IP
HA Blot
Lysate IP
TAP Blot
Lysate IP

Figure 2.

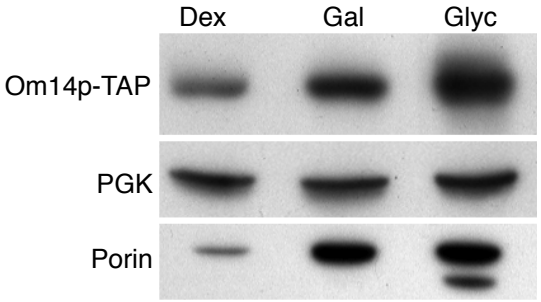

Figure 3.

A

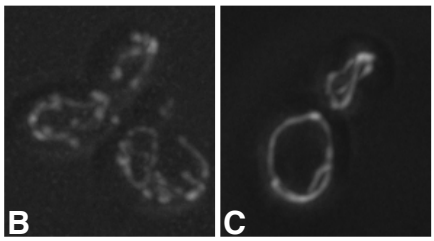

	Tubular	Simple Networks
Glycerol		
Wild type	93.5	6.5
*om14*Δ	38	62
Galactose		
Wild type	89.5	10.5
*om14*Δ	76	24
Dextrose		
Wild type	100	0
*om14*Δ	100	0

D

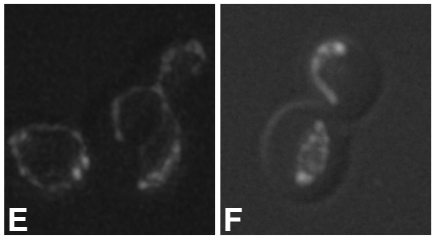

	Spread Nets	Compact Nets
Glycerol		
*dnm1*Δ	87	13
*dnm1*Δ *om14*Δ	26	74

Figure 4.

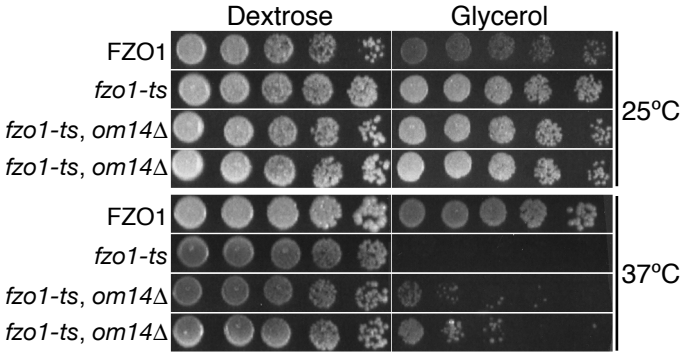
Dextrose
Glycerol
FZO1
fzo1-ts
fzo1-ts, om14Δ
fzo1-ts, om14Δ
25ºC
FZO1
fzo1-ts
fzo1-ts, om14Δ
fzo1-ts, om14Δ
37ºC

Figure 5.

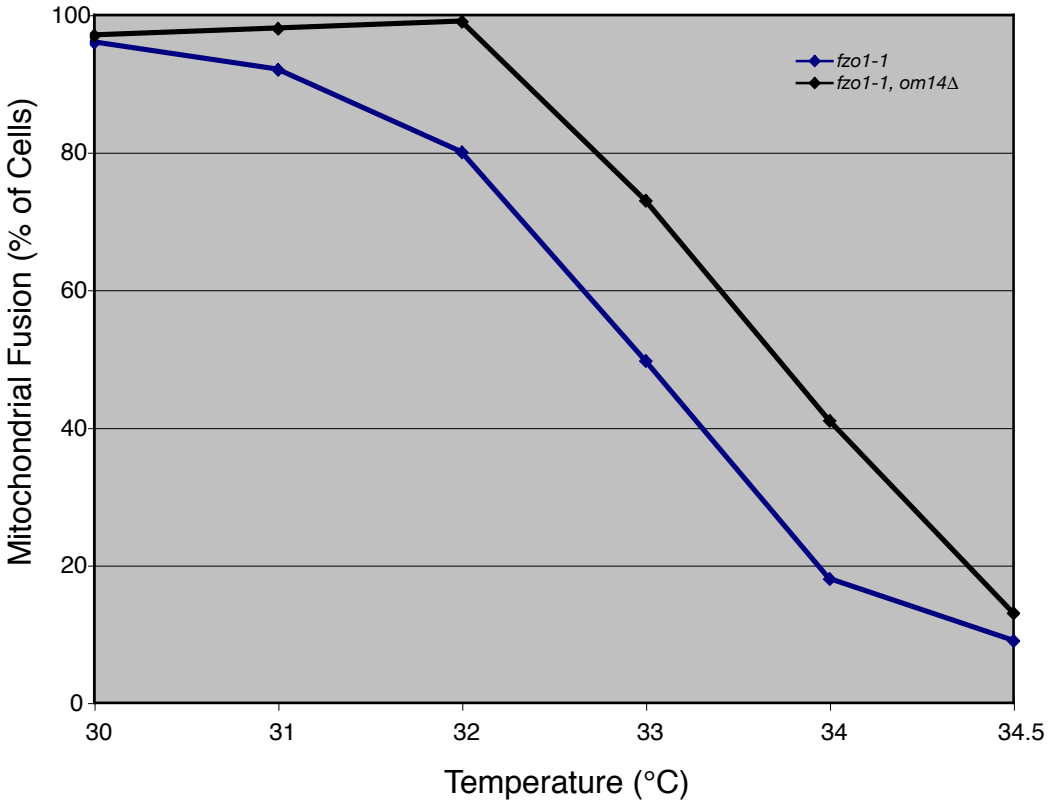
100
80
60
40
20
0
Mitochondrial Fusion (% of Cells)
30
31
32
33
34
34.5
Temperature (°C)
fzo1-1
fzo1-1, om14Δ